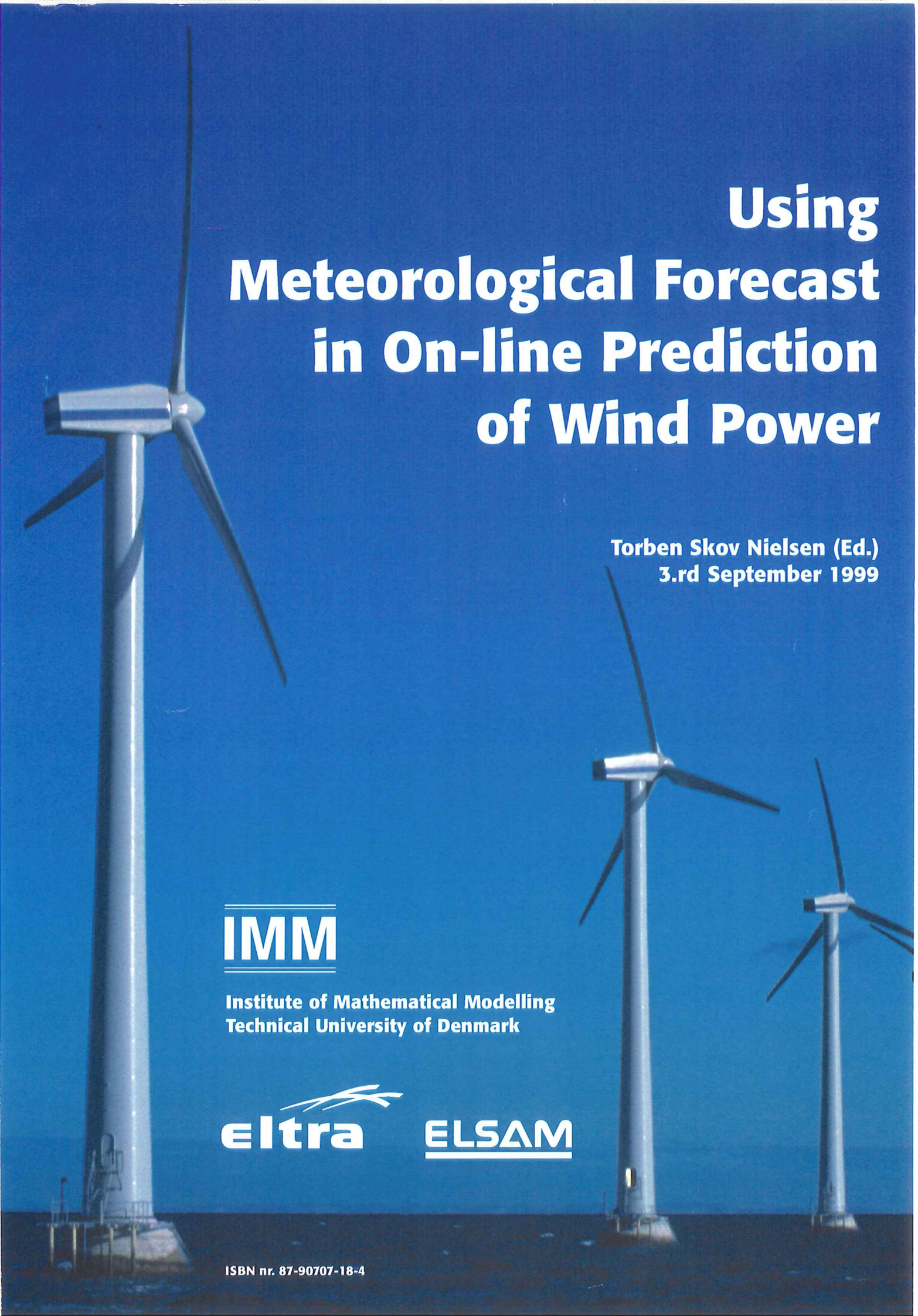

Using Meteorological Forecast in On-line Prediction of Wind Power

Torben Skov Nielsen (Ed.)

3.rd September 1999

IMM

Institute of Mathematical Modelling
Technical University of Denmark

eltra

ELSAM

ISBN nr. 87-90707-18-4

Using Meteorological Forecasts in On-line Predictions of Wind Power

Torben Skov Nielsen (Ed.)

3rd September 1999

IMM

Institute of Mathematical Modelling
Technical University of Denmark

Contents

Preface

Authors

Several authors have contributed significantly by writing sections of the present report:

John Tøfting	– Elsam
Arne Grud	– Eltra
Aksel Gruelund Sørensen	– Eltra
Henning Parbo	– Eltra
Henrik Madsen	– IMM
Henrik Ålborg Nielsen	– IMM
Torben Skov Nielsen	– IMM

The contributions of the different authors have been specified in more detail in the following:

- **Chapter 1 – Summary** is written by Torben Skov Nielsen with comments and helpful suggestions from Henrik Madsen and Henrik Ålborg Nielsen.
- **Chapter 2 – Introduction** is written by Torben Skov Nielsen with comments and helpful suggestions from Henrik Madsen.
- **Chapter 3 – Measurements** is written by Torben Skov Nielsen and Arne Grud with comments and helpful suggestions by Henrik Madsen and Henrik Ålborg Nielsen.
- **Chapter 4 – Meteorological data** is written by Torben Skov Nielsen with comments and helpful suggestions from Henrik Madsen and Henrik Ålborg Nielsen.
- **Chapter 5 – Estimation methods** is written by Henrik Ålborg Nielsen and Torben Skov Nielsen with comments and helpful suggestions from Henrik Madsen.
- **Chapter 6 – Models for predicting wind speed and power** is written by Torben Skov Nielsen with comments and helpful suggestions by Henrik Madsen and Henrik Ålborg Nielsen.
- **Chapter 7 – Upscaling** is written by Henning Parbo with comments and helpful suggestions by Henrik Madsen, Henrik Ålborg Nielsen and Torben Skov Nielsen.
- **Chapter 8 – Utility experiences** is written by John Tøfting (utility experiences) and Aksel Gruelund Sørensen (network losses) with comments and suggestions from Henrik Madsen and Torben Skov Nielsen.
- **Chapter 9 – Implementation** is written by Torben Skov Nielsen with comments and helpful suggestions from Henrik Madsen.

Project participants

The following people have participated in the project group during the three year lifespan of the project:

Bjarne Korshøj	– Elsam
John Tøfting	– Elsam
Jens K. Vesterdal	– Elsam
Gitte Agersbæk	– Eltra
Henning S. Christensen	– Eltra
Arne Grud	– Eltra
Henning Palmelund	– Eltra
Henning Parbo	– Eltra
Henrik Madsen	– IMM
Torben Skov Nielsen	– IMM

Acknowledgements

The work presented in the present report has been partially founded by the European Commission as a part of the project "Implementing Short-term Wind Power Predictions at Utilities", contract JOR3-CT95-0008.

Torben Skov Nielsen,
Juli 1999.

Chapter 1

Summary

During the present project a software system – WPPT[1] – for predicting the total wind power production in the Jutland/Funen supply area has been developed and subsequently installed at the control centres of Elsam and Eltra.

In WPPT statistical methods are applied for predicting the expected wind power production in a larger area using on-line data covering only a subset of the total population of wind turbines in the area. The approach is to divide the area of interest into sub-areas each covered by a wind farm (a reference wind farm). Predictions of wind power with a horizon from 30 minute up to 39 hours are then formed using local measurements of climatic variables as well as meteorological forecasts of wind speed and direction. The wind farm power predictions for each sub-area are subsequently up-scaled to cover all wind turbines in the sub-area before the predictions for sub-areas are summarized to form a prediction for the entire area. An overview of WPPT is found in Figure 1.1.

The WPPT application has been developed as a co-work between Elsam/Eltra and the Department of Mathematical Modeling (IMM) at the Technical University of Denmark (DTU). The work was initiated in 1992 as a part of a project, *Wind Power Prediction Tool in Control Dispatch Centres*, sponsored by the European Commission. During this project a statistical model utilizing only measurements of wind power and wind speed was developed and together with a graphical user interface implemented at Elsam's control center at Fredericia. WPPT version 1 went into operation in October 1994 and was subject to a three months trial period. The experience gained as well as further details regarding the models and user interface developed can be found in [H. Madsen (Ed.), 1995] and [H. Madsen (Ed.), 1996]. In short it became apparent that WPPT 1.0 was capable of providing the operators with useful predictions up to 8 to 12 hours ahead, but for larger prediction horizons further model development was needed.

In ([Landberg et al., 1997], [Landberg, 1997]) physical models describing the wind farm layout and the influence of the surroundings are used in combination with meteorological forecasts of wind speed and direction to make predictions of power production with a horizon of up to 36 hours ahead. Promising results were found for the longer prediction horizons, but the approach had poor performance on shorter horizons. The purpose of the project described in this report has therefore been to improve the previous developed models in WPPT by using meteorological forecasts from the national weather service as input to the

[1] Wind Power Prediction Tool

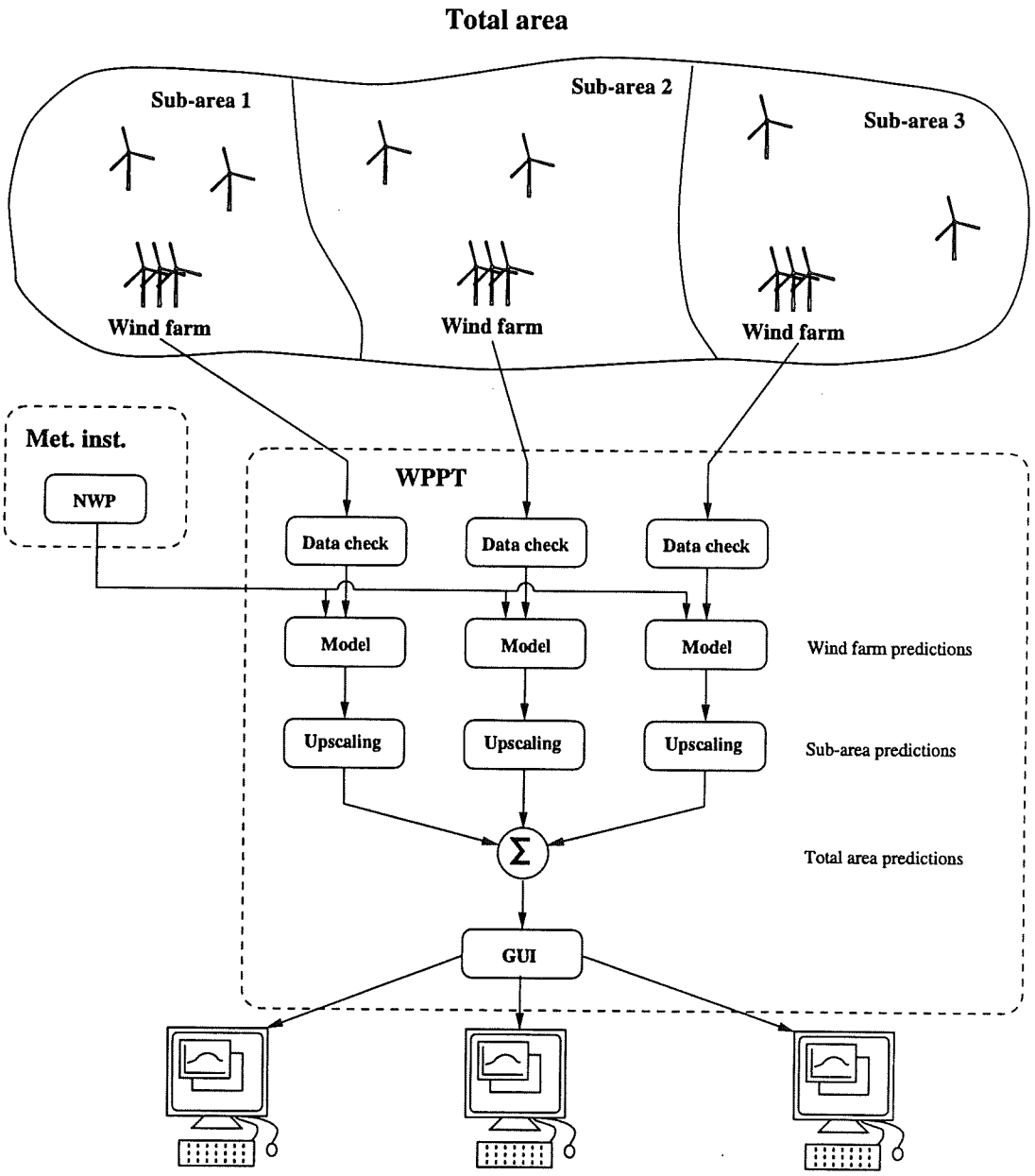

Figure 1.1: *Overview over WPPT. In WPPT the wind power production in a larger area are predicted using on-line data covering only a subset of the total population of wind turbines in the area. The area of interest is divided into sub-areas each covered by a wind farm (a reference wind farm) and for each sub area predictions of wind power are calculated using local measurements of climatic variables as well as meteorological forecasts of wind speed and direction. The wind farm power predictions for each sub-area are subsequently up-scaled to cover all wind turbines in the sub-area before the predictions for sub-areas are summarized to form a prediction for the entire area.*

models.

The most important model analysis and the main conclusions are listed below.

- **Meteorological models.** It has been shown how fundamental characteristics such as mean value and variance of the meteorological forecasts of wind speed and wind

direction from the HIRLAM model change as a function of the forecast horizon (lead time). Especially the change in mean value is undesirable and should be countered by a statistical correction before further use of the meteorological forecasts of wind speed and wind direction.

Also the diurnal variation of observed as well as forecasted wind speeds have been investigated. As expected the diurnal variation of the observed wind speeds is found to follow a annual pattern with larger variations during summer time and only minor variations during winter time. The diurnal variation in the observed wind speed is found to vary greatly between the wind farms but a similar pattern can not be recognized in the diurnal variation of the forecasted wind speeds. It is thus concluded, that the diurnal variation in the wind speed can not be assumed contained in the forecasts of wind speed from the HIRLAM model.

- **Models relating power production to the wind speed (power curve models).** Power curves describing the relationship between observed power production and observed wind speeds as well as the HIRLAM analysis of the wind speed have been estimated using non-linear models. Models with as well as without wind direction dependency have been considered.

  The power curves without wind direction dependency and estimated using the observed wind speeds as input seems to give a good description of the physics in the wind farms. Coefficient of determination (R^2) for the estimated power curve models range from 0.86 up to 0.96 depending on wind farm and the wind speed used as input. When considering the wind direction dependent power curves also the estimated wind direction dependency seems to give a good indication of physical conditions in the wind farms. In general the wind direction dependency estimated using measured wind speeds as input does not give a clear indication of the situation or layout of the wind farm whereas local conditions influencing the anemometers them self such as shading effects from nearby wind turbines are readily discerned. The wind direction dependency estimated using the analysis wind speed as input by contrast seems to resemble what must be expected when the siting of the wind farms is considered and also the influence of the wind farm layout can in some cases be deducted. When comparing with the power curves estimated without wind direction dependencies improvements in R^2 ranging from 0.01 to 0.07 depending on wind farm and wind speed used as input are observed.

  The performance of the power curve models have been evaluated when using meteorological forecasts of wind speed and direction as input in order to calculate predictions of the power production for the wind farms. The power curves models investigated are the power curve model without wind direction dependency as well as the most promising of the wind direction dependent models estimated using either observed wind speed or the analysis as input. The results have been evaluated using R^2 as a measure.

  In the context of prediction it seems generally to be advantageous to use models estimated on basis of the analysis and this is especially true for the models with wind direction dependency. Furthermore it is found that, with the exception of Fjaldene, it is clearly beneficial to model the wind direction dependency and especially Dræby

and Hollandsbjerg show a very distinct improvement in performance. There seems, however, to be a reduced improvement as the prediction horizon increases. For the two prediction horizons 0 hours and 36 hours the R^2 values range from between 0.73 and 0.81 for Dræby and Sydthy, respectively, and down to between 0.40 and 0.51 for Dræby and Fjaldene, respectively.

- **Models for multi-step prediction of power production.** The models considered belong to the class of linear autoregressive models with exogenous input and are formulated directly as k-step prediction models. The input is transformed values of observed wind speed as well as forecasted wind speed, where the transformation is either by a second order polynomial expansion or by the power curves estimated in Section 6.4.2. The model parameters are estimated adaptively in order to accommodate slow changes in the system using the Recusive Least Squares algorithm with exponential forgetting. The prediction horizon range from half an hour to 39 hours in half hourly steps, thus the prediction horizon for the models investigated range from 1-step to 78-step.

  A set of models have been proposed and based on exhaustive search among all possible combinations of the model terms a candidate for a best overall adaptive prediction model is identified. Two characteristics are noted for this model. First of all the transformed meteorological wind speeds are needed in the model for all prediction horizons. Secondly for the shorter prediction horizons the model relies on observed values of power, and to a less extent, wind speed, but as the prediction horizon increases the emphasis shifts to terms related to diurnal variation and for a prediction horizon larger than or equal to 18 hours no observations enter the model.

  For the two prediction horizons 1 hours and 36 hours the R^2 values for the candidate model range from between 0.88 and 0.93 for Rejsby and Sydthy, respectively, and down to between 0.43 and 0.52 for Dræby and Sydthy, respectively.

In order to handle errors in the data methods for robust estimation and detection of outliers (bad measurements) have been developed. If measurements are classified as erroneous this is automatically indicated in the implemented system.

WPPT was installed in the control centres of Elsam and Eltra in October 1997 and has been used operationally since January 1998.The assessment by the operators is that WPPT generally produces reliable predictions, which are used directly in the economic load dispatch and the day to day electricity trade. In periods with unstable weather the operators may choose to modify the predictions (typically smooth the pattern of the prediction) before further usage though. The economical value of the wind power predictions is difficult to evaluate directly mainly due to the problem of assessing the course of action had the predictions not been available. Instead three cases have been analysed in order to illustrate how the predictions are used and with which consequences. The examples indicate that the operators rely on the wind power production from WPPT in the daily planning. The predictions are markedly better than what can be derived from other sources. This is not to say, that there is no room for improvement, and thus WPPT is subject to continues improvements based on the experiences of the operators.

Chapter 2

Introduction

The purpose of the Wind Power Prediction Tool (WPPT) project is to develop, implement and test a forecasting model for the prediction of wind power production to be used in the daily planning at the control centres of Elsam and Eltra.

2.1 Background

The background for the WPPT project is primarily the increasing amount of wind power installed Jutland/Funen supply area – 1000 MW by the end of 1998 – which might be put into relation by comparing with an yearly minimum and maximum load in the supply area of 1200 MW and 3700 MW, respectively. Furthermore it is foreseen that the amount of wind power will double within the next 10 years. Such a high level of wind energy penetration clearly calls for reliable methods for predicting the future wind power production not only for planning purposes (minimization of spinning reserves, short term network maintenance, etc.), but also the marked value of wind energy on Europe's future free energy markets will depend on the availability of such methods.

From January 1998 the old Elsam has been divided into two companies:

- Eltra is the independent system operator for the western part of Denmark. Eltra are responsible for the production with priority (small combined powerplants and wind-turbines) and are the owners of the 400, 220 kV and HVDC transmission lines.
- The new Elsam now concentrates on trade and export of electricity, purchase of fuel and co-ordination of the combined heat and electricity production in six primary power stations and utility owned wind turbines.

Eltra and Elsam operate in the western part of Denmark (the peninsula Jutland and the island Funen).

2.2 Aim of the project

It has first of all been the aim of the WPPT project to develop and implement an on-line prediction tool which is capable of prediction the power production in the Jutland/Funen

supply area with a sufficently high accuracy to make it usefull in the daily planning of the operations. Furthermore it has been the aim to test the implemented tool and to evaluate the benefits of such an on-line model.

2.3 Brief outline of the report

The report addresses the following eight main topics:

- Description of measurements.
- Description of meteorological forecasts.
- Analysis of the meteorological forecasts of wind speed and wind direction.
- Identification and estimation of power curve models for the individual wind farms.
- Identification and estimation of power prediction models for the individual wind farms.
- Calculation of the the total wind power production from the power production in selected wind farms.
- Description of the practical experiences with WPPT in the control centres of the utilities.
- Description of the software system.

The report is organized as follows. Chapter 3 and 4 describes the data used in WPPT as well as the data collection system. The estimation methods, linear as well as non-linear, which are employed in the model study, are described in Chapter 5. The developed models as well as the results obtained are described in Chapter 6. Chapter 7 motivates the upscaling algorithm which is emloyed in WPPT. The methods applied by Elsam/Eltra when planning with the wind power are presented in Chapter 8 where also the experience gained by the operators in Elsam/Eltra's control centres are outlined. Finally Chapter 9 discusses the implementation of WPPT and describes briefly some parts of the user interface.

Chapter 3

Measurements

The wind power prediction tool (WPPT) is developed and implemented on the basis of power predictions at fourteen reference wind farms in the Jutland/Funen supply area. These fourteen wind farms have been selected in order to reflect the geographical distribution of wind power in the supply area. The siting of the fourteen wind farms are illustrated in Figure 3.1.

Among the fourteen reference wind farms five wind farms, Dræby Fedsodde, Fjaldene, Hollandsbjerg, Rejsby Hede and Sydthy Kabellaug are selected in order to establish a data foundation for further model development. The main criterion for selecting these five wind farms has been a high availability of the measured data, but it has also been of importance to ensure, that the selected wind farms are representative for the total rated wind power in the Elsam/Eltra supply area both with respect to geographical distribution as well as wind turbine technology.

In Section 3.1 the measurements available at the reference wind farms and the equipment involved in the data collection are described, further details regarding the five wind farms selected for the model study are found in Section 3.2 and finally the corrective actions performed to remove erroneous data values are explained in Section 3.3.

3.1 Description of measured data

WPPT rely on the availability of on-line measurements of power production and meteorological variables for the reference wind farms. For each of the fourteen reference wind farms the following five measurements are collected on-line:

- *Wind speed 1 and 2* $[m/s]$. For most of the reference wind farms the measurements of wind speed are established utilizing one anemometer per measurement. The exception is the measurement of wind speed 1 at the Hollandsbjerg and Torrild wind farms, where the recorded value is constructed as the average of readings from two anemometers sited in opposite ends of the wind farm(s). For all wind farms the anemometers are placed in one or more meteorology towers which in all cases are sited within 1 km from the nearest wind turbine. It should be noted, though, that the power measurement for some of the wind farms covers wind turbines with a considerable geographical distribution.

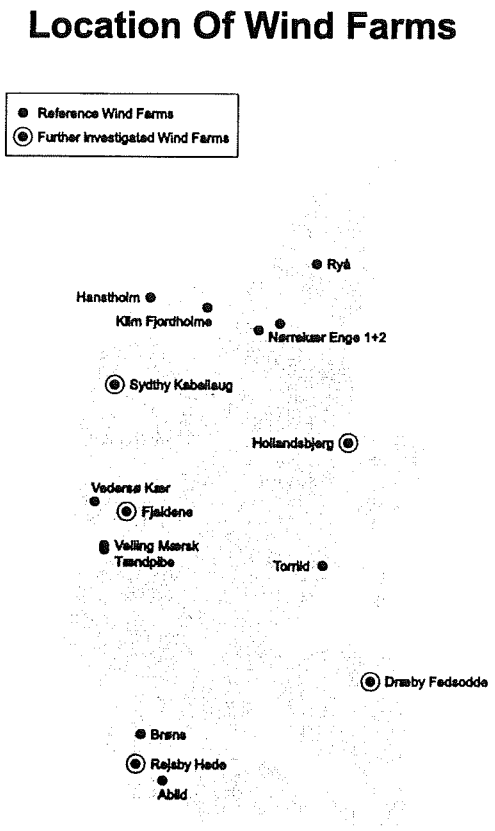

Figure 3.1: *The fourteen reference wind farms marked by a dot. The five wind farms selected for further scrutiny is marked by a surrounding circle.*

Furthermore none of the anemometers are placed so high above ground level that they can be assumed to be unaffected by shading effects from wind turbines in the vicinity.

- *Wind direction* [°]. The wind direction is in all cases except for Rejsby measured through a transducer in connection with the anemometer related to the wind speed 2 measurement.

- *Ambient air temperature* [$°C$]. The ambient air temperature is measured from either the meteorology tower or from a north facing wall on the control station for the wind farm. The transducer is typically placed a couple of meters above ground level.

- *Power production* [kW]. The power production in the wind farm is measured just before the accounting point for energy supplied to the grid. Hence the power measurement is independent of internal wiring in the wind farm and is presumed to give a reliable representation of the actual power production for the wind farm.

The data communication between the central SCADA[1] system running at Eltra and the data retrieval equipment installed in the reference wind farms is established through the

[1]System Control And Data Acquisition.

technical network operated by TeleDanmark[2]. The SCADA system running at the Eltra Dispatch Center is a Becos 32 system for which the host station is based on Alpha/VMS.

All measurements are integrated locally to form 5 minute average values, which are transmitted to the host station every 5 minutes. The models developed later in this study are based on 30 minute (average) values. It is therefore necessary to change the sampling period of the measurements by sub-sampling the 5 minute average values to 30 minute values. The 30 minute values is calculated as the average of the preceding 6 5 minute values[3]. The sub-sampling is performed by WPPT.

3.2 Description of the selected wind farms

The layout of the five wind farms selected for further investigation as well as the measurement equipment installed in the wind farms are described in the following sections. Furthermore some summary statistics as well as an overview of the availability of the measurements is presented for each of the five wind farms.

3.2.1 The Dræby wind farm

The Dræby wind farm is situated on the north coast of a small point (Fedsodde) in Odense Fjord, a inlet on the north coast of Funen (See Figure 3.1). The wind farm consists of 12 Wind World 220 kW (total rated power 2.64 MW – hub height 31 m) wind turbines located within an area of approximately 1.5 kilometers. The layout of the wind farm is depicted in Figure A.1. The wind farms was put into operation in 1991.

The data set covers the period from the 26th of May 1997 to the 17th of May 1998. The measurement equipment is configured as follows:

- *Meteorological tower.* The tower is located south west of the wind farm approximate 10 m from the host station. The two wind speeds as well as the wind direction are measured from the tower approximately 25 m above the ground.
- *Wind speed 1.* The anemometer of type Penny & Giles is positioned southerly on a sliding bar. The bar is positioned in the direction north north east - south south west.
- *Wind speed 2.* The anemometer of type Penny & Giles is positioned northerly on the sliding bar.
- *Wind direction.* Measured by anemometer 2.
- *Temperature transducer.* Positioned on north facing wall approximately 2 m above ground level.

An overview over the measurements from the Dræby wind farm is found in Table 3.1.

[2]TeleDanmark is the major telecommunication operator in Denmark.

[3]The 30 minute value given at, say 11 am., is the average of the 5 minute values from 10:35 to 11:00.

Obs.	Unit	Mean	Min.	Max.	No. NA
w_1	[m/s]	4.0	-0.2	15.3	20199
w_2	[m/s]	4.3	-0.5	16.3	157
θ	[°]	-	-	-	307
T_a	[°C]	9.6	-8.5	31.8	178
p	[kW]	399	-79	3002	85

Table 3.1: *Mean, minimum, maximum and number of erroneous or missing observations for wind speed 1 (w_1) and 2 (w_2), wind direction (θ), ambient air temperature (T_a) and power production (p) at the Dræby wind farm. The large difference in estimated mean value for the two anemometers is most likely due to a long period of missing observations for anemometer 1 covering most of the first quarter of 1998. The total number of observations is 102815.*

3.2.2 The Fjaldene wind farm

The Fjaldene wind farm is sited approximately 28 km inland from the west coast of Jutland some 20 km north-east of Ringkøbing Fjord. The wind farm consists of 18 Vestas V39 500 kW (total rated power 9.0 MW – hub height 42 m) wind turbines located within an area of 1.5 kilometers. Figure A.3 in shows the layout of the Fjaldene wind farm. The wind farm was put into operation in 1995.

The data set covers the period from the 26th of May 1997 to the 17th of May 1998. The measurement equipment is configured as follows:

- *Meteorological tower.* The tower is located in the middle of the wind farm 3 m from the station.The two wind speeds as well as the wind direction are measured from the tower approximately 32 m above the ground.
- *Wind speed 1.* The anemometer of type Penny & Giles is positioned southerly on a sliding bar. The bar is oriented in a north-south direction.
- *Wind speed 2.* The anemometer of type Penny & Giles is positioned northerly on the sliding bar.
- *Wind direction.* Measured by anemometer 2.
- *Temperature transducer.* Positioned on the tower 2 m above ground level.

An overview of the measurements from the Fjaldene wind farm is found in Table 3.2.

3.2.3 The Hollandsbjerg wind farm

The Hollandsbjerg wind farm is located next to Randers Fjord, an inlet on the east coast of Jutland, some 10 km inland from the shore line of the east cost (See Figure 3.1). The wind farm is equipped with 30 Nordtank 130 kW wind turbines and 2 Nordtank 300 kW turbines (total rated power 4.5 MW – hub height 26 m and 31 m, respectively) located within an area of approximately 2 kilometers. Figure A.5 in shows the layout of the Hollandsbjerg wind farm. The wind farm was put into operation in 1989.

The data set covers the period from the 26th of May 1997 to the 17th of May 1998. The measurement equipment is configured as follows:

Obs.	Unit	Mean	Min.	Max.	No. NA
w_1	[m/s]	4.4	-0.5	16.6	41395
w_2	[m/s]	4.6	-0.5	18.7	5033
T_a	[°C]	9.3	-7.1	31.7	5055
θ	[°]	-	-	-	5189
p	[kW]	1896	-94	8593	103

Table 3.2: *Mean, minimum, maximum and number of erroneous or missing observations for wind speed 1 (w_1) and 2 (w_2), wind direction (θ), ambient air temperature (T_a) and power production (p) at the Fjaldene wind farm. The large difference in estimated mean value for the two anemometers is most likely due to the fact that the observations for anemometer 1 are missing from Christmas 1997 and onwards. The total number of observations is 102815.*

- *Meteorological towers.* The wind farm has three meteorological towers. Tower 1 is located in the eastern part of the wind farm, tower 2 in the north western part and tower 3 in the middle of the wind farm 5 m from the station.
- *Wind speed 1.* Wind speed measurement 1 is calculated as the average of two measurements recorded in tower 1 and 2. The anemometers of type Malling are positioned on bars and have a hub height of 25.8 m above ground level.
- *Wind speed 2.* The anemometer of type Penny & Giles is placed in tower 3 on the top of a vertical pole and has a hub height of 13 m above ground level.
- *Wind direction.* Measured by anemometer 2.
- *Temperature transducer.* Positioned on tower 1 approximately 3 m above ground level.

An overview of the measurements from the Hollandsbjerg wind farm is found in Table 3.3.

Obs.	Unit	Mean	Min.	Max.	No. NA
w_1	[m/s]	4.7	0.0	21.2	14463
w_2	[m/s]	3.5	-0.5	15.6	15351
T_a	[°C]	9.0	-8.2	30.4	7317
θ	[°]	-	-	-	5707
p	[kW]	522	-216	4263	3569

Table 3.3: *Mean, minimum, maximum and number of erroneous or missing observations for wind speed 1 (w_1) and 2 (w_2), wind direction (θ), ambient air temperature (T_a) and power production (p) at the Hollandsbjerg wind farm. The difference between the estimated mean for the two wind speed measurements is only to be expected when the differences in measurement equipment and siting is taken into consideration. The total number of observations is 102815.*

3.2.4 The Rejsby Hede wind farm

The Rejsby Hede wind farms is situated on the west coast of Jutland some 1.5 km inland from the shore line (See Figure 3.1). The wind farm consists of 40 Micon M1500 600/150 kW

wind turbines (total rated power 24.0 MW – hub height 46 m) located within approximately 2.5 kilometers. The layout of the Rejsby wind farm is shown in Figure A.7. The wind farm was put into operation in 1995.

The data set covers the period from the 26th of May 1997 to the 17th of May 1998. The measurement equipment is configured as follows:

- *Meteorological tower.* The tower is located 500 m west of the wind farm and 1.5 km from the station. The two wind speeds and the wind direction are measured from the tower.
- *Wind speed 1.* The anemometer of type DNI 9501 is placed on top of lattice tower and has a hub height of 46 m.
- *Wind speed 2.* The anemometer of type WSI 0141 is placed on a bar and has a hub height of 45 m.
- *Wind direction.* Measured by separate anemometer next to anemometer 1.
- *Temperature transducer.* Positioned on north facing gable end 2.5 m above the ground.

An overview of the measurements from the Rejsby wind farm is found in Table 3.4.

Obs.	Unit	Mean	Min.	Max.	No. NA
w_1	[m/s]	7.5	0.0	28.6	14606
w_2	[m/s]	6.7	0.0	28.3	14620
T_a	[°C]	9.6	-9.6	31.8	236
θ	[°]	-	-	-	14805
p	[kW]	6079	-400	25870	615

Table 3.4: *Mean, minimum, maximum and number of erroneous or missing observations for wind speed 1 (w_1) and 2 (w_2), wind direction (θ), ambient air temperature (T_a) and power production (p) at the Rejsby wind farm. The large difference between the estimated mean for the two wind speed measurements must be due to either the difference in measurement equipment or shading effects from the meteorological tower. The total number of observations is 102815.*

3.2.5 The Sydthy Kabellaug wind farm

The Sydthy Kabellaug wind farm is located on the west coast of Jutland on the shoreline of Nissum Bredning (See Figure 3.1). It is not a wind farm in the traditional sense but more a collection of independently owned wind turbines sharing a common power line, which explains the rather casual layout of the wind farm revealed in Figure A.9. The wind farm consists in total of 26 wind turbines: 23 Vestas V27 225 kW turbines, 1 Vestas V39 500 kW turbine and 2 Vestas V42 600 kW (total rated power 6.875 MW – hub height 32 m, 41 m and 41 m, respectively), located within approximately 5 kilometers.

The data set covers the period from the 11th of July 1997 to the 17th of May 1998. The measurement equipment is configured as follows:

- *Meteorological tower.* The tower is located north east of the wind farm 15 m from the station.The two wind speeds as well as the wind direction are measured from the tower approximately 20 m above the ground.
- *Wind speed 1.* The anemometer of type Penny & Giles is positioned easterly on a sliding bar. The bar is oriented east-west.
- *Wind speed 2.* The anemometer of type Penny & Giles is positioned westerly on the sliding bar.
- *Wind direction.* Measured by anemometer 2.
- *Temperature transducer.* Positioned on north facing wall approximately 3 m above ground level.

An overview of the measurements from the Sydthy wind farm is found in Table 3.5.

Obs.	Unit	Mean	Min.	Max.	No. NA
w_1	[m/s]	4.5	-0.1	15.7	404
w_2	[m/s]	4.3	-0.3	15.5	453
T_a	[°C]	8.6	-6.7	32.3	402
θ	[°]	-	-	-	759
p	[kW]	2058	-270	6456	1266

Table 3.5: *Mean, minimum, maximum and number of erroneous or missing observations for wind speed 1 (w_1) and 2 (w_2), wind direction (θ), ambient air temperature (T_a) and power production (p) at the Sydthy wind farm. The large difference between the estimated mean for the two wind speed measurements must be due inaccuracies in the zero point calibration of the measurement equipments as the difference is found between mean, minimum and maximum for the two measurements is the same in all three cases. The total number of observations is 89567.*

3.3 Correction of measured data

The figures in Appendix B show plots of the two wind speeds, wind direction, power production and ambient air temperature for the selected five wind farms. The figures reveal, that different kinds of errors are present in data:

- *Periods with missing values.* Only very few observations have been missing from the data set.
- *Single extreme values.* A few single extreme values are present in the data set but, as they are easily detected and removed, they do not constitute a problem in the modelling.
- *Periods with erroneous constant measurement.* The data set contains several periods where measurements have remained constant for a longer period of time. The only measurements which are expected to remain constant for longer periods of time are

those of wind speed and especially power production where constant readings close to zero will occur in periods with very low wind speed. For wind direction and ambient air temperature these periods are easily detected but the measurement equipment for wind speed and power production are unfortunately constructed so that most situations with erroneous constant measurements lead to readings close to zero. This makes it difficult to distinguish between periods with low wind speed and periods with erroneous constant wind speed and/or power production.

- *Periods with unreliable wind speed measurements.* The data set contains several long periods where the wind speed readings are either constant or systematically too low. Most of the installed anemometers have been supplied by Penny & Giles and the cause for the aforementioned problems has in many cases been that the bearings used in these anemometers are of a poor quality leading to premature failure. In these situations the increased friction in the anemometers manifests it self as sticktion for low wind speeds and/or too low readings for higher wind speeds.

- *Periods with unreliable power production measurements.* These are few and, with the exception of Hollandsbjerg, of short duration, say 1 to 2 samples. The experiences gathered during this project indicate that measurements of the power production based on the accounting system can be considered very reliable. During periods with extreme wind speeds, where the wind turbines reduce the production, it can be difficult/impossible to estimate a reliable relationship between observed values of wind speed and power production as the power production will depend on unmeasured phenomena such as guests in the wind. Consequently the power production during these periods are treated as erroneous even though there is nothing wrong with the actual measurements.

- *Erroneous wind direction.* The wind direction has for most of the wind farms been measured through a wind vane built into the Penny & Giles anemometers. The first batch of anemometers installed in the wind farms was affected by a construction error allowing the wind direction measurement to change back and forth between 360 °and 0 °. As the wind direction is collected as an average value this leads to erroneous readings for northerly wind directions. This error was rectified during autumn 1998 where a new batch of anemometers with hysteresis build into the wind direction measurement was installed in the wind farms. For some of the wind farms periods with excessive noise on the wind direction measurement have been observed (See e.g. Hollandsbjerg in the period from the 7th of November 1997 to the 12th of January 1998, Figure B.22 to B.24). The cause of this phenomena has not been clarified.

The dubious observations have been removed from the data set using the procedure outlined in the following:

1. Periods with missing observations are identified using time stamps associated with the individual observations.

2. Single extreme values are identified by visual inspection and removed.

3. Periods with constant readings are identified by visual inspection and removed from the data set. For power production and wind speeds scatter plots of power production versus the two wind speeds is a very useful tool in this connection.

4. Unreliable measurements are identified using model based statistics. Statistical models describing the correlation within a time series or the relationship between different time series are estimated and the observations which give rise to large residuals are selected for further scrutiny and rejected if deemed unreliable. The following models have been employed in this context:

   - Power curve models describing the relationship between power production and wind speed.
   - The Kalman filter has been used to reconstruct the wind direction measurement in situations where it has been corrupted by the inexpedient construction of the wind direction measurement equipment prior to the upgrade of aforementioned equipment.

After missing or erroneous observations have been identified and marked as being unavailable the remaining data set has been sub-sampled to form 30 minute values.

Chapter 4

Meteorological data

The forecasts used in this study are provided by the Danish Meteorological Institute (DMI). DMI is running a regional atmospheric forecasting system based on the HIgh Resolution Limited Area Model (HIRLAM) system. For further details refer to [Landberg et al., 1994] or [Landberg et al., 1997].

4.1 Data Description

The forecasts used in this study are provided by the so called "fine scale model" (the DKV model) - a sub model within the HIRLAM modelling system. The DKV model covers most of west Europe with a horizontal resolution of approximately $17km$ and a vertical resolution in 31 model layers ranging from approximately $1km$ above ground level and downwards[1]. The forecasts used here are from model level 30 and 31 corresponding to $104m$ and $32m$, respectively, above ground level. These forecasts give an area wind speed without any corrections for the effect of local conditions such as trees or buildings.

DMI provide local forecasts for each of the fourteen reference wind farms. As the forecasts are calculated in a grid with a horizontal resolution of $17km$, it has been necessary for DMI to calculate intermediate values for the reference wind farms. These calculations are based on a simple linear interpolation scheme between the grid points.

The forecasts provided by DMI are updated 4 times a day with calculations initiated at 00, 06, 12 and 18 UTC. Each forecast update covers a period from 0 to 48 hours ahead starting at the time of initiation (00, 06, 12 and 18 UTC) and in steps of 1 hour. The 0 hour "forecast" is also called the analysis.

An full update of the HIRLAM model is a substantial task and calculation as well as validation of the forecasts will normally be finished in just above 2 hours. This means, that the forecasts are delivered to Eltra (by e-mail) just after 02, 08, 14 and 20 UTC. Considering that the 48 hour forecasts are updated with 6 hours intervals and allowing for some time slack in the calculations and data transmission, this leads to an effective forecast horizon[2] of 39 hours, which also is the prediction horizon used in WPPT.

The meteorological forecasts are only updated 4 times a day implying, that a time series

[1]The actual height of the model layers are pressure dependent.

[2]By effective forecast horizon is meant the minimum forecasting horizon available at any time of day.

consisting entirely of values for a given forecast horizon only has 4 "observations" per day. It is a requirement for the modelling scheme applied in WPPT, that the various input time series have a common and equidistant time period. In the case of WPPT a time period of 30 minutes has been chosen. In order to convert the raw HIRLAM forecasts to 79 equidistant time series with a time period of 30 minutes which each contains a forecast horizon from 0 to 39 hour in steps of 30 minute the interpolation scheme described in Section 6.4.2 is applied.

Plots of forecasted wind speed and wind direction are provided in Appendix C for some selected forecast horizons.

4.2 Data Correction

The meteorological forecasts have been checked for missing updates. The inspection revealed that only 21 updates are missing from the data set. In Table 4.1 the missing updates are denoted by their UTC time.

Update time			
1997-05-26 00:00			1997-05-26 18:00
	1997-06-09 06:00		
			1997-08-11 18:00
			1997-08-25 18:00
		1997-09-01 12:00	1997-09-01 18:00
1997-09-13 00:00	1997-09-13 06:00		
		1997-09-28 12:00	1997-09-28 18:00
			1997-09-29 18:00
			1997-09-30 18:00
		1997-12-13 12:00	1997-12-13 18:00
1997-12-14 00:00	1997-12-14 06:00	1997-12-14 12:00	
			1998-01-24 18:00
			1998-03-07 18:00
1998-04-04 00:00			

Table 4.1: *Missing updates in the data set generated by the meteorological weather model.*

As only very few updates are missing in the data set DMI has not been asked to fill in the missing updates, which instead have been marked as not available.

Chapter 5

Estimation methods

This chapter presents the model classes and estimation methods applied in the modelling and prediction of power production in a wind farm.

Two different approaches exist for estimation of parameters in a model. One possibility is to estimate the parameters using an off-line technique. The advantage of this approach is that it is possible to estimate models being linear as well as non-linear in the parameters. The disadvantage is that whenever new data becomes available the model has to be re-estimated on the full set of data.

Another possibility is recursive or on-line estimation. For this approach the model parameters are estimated in a sequential manner enabling new data to be included in the parameter estimation without having to reestimate the parameters on the entire set of data. Compared to off-line estimation this leads to considerable savings in computational effort. A further advantage of the on-line estimation approach is that the estimation rather easily can be made adaptive. This enables the model to adjust to slow changes in the system, which often is of great importance in on-line applications.

The drawback of the recursive methods is, however, that it can not be guaranteed, that the estimated parameters will converge towards the true values for non-linear models. Hence for practical purposes it is not considered desirable to use recursive methods for models being non-linear in the parameters.

The estimation of models being non-linear in the parameters give rise to further difficulties in on-line applications. Most often the non-linear estimation problem has no closed form solution, and a solution has to be found by numerical optimization. This implies, that it is difficult to guaranty, that a solution always can be found within a sampling period - a requirement for on-line deployment.

For the reasons stated above traditional non-linear models are not well suited for on-line applications and have thus not been considered further in this study. Instead non-linear relationships have been estimated using local regression and conditional parametric models, for which the estimation problem has close resemblance to that known from ordinary linear models.

For ordinary linear models the off-line and on-line estimation methods are described in Section 5.1 and the similar topics are covered in Section 5.2 for conditional parametric models. Section 5.3 introduces some standard statistical performance measures as well as some measures specifically related to prediction models and finally Section 5.4 introduces

the notion of overfitting and describes how the problem can be avoided.

5.1 Linear models

5.1.1 Off-line estimation for linear models

A linear regression model is a model, where the expected value of a response variable can be written as a linear function of some explanatory variables

$$Ey_s = \mathbf{x}_s^T \boldsymbol{\theta} \tag{5.1}$$

Here Ey_s is the expected value of the response (or dependent) variable at time s, $\mathbf{x}_s$ is a vector containing the explanatory (or independent) variables at time s, and $\boldsymbol{\theta}$ is the parameter vector. Assuming that observations at time $s = 1, \ldots, t$ are available, the unweighted least squares (LS) estimate of $\boldsymbol{\theta}$ is given as

$$\hat{\boldsymbol{\theta}} = \underset{\boldsymbol{\theta}}{\text{Argmin}} \sum_{s=1}^{t} \left(y_s - \mathbf{x}_s^T \boldsymbol{\theta}\right)^2 \tag{5.2}$$

Using matrix notation (5.2) can be written

$$\hat{\boldsymbol{\theta}} = \underset{\boldsymbol{\theta}}{\text{Argmin}} \, (\mathbf{y} - \mathbf{X}\boldsymbol{\theta})^T (\mathbf{y} - \mathbf{X}\boldsymbol{\theta}) \tag{5.3}$$

where $\mathbf{y} = [y_1 \ \ldots y_t]^T$ is a vector of the observations and

$$\mathbf{X} = \begin{bmatrix} \mathbf{x}_1^T \\ \vdots \\ \mathbf{x}_t^T \end{bmatrix}$$

is a (design) matrix, where row s is equal to $\mathbf{x}_s^T$. It is easily shown (see e.g. [Ljung, 1987]), that the solution to (5.3) is written explicitly as

$$\hat{\boldsymbol{\theta}} = \left(\mathbf{X}^T\mathbf{X}\right)^{-1} \mathbf{X}^T\mathbf{y} \tag{5.4}$$

5.1.2 On-line estimation for linear models

In many applications it is useful or even necessary to implement a model as (5.1), where the model parameters are updated on-line as the observations become available. If the parameters have to be estimated using (5.4), this implies, that the parameters have to be re-estimated using the entire and forever growing data set. It is clear, that ultimately such an update scheme must fail. A recursive version of (5.4) is easily derived though. Using the matrix multiplication rules the estimate corresponding to (5.4) at time t may be written as

$$\hat{\boldsymbol{\theta}}_t = \left[\sum_{s=1}^{t} \mathbf{x}_s \mathbf{x}_s^t\right]^{-1} \sum_{s=1}^{T} \mathbf{x}_s \mathbf{y}_s \tag{5.5}$$

Now introduce

$$\begin{aligned}\mathbf{R}_t &= \sum_{s=1}^{t} \mathbf{x}_s \mathbf{x}_s^T \\ \mathbf{f}_t &= \sum_{s=1}^{T} \mathbf{x}_s y_s\end{aligned}$$

into (5.5) and consider the update from $t-1$ to t

$$\begin{aligned}\hat{\boldsymbol{\theta}}_t &= \mathbf{R}_t^{-1}\mathbf{f}_t \\ &= \mathbf{R}_t^{-1}\left[\mathbf{f}_{t-1} + \mathbf{x}_t\, y_t\right] \\ &= \mathbf{R}_t^{-1}\left[\mathbf{R}_{t-1}\hat{\boldsymbol{\theta}}_{t-1} + \mathbf{x}_t y_t\right] \\ &= \mathbf{R}_t^{-1}\left[\left(\mathbf{R}_t - \mathbf{x}_t\mathbf{x}_t^T\right)\hat{\boldsymbol{\theta}}_{t-1} + \mathbf{x}_t\, y_t\right] \\ &= \hat{\boldsymbol{\theta}}_{t-1} + \mathbf{R}_t^{-1}\mathbf{x}_t\left[y_t - \mathbf{x}_t^T\hat{\boldsymbol{\theta}}_{t-1}\right]\end{aligned}$$

The recursive least squares (RLS) algorithm can thus be summarized as

$$\begin{aligned}\mathbf{R}_t &= \mathbf{R}_{t-1} + \mathbf{x}_t\mathbf{x}_t^T \\ \hat{\boldsymbol{\theta}}_t &= \hat{\boldsymbol{\theta}}_{t-1} + \mathbf{R}_t^{-1}\mathbf{x}_t\left[y_t - \mathbf{x}_t^T\hat{\boldsymbol{\theta}}_{t-1}\right]\end{aligned} \tag{5.6}$$

The algorithm has to be initialized. The initial estimates may be chosen quite arbitrarily – often zero is used. The initial values of $\mathbf{R}$ has to be chosen in such a way, that the matrix is invertible and the covariance of the initial estimates large – often $\mathbf{R}_0$ is selected as a diagonal matrix with all elements on the diagonal set to $\frac{1}{100}$ or $\frac{1}{1000}$.

It is often advantageous to allow the model parameters to change slowly over time or in other words let the parameter estimation become adaptive. One frequently used adaptive estimation scheme – least squares with exponential forgetting – is established by introducing an exponential weighting of the squared residuals in the LS estimation criterion (5.2) as

$$\hat{\boldsymbol{\theta}} = \underset{\boldsymbol{\theta}}{\text{Argmin}} \sum_{s=1}^{t} \lambda^{t-s}\left(y_s - \mathbf{x}_s^T\boldsymbol{\theta}\right)^2 \tag{5.7}$$

where λ is a forgetting factor ($0 < \lambda \leq 1$). The exponential weights allow the influence of an observation to tail off as the observation becomes (grows) older.

The choice of the forgetting factor λ is determined by a trade-off between the needed ability to track time-varying parameters and the noise sensitivity of the estimate. A low value of λ results in a system with a good ability to track time-varying parameters, but a higher sensitivity against noise in the data. A typical choice of λ is in the range $0.95 \leq \lambda \leq 0.999$. The effective number of observations is given as

$$\begin{aligned}N_{eff} &= \sum_{i=0}^{\infty}\lambda^i \\ &\approx \frac{1}{1-\lambda}\end{aligned} \tag{5.8}$$

The effective number of observations is also know as the memory time constant. Notice that for $\lambda = 1$ the LS criterion in (5.2) is obtained.

As for the recursive least squares algorithm the recursive formulation of the solution to (5.7) is easily deduced - for details see e.g. [Ljung, 1987]. Without proof the adaptive least squares algorithm is stated as

$$\begin{aligned} \hat{\boldsymbol{\theta}}_t &= \hat{\boldsymbol{\theta}}_{t-1} + \mathbf{R}_t^{-1}\mathbf{x}_t \left[y_t - \mathbf{x}_t^T \hat{\boldsymbol{\theta}}_{t-1} \right] \\ \mathbf{R}_t &= \lambda \mathbf{R}_{t-1} + \mathbf{x}_t \mathbf{x}_t^T \end{aligned} \tag{5.9}$$

As it is seen from (5.9), the 1-step prediction error $(y_t - \mathbf{x}_t^T \hat{\boldsymbol{\theta}}_{t-1})$ is used in the update of the parameter estimates. If a prediction horizon larger than one is applied, a choice between two alternative ways of updating the estimates must be made:

- The estimates $\hat{\boldsymbol{\theta}}_{t-k}$ and the regressors $\mathbf{x}_{t-k+1}$ are used instead of $\hat{\boldsymbol{\theta}}_{t-1}$ and $\mathbf{x}_t$ in the algorithm described above, or
- pseudo prediction errors are used in the update of estimates. The pseudo prediction error at time t is calculated as

$$\tilde{y}_{t|t-k}^{pseudo} = y_t - \mathbf{x}_{t-k}^T \hat{\boldsymbol{\theta}}_{t-1}, \tag{5.10}$$

  from this equation it is seen that the pseudo prediction error corresponds to variables known at time $t-k$ (i.e. $\mathbf{x}_{t-k}$) and the most recent estimates (i.e. $\hat{\boldsymbol{\theta}}_{t-1}$).

In both cases the true k-step prediction is calculated as

$$\hat{y}(t+k|t) = \mathbf{x}_{t+k}^T \hat{\boldsymbol{\theta}}_t.$$

In this study the latter approach for updating the parameter estimates is applied. Using the true k-step prediction error in the update of the most recent estimates will result in highly inappropriate estimates. This is due to the fact, that the prediction error will give a feed-back not corresponding to the estimates, which are being updated.

5.2 Non-linear models

In this study conditional parametric models are used to estimate non-linear relationships, for which the exact parametric form is unknown. The conditional parametric model is the well known linear regression model (5.1) in which the parameters are replaced by smooth, but otherwise unknown functions of one or more explanatory variables. These functions are called coefficient-functions. The estimation method for the classical case, where the coefficient functions are considered constant over time, is described in Section 5.2.1. For on-line applications it is advantageous to allow the function estimates to be modified as data become available. Furthermore, because the system may change slowly over time, observations should be down-weighted as they become older. For this reason an adaptive and recursive procedure which is a combination of the adaptive recursive least squares method [Ljung, 1987] and locally weighted polynomial regression [Cleveland and Devlin, 1988] has been proposed in [Nielsen et al., 1999a]. This new method for on-line estimation in non-linear systems is outlined in Section 5.2.2.

5.2.1 Off-line estimation for non-linear models

This section describes non-adaptive estimation in conditional parametric models. The model is of the form

$$y_s = \mathbf{x}_s^T \boldsymbol{\theta}(\mathbf{u}_s) + e_s; \quad s = 1, \ldots, N, \tag{5.11}$$

where the response y_s is a stochastic variable, $\mathbf{u}_s$ and $\mathbf{x}_s$ are explanatory variables, e_s is i.i.d. $N(0, \sigma^2)$, $\boldsymbol{\theta}(\cdot)$ is a vector of unknown but smooth functions with values in $\mathbb{R}^p$, and $s = 1, \ldots, N$ are observation numbers. When $\mathbf{u}_s$ is constant across observations the model reduces to a linear model, hereof the name.

Estimation in (5.11) aims at estimating the functions $\boldsymbol{\theta}(\cdot)$ within the space spanned by the observations of $\mathbf{u}_s$; $s = 1, \ldots, N$. The functions are only estimated for distinct values of the argument $\mathbf{u}$. Below $\mathbf{u}$ denotes one single of these fitting points and $\hat{\boldsymbol{\theta}}(\mathbf{u})$ denotes the estimates of the coefficient-functions, when the functions are evaluated at $\mathbf{u}$.

One solution to the estimation problem is to replace $\boldsymbol{\theta}(\mathbf{u}_s)$ in (5.11) with a constant vector $\boldsymbol{\theta}_u$ and fit the resulting model locally to $\mathbf{u}$, using weighted least squares. Below two similar methods of allocating weights to the observations are described. For both methods the weight function $W : \mathbb{R}_0 \to \mathbb{R}_0$ is a nowhere increasing function. In this study the tri-cube weight function

$$W(u) = \begin{cases} (1 - u^3)^3, & u \in [0; 1] \\ 0, & u \in [1; \infty[\end{cases}$$

is used. Hence, $W : \mathbb{R}_0 \to [0, 1]$

In the case of a spherical kernel the weight on observation s is determined by the Euclidean distance $||\mathbf{u}_s - \mathbf{u}||$ between $\mathbf{u}_s$ and $\mathbf{u}$, i.e.

$$w_s(\mathbf{u}) = W\left(\frac{||\mathbf{u}_s - \mathbf{u}||}{\hbar(\mathbf{u})}\right).$$

A product kernel is characterized by distances being calculated for one dimension at a time, i.e.

$$w_s(\mathbf{u}) = \prod_j W\left(\frac{|u_{j,s} - u_j|}{\hbar(\mathbf{u})}\right),$$

where the multiplication is over the dimensions of $\mathbf{u}$. The scalar $\hbar(\mathbf{u}) > 0$ is called the bandwidth. If $\hbar(\mathbf{u})$ is constant for all values of $\mathbf{u}$ it is denoted a fixed bandwidth. If $\hbar(\mathbf{u})$ is chosen so that a certain fraction (α) of the observations fulfill $||\mathbf{u}_s - \mathbf{u}|| \leq \hbar(\mathbf{u})$ it is denoted a nearest neighbor bandwidth. If $\mathbf{u}$ has the dimension two or larger, scaling of the individual elements of $\mathbf{u}_s$ before applying the method should be considered, see e.g. [Cleveland and Devlin, 1988]. Rotating the coordinate system in which $\mathbf{u}_s$ is measured may also be relevant. In this study only models with one-dimensional $\mathbf{u}$ is considered though in which case the spherical kernel is equal to the product kernel.

If the bandwidth $\hbar(\mathbf{u})$ is sufficiently small the approximation of $\boldsymbol{\theta}(\cdot)$ as a constant vector near $\mathbf{u}$ is good. This implies that a relatively low number of observations is used to estimate

$\boldsymbol{\theta}(\mathbf{u})$, resulting in a noisy estimate or large bias if the bandwidth is increased. See also the comments on kernel estimates in [Anderson et al., 1994].

It is, however, well known that locally to $\mathbf{u}$ the elements of $\boldsymbol{\theta}(\cdot)$ may be approximated by polynomials, and in many cases these will be good approximations for larger bandwidths than those corresponding to local constants. Local polynomial approximations are easily included in the method described. Let $\theta_j(\cdot)$ be the j'th element of $\boldsymbol{\theta}(\cdot)$ and let $\mathbf{p}_d(\mathbf{u})$ be a column vector of terms in a d-order polynomial evaluated at $\mathbf{u}$, if for instance $\mathbf{u} = [u_1\ u_2]^T$ then $\mathbf{p}_2(\mathbf{u}) = [1\ u_1\ u_2\ u_1^2\ u_1u_2\ u_2^2]^T$. Furthermore, let $\mathbf{x}_s = [x_{1s} \dots x_{ps}]^T$. With

$$\mathbf{z}_s^T = [x_{1s}\mathbf{p}_{d(1)}^T(\mathbf{u}_s) \dots x_{js}\mathbf{p}_{d(j)}^T(\mathbf{u}_s) \dots x_{ps}\mathbf{p}_{d(p)}^T(\mathbf{u}_s)]$$

and

$$\hat{\boldsymbol{\phi}}^T(\mathbf{u}) = [\hat{\boldsymbol{\phi}}_1^T(\mathbf{u}) \dots \hat{\boldsymbol{\phi}}_j^T(\mathbf{u}) \dots \hat{\boldsymbol{\phi}}_p^T(\mathbf{u})],$$

where $\hat{\boldsymbol{\phi}}_j(\mathbf{u})$ is a column vector of local constant estimates at $\mathbf{u}$ corresponding to $x_{js}\mathbf{p}_{d(j)}(\mathbf{u}_s)$, estimation is handled as described above, but fitting the linear model

$$y_s = \mathbf{z}_s^T\boldsymbol{\phi}_u + e_s; \quad s = 1, \dots, N,$$

locally to $\mathbf{u}$. Hereafter the elements of $\boldsymbol{\theta}(\mathbf{u})$ is estimated by

$$\hat{\theta}_j(\mathbf{u}) = \mathbf{p}_{d(j)}^T(\mathbf{u})\,\hat{\boldsymbol{\phi}}_j(\mathbf{u}); \quad j = 1, \dots p.$$

This method is identical to the method described in [Cleveland and Devlin, 1988] when $\mathbf{x}_j = 1$ for all j with the exception that in [Cleveland and Devlin, 1988] the elements of $\mathbf{u}_s$ used in $\mathbf{p}_d(\mathbf{u}_s)$ are centered around $\mathbf{u}$ and hence $\mathbf{p}_d(\mathbf{u}_s)$ must be recalculated for each value of $\mathbf{u}$ considered.

5.2.2 On-line estimation for non-linear models

The method is described as a generalization of exponential forgetting described in Section 5.1.2. Bringing (5.7) on matrix form and solving with respect to $\hat{\boldsymbol{\theta}}_t$ the explicit solution may be written as

$$\hat{\boldsymbol{\theta}}_t = \left(\mathbf{X}_t^T\boldsymbol{\Lambda}_t\mathbf{X}_t\right)^{-1}\mathbf{X}_t^T\boldsymbol{\Lambda}_t\mathbf{y}_t, \tag{5.12}$$

where $\boldsymbol{\Lambda}_t = \mathrm{diag}(\lambda^{t-1}, \lambda^{t-2}, \dots, \lambda, 1)$ is a diagonal weight matrix. When the estimator is written as the local (time) weighted least squares solution (5.12) this suggests that the estimator may also be defined locally to some other explanatory variables $\mathbf{u}_t$. If the estimates are defined locally to some fixed point $\mathbf{u}$ the adaptive estimate corresponding to this point can be expressed as

$$\hat{\boldsymbol{\theta}}_t(\mathbf{u}) = \left(\mathbf{X}_t^T\boldsymbol{\Lambda}_t\mathbf{W}_{ut}\mathbf{X}_t\right)^{-1}\mathbf{X}_t^T\boldsymbol{\Lambda}_t\mathbf{W}_{ut}\mathbf{y}_t, \tag{5.13}$$

where $\mathbf{W}_{ut} = \mathrm{diag}(w_u(\mathbf{u}_1), \dots, w_u(\mathbf{u}_t))$ is a diagonal weight matrix in which the weights depend on the observations $\mathbf{u}_s$; $s = 1, \dots, t$, see Section 5.2.1. Estimators like (5.13) can be applied in parallel to a number of fitting points $\mathbf{u}$ and hence it corresponds to adaptive

estimation in the model $Ey_s = \mathbf{x_s}^T\boldsymbol{\theta}(\mathbf{u}_s)$, i.e. the functions $\boldsymbol{\theta}(\mathbf{u})$ are estimated adaptively at a number of points. Interpolation is used, if the estimated function values are needed for other values of the argument(s).

It is clear that (5.13) is the solution to

$$\underset{\boldsymbol{\theta}}{\text{Min}} \sum_{s=1}^{t} \lambda^{t-s} w_u(\mathbf{u}_s)(y_s - \mathbf{x}_s^T\boldsymbol{\theta})^2.$$

Following (5.9) the solution can be found recursively as

$$\mathbf{R}_{u,t} = \lambda \mathbf{R}_{u,t-1} + w_u(\mathbf{u}_t)\mathbf{x}_t\mathbf{x}_t^T \tag{5.14}$$

and

$$\begin{aligned} \hat{\boldsymbol{\theta}}_t(\mathbf{u}) &= \hat{\boldsymbol{\theta}}_{t-1}(\mathbf{u}) + \\ & \quad w_u(\mathbf{u}_t)\mathbf{R}_{u,t}^{-1}\mathbf{x}_t \left[y_t - \mathbf{x}_t^T\hat{\boldsymbol{\theta}}_{t-1}(\mathbf{u})\right]. \end{aligned} \tag{5.15}$$

It is seen that existing numerical procedures can be applied by replacing $\mathbf{x}_t$ and y_t with $\mathbf{x}_t\sqrt{w_u(\mathbf{u}_t)}$ and $y_t\sqrt{w_u(\mathbf{u}_t)}$, respectively. Note that although $\mathbf{x}_t^T\hat{\boldsymbol{\theta}}_{t-1}(\mathbf{u})$ may be regarded as a predictor of y_t it is not very appropriate. If such a predictor is required we should first seek a predictor for $\mathbf{u}_t$ and use this instead of $\mathbf{u}$.

When $\mathbf{u}_t$ is far from $\mathbf{u}$ it is clear from (5.14) that $\mathbf{R}_{u,t} \approx \lambda\mathbf{R}_{u,t-1}$. This may result in abruptly changing estimates if $\mathbf{u}$ is not visited regularly. This is considered a serious practical problem and consequently (5.14) has to be modified to ensure that the past is weighted down only when new information become available, i.e.

$$\mathbf{R}_{u,t} = \lambda v(w_u(\mathbf{u}_t);\lambda)\mathbf{R}_{u,t-1} + w_u(\mathbf{u}_t)\mathbf{x}_t\mathbf{x}_t^T, \tag{5.16}$$

where $v(\cdot\,;\lambda)$ is a nowhere increasing function on $[0;1]$ fulfilling $v(0;\lambda) = 1/\lambda$ and $v(1;\lambda) = 1$. Note that this requires that the weights span the interval ranging from zero to one. Here only the linear function

$$v(w;\lambda) = 1/\lambda - (1/\lambda - 1)w,$$

is considered. Thus (5.16) becomes

$$\begin{aligned} \mathbf{R}_{u,t} &= (1 - (1-\lambda)w_u(\mathbf{u}_t))\mathbf{R}_{u,t-1} \\ & \quad + w_u(\mathbf{u}_t)\mathbf{x}_t\mathbf{x}_t^T. \end{aligned} \tag{5.17}$$

It is obvious to denote $1 - (1-\lambda)w_u(\mathbf{u}_t)$ the effective forgetting factor for point $\mathbf{u}$ at time t; $\lambda_{eff}^u(t)$.

5.3 Model evaluation measures

In order to evaluate the performance of the various models investigated in Chapter 6 some performance measures are needed. Section 5.3.1 introduces four standard statistical measures: mean error (ME), mean square error (MSE), error variance (SDE^2) and coefficient of determination (R^2). Section 5.3.2 presents two simple reference models which are of relevance for meteorological applications.

5.3.1 Some statistical performance measures

Estimated mean value and estimated variance (or variability) are two fundamental statistical measures used in characterizing a measured variable y, where y is assumed to be generated by a second order stationary process. The estimated mean value, $\bar{y}$, is given as

$$\bar{y} = \frac{1}{N}\sum_{i=1}^{N} y_i \tag{5.18}$$

where N is the number of observations and y_i is the observed value at time i. An unbiased estimate for the variance, s_y^2, for y is

$$s_y^2 = \frac{1}{N-1}\sum_{t=1}^{N}(y_i - \bar{y})^2 . \tag{5.19}$$

In order to obtain the estimated mean error (ME) and error variance for a given model simply substitute y_i in (5.18) and (5.19) with the estimated model error

$$\hat{e}_i = y_i - \hat{y}_i$$

where $\hat{y}_i$ is the model prediction at time i and get

$$\begin{aligned} ME &= \frac{1}{N}\sum_{i=1}^{N}\hat{e}_i \\ SDE^2 &= \frac{1}{N-1}\sum_{t=1}^{N}\left(\hat{e}_i - \bar{\hat{e}}\right)^2 . \end{aligned} \tag{5.20}$$

An often used model residual measure which also will be used in this study is mean square error (MSE)

$$MSE = \frac{1}{N}\sum_{t=1}^{N}\hat{e}_i^2. \tag{5.21}$$

The overall goodness of fit for a model can be evaluated using the coefficient of determination

$$R^2 = 1 - \frac{s_e^2}{s_y^2}. \tag{5.22}$$

The coefficient of determination is interpreted as the proportion of the observed variability in the dependent variable which is explained by a given model.

5.3.2 Two simple reference models

The naive (or persistent) predictor is often used as a reference model within meteorological application, when the performance of a particular models is to be evaluated. The persistent predictor is given as

$$\hat{y}_{t+k|t} = y_t \tag{5.23}$$

where $\hat{y}_{t+k|t}$ is the predicted value of process y at time $t+k$ given information up to time t. The persistent predictor simple states that the predicted future value of y is given as the currently observed value of y.

For shorter prediction horizons[1] the persistent predictor performs rather well but it is easily shown that as the correlation between y_{t+k} and y_t goes towards zero with increasing k the expected variance of the prediction error will be 2 times the variance of y.

For larger k comparing with the persistent predictor will thus tend to over-inflate the performance of a model. As a consequently a new statistical reference model has been proposed in [Nielsen et al., 1999b].

In this new reference model the predictions are calculated as a weighting between the persistence predictor and the mean predictor where the weighting for different prediction horizons is determined by the correlation between y_t and y_{t+k}. The predictor is given as

$$\begin{aligned} \hat{y}_{t+k|t} &= a_k y_t + (1-a_k)\bar{y} \\ a_k &= \frac{\sum_{t=1}^{N-k} \tilde{y}_t \tilde{y}_{t+k}}{\sum_{t=1}^{N-k} \tilde{y}_t^2} \\ \tilde{y}_t &= y_t - \bar{y} \end{aligned} \tag{5.24}$$

When considering the prediction performance over a wide range of prediction horizons it is demonstrated in [Nielsen et al., 1999b] that the new reference model give more reasonable results than either the persistence or the mean value predictor. It should also be noted that the new reference predictor does not require addition input compared to the persistence and mean predictors as well as being very simple to calculate.

5.4 Model selection

This section describes how the model selection between different model structures is carried out in the present study. In order to compare different model structures a performance measure has to be defined. In this study the coefficient of determination (R^2) will be used. This measure is, as it appears from Section 5.3.1, directly related to the much used mean square error criterion (MSE), but, as it is a relative measure, R^2 is better suited for making comparisons between the different wind farms than MSE. It should also be noted that using R^2 as the model selection and model evaluation criterion relates nicely with using Least Squares or Weighted Least Squares as the model parameter fit criterion.

When a model structure is fitted to a given data set using a global method, where a (global) parameter set is estimated on basis of the entire data set, the fit criterion will decrease monotonously as the model structure increases. In the beginning, when the increase in the model structure contributes in explaining relevant features in data, the decrease in fit criterion will be significant, but, as the model structure continues to increase, the extra flexibility will allow the model to adapt to specific features of the noise realization for this particular data set and the decrease in fit criterion will become less significant. This

[1] That is prediction horizons comparable with the characteristic time scale in the atmosphere. [Landberg et al., 1997] states the characteristic time scale in the atmosphere for wind phenomena to be approximate 3 hours.

phenomenon, where a model is extented with non-significant parameters, is known as "over-fitting". A widely used method to overcome this problem is known as Cross-validation. Here the available data set is separated in two: a data set used for model estimation and a data set used for validation of the estimated model. Thereby it is ensured that superfluous model structure will not account for any features of the specific noise realization in the validation set and thus that the validation criterion will not continue to decrease as the model size increases.

The estimation and validation data set should be independent as well as be consistent with respect to process dynamics. In this study this has been accomplished by allocating every second week of data to either the estimation set or the validation set. Hereby it is ensured that the two data sets are (almost) independent and at the same time that both data sets contain data from the entire year and thus exhibit the same process dynamics.

The problem of over-fitting at model structure is less obtrusive when the model estimation is based on recursive or local methods. Here the model prediction of the dependent variable at time t is calculated using a parameter estimate based on data up to time $t-1$. It is therefore not possible for any superfluous model parameters to adjust for the system error at time t, and thus the validation criterion will (normally) not decrease when superfluous parameters are included in the model.

Chapter 6

Models for predicting wind speed and power

The aim of this study is to investigate methods for predicting the total power production for the wind turbines in the western part of Denmark up to 39 hours ahead with a time resolution of 30 minutes. The approach taken is to model and predict the power production for fourteen reference wind farms and subsequently upscale the predictions for the reference wind farms to cover the entire area of Jutland and Funen.

This chapter presents results concerning the issue of modelling and predicting wind speed and power production in a wind farm, whereas the subject of upscaling is referred to Chapter 7. The present investigation forms the basis for selecting the prediction models implemented in the Wind Power Prediction Tool, WPPT.

In [H. Madsen (Ed.), 1995] power prediction models for wind farms based on local observations of power production and wind speed are investigated. The results obtained suggest, that for prediction horizons larger than 12 hours it is necessary to include meteorological forecasts of wind speed as input to the model, if a satisfactory performance is to be obtained. This has later been confirmed in [Nielsen and Madsen, 1996].

When employing meteorological forecasts and local observations of weather variables, primarily wind speed, in the modelling and prediction of power production for a wind farm two conceptually different approaches for establishing the power prediction models can be taken:

1. A model of the wind speed is used to calculate predictions of wind speed as a function of forecasted and observed weather variables. The wind speed predictions are then used as input to another model describing the relationship between wind speed and power production[1] in order to obtain predictions of power production. That is, the power predictions are obtained in a two stage approach, where the two models are estimated separately.

2. One model containg a description of both the correlation structure of wind speed and power production is used to obtain the power predictions. The relation between wind

[1]The relationship between wind speed and power production for a wind farm will be denoted the wind farm power curve. This relationship might include the influence of other weather variables, e.g. wind direction is an obvious candidate.

speed and power production can either be contained in the model or be estimated seperately.

Earlier findings in [H. Madsen (Ed.), 1995] and [Nielsen and Madsen, 1996] suggest, that the performance of the two stage models, where the correlations structure of the power observations is disregarded, generally are inferior to models taking this structure into account. Consequently the power prediction models considered in the present study all belong to the class of autoregressive models with exogenous input - a model class where the correlation structure between current and future values of the dependent (output) variable is modelled directly.

The analysis of power prediction in a wind farm presented in this chapter is divided into the following topics:

- The relationship between forecasted and observed wind speed for a given location is treated in Section 6.1. The analysis aims to determine, whether any dependency on prediction horizon is present in the statistical properties of the meteorological forecasts.
- The relationship between forecasted and observed wind direction is investigated in Section 6.2. It is also here considered, whether the relation between observed and forecasted wind direction is depending on the prediction horizon.
- The estimation of power curves for a wind farm is investigated in Section 6.4. Both power curve models with and without wind direction dependency are considered.
- The estimation of power prediction models for a wind farm is covered in Section 6.5.

In the subsequent sections the following nomenclature is used for the measured and forecasted variables at the five wind farms:

- t. The time index. The index denotes hourly values in Section 6.1 and 6.2 and half hourly values in Section 6.4 and 6.5. The two data sets are described in Section 6.1 and 6.4, respectively.
- w_t^1. The observed wind speed at time t for anemometer 1.
- w_t^2. The observed wind speed at time t for anemometer 2.
- w_t. The observed wind speed for anemometer 2 has throughout this study been used as the default wind speed. w_t will therefore be used as a reference to wind speed 2.
- ϕ_t. The observed wind direction at time t.
- p_t. The observed power production at time t.
- $w^m_{t+k|t}$. The forecasted wind speed from the national weather service for time $t+k$ given at time t.
- $\phi^m_{t+k|t}$. The forecasted wind direction from the national weather service for time $t+k$ given at time t.

- h_t^{24}. Time of day. At e.g. 01:00 PM h_t^{24} is equal to 13 hours.

The following abbreviations are used throughout the remaining sections:

- R^2. Coefficient of determination.
- *i.i.d.* Independent identical distributed.
- WF. Wind farm.
- DR. The Dræby wind farm.
- FJ. The Fjaldene wind farm.
- HO. The Hollandsbjerg wind farm.
- RB. The Rejsby wind farm.
- SY. The Sydthy wind farm.

6.1 Meteorological wind speed models

This section describes the initial investigation of the characteristics for the meteorological forecasts of wind speed provided by the HIRLAM forecasting model running at DMI. The meteorological data delivered by DMI for each of the five model wind farms consists, as described in Chapter 4, of forecasted wind speed and wind direction for the lowest and second lowest model layers in the HIRLAM model. Each forecast covers a period from 0 to 48 hours ahead in hourly steps and the forecasts are updated 4 times a day.

The aim of this investigation has been twofold:

- To evaluate whether the forecasts from HIRLAM model level 30 (second lowest layer $\sim$ 104 m above ground level) or level 31 (lowest layer $\sim$ 32 m above ground level) is the most appropriate for this application.
- To identify suitable models for the relation between observed wind speed and forecasted wind speed. One important consideration is here how the characteristics of the forecasted meteorological variables changes as a function of the prediction horizon.

The meteorological forecasts used in this section are the raw HIRLAM forecast, that is no interpolation has been done between forecast updates or within the hourly steps in an individual forecast. This implies, that for each of the 49 horizons the forecasted wind speed or wind direction is only updated 4 times a day.

The dynamics of the forecasted wind speed is, according to DMI, comparable to the dynamics of 30 to 45 minute averages of a measured wind speed. The measured wind speeds and wind directions used in the following has thus been constructed by sub-sampling the original 5 minute average values into 30 minute values as described in Chapter 3 and then leaving every second sample out.

As argued in the beginning of this chapter the subject of making (optimal) predictions of wind speed at a location will not be considered in this study. Consequently the analysis presented in this section is restricted to models describing the static relations between forecasted and observed wind speeds. Both linear and non-linear models will be considered, but as this section focuses on the static relationship between observed and forecasted wind speed only off-line estimation techniques will be used in this section.

This section considers models for predicting the observed wind speed as a function of forecasted wind speed, wind direction as well as time of day, that is models of the type

$$w_{t+k} = f_k(w^m_{t+k|t}, \phi^m_{t+k|t}, h^{24}_{t+k}) + e_{t+k}, \quad e_{t+k} \in N(0, \sigma^2_k), \tag{6.1}$$

where w_{t+k} is the observed wind speed at time $t+k$, $w^m_{t+k|t}$ and $\phi^m_{t+k|t}$ is the meteorological forecasts of wind speed and direction at time $t+k$ given at time t, h^{24}_{t+k} denotes time of day and e_{t+k} is an error term. As the k subscript indicates, it is in (6.1) assumed, that f_k is dependent of the prediction horizon. Not only does this mean, that it is necessary to estimate (and identify) one model for each prediction horizon, but as each prediction horizon is only updated four times a day, it decreases the amount of data available for the estimation to $\frac{1}{6}$ of the full set of data. It is thus clear, that if the model with reason can be assumed independent of the prediction horizon, this will be a considerable advantage for the modelling.

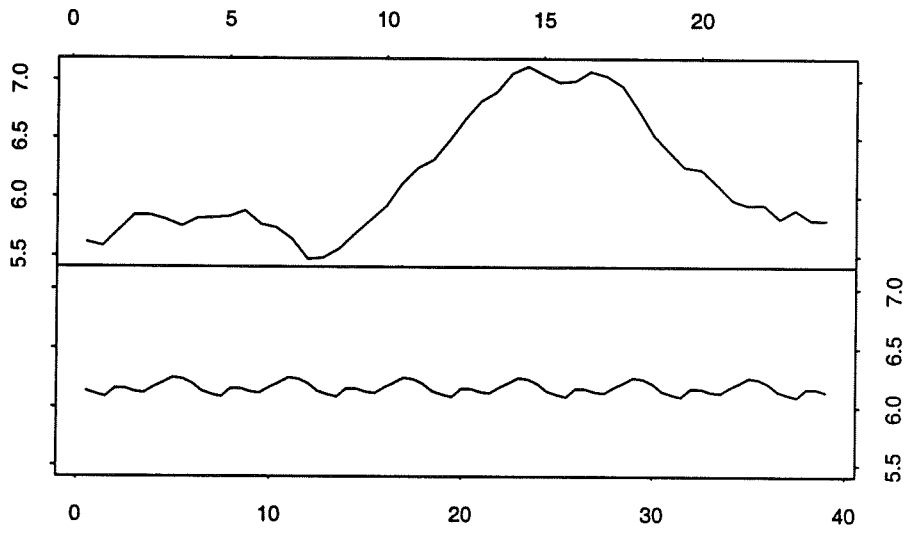

Figure 6.1: *The diurnal variation for the local wind speed at the Rejsby wind farm estimated on basis of data for the period from 26th of May 1997 to the 25th of September 1997 [m/s] (top) together with the derived prediction horizon dependent variation of a perfect – and thus unbiased – forecast updated 4 times a day [m/s] (bottom).*

Since the mean of w_t is constant a necessary requirement in order to make such an assumption valid is, that the expected value of the input variables in (6.1) is independent of k. Here it should be noted though, that the expected value of even a perfect – and thus unbiased – forecast of the local wind speed can not be assumed to be independent of the prediction horizon. This is caused by the diurnal variation exhibited by the local wind speed combined with the fact that the forecast only are updated 4 times a day. Figure 6.1

shows the estimated diurnal variation in the wind speed at the Rejsby wind farm for the period from the 26th of May 1997 to the 25th of September 1997 together with the derived prediction horizon dependent variation of a perfect forecast updated 4 times a day. From the plot it is evident that even a quite pronounced diurnal variation only results in a minor prediction horizon dependent variation of the forecasted wind speed for the case where the forecasts are updated 4 times a day.

In order not to compromise the clearness of the presentation unnecessarily the various plots and figures are related to the Rejsby wind farm as a recurrent example. Plots and figures for the remaining four wind farms considered are referred to Appendix D.

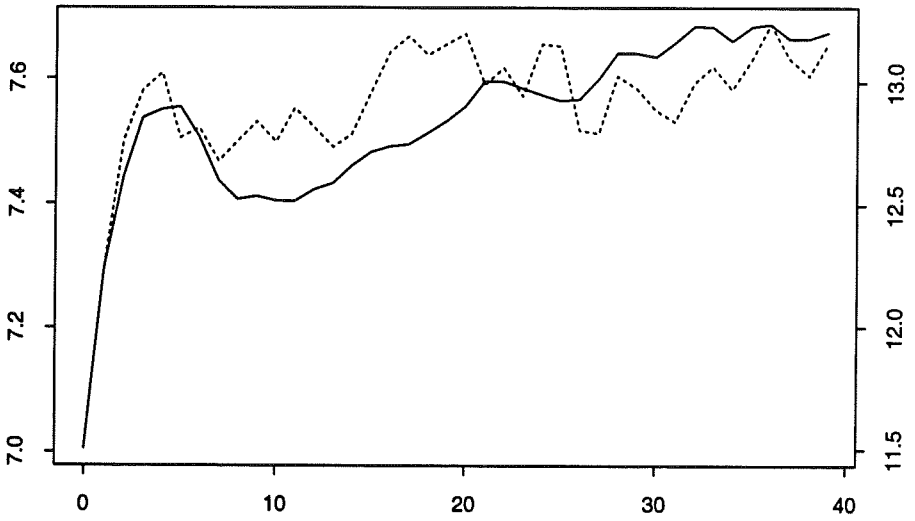

Figure 6.2: *(Rejsby) Estimated mean (full line, left hand axis $[m/s]$) and variance (dotted line, right hand axis $[m^2/s^2]$) versus prediction horizon (hours) for the forecasted wind speed at model level 31.*

Figure 6.2 depicts the estimated mean and variance of the forecasted wind speed as a function of the prediction horizon for the Rejsby wind farm. From the figure it is seen, that the mean value curve displays a step peak for a prediction horizon between 0 and 6-8 hours before settling into a steady almost linear increase as the prediction horizon increases. A similar pattern is found for the other four wind farms.

It is thus evident, that the prediction horizon dependent variation of mean value (and variance) for the forecasted wind speed exhibits a pronounced deviation from what would be expected with Figure 6.1 in mind, and hence that the mapping between observed and forecasted wind speed has to be handled individually for each prediction horizon.

6.1.1 Relations between observed and forecasted wind speed

Scatter plots are useful in the initial evaluation of the relationship between two variables. Figure 6.3 shows scatter plots of observed wind speed versus forecasted wind speed at level 31 for prediction horizons of 0 hour (the analysis), 12 hours, 24 hours and 36 hours for the Rejsby wind farm. Similar plots for the Dræby, Fjaldene, Hollandsbjerg and Sydthy wind farms are found in Figure D.5 to D.8. Even though the scatter is considerable, in particular

for prediction horizons of 24 and 36 hours, the plots suggest a linear relationship between observed and forecasted wind speed. The model thus becomes

$$w_{t+k} = b_0 + b_1 w^m_{t+k|t} + e_{t+k} \tag{6.2}$$

where w_{t+k} is the observed wind speed[2] at time $t+k$, $w^m_{t+k|t}$ is the forecasted wind speed for time $t+k$ given at time t, e_{t+k} is an i.i.d. noise term and b_0, b_1 are model parameters to be estimated.

Model (6.2) is estimated using ordinary least squares as described in Section 5.1.1. The data set is separated into two independent sets as described in Section 5.4, where one set is used for estimation and the second set is used for model validation. The model as been estimated and evaluated using forecasts from both model layer 30 and 31.

The coefficient of determination (R^2) for the validation data set is tabulated under label "l30 ml" and "l31 ml" for selected prediction horizons between 0 and 36 hours in Table 6.1 for the five wind farms. Especially for the larger prediction horizons the performance of the model varies between the wind farms with a R^2 ranging from 0.45 for Dræby to 0.56 for Rejsby (level 31) for a prediction horizon of 36 hours.

The comparison between models using input from model layer 30 respectively model layer 31 is referred to the end of this section.

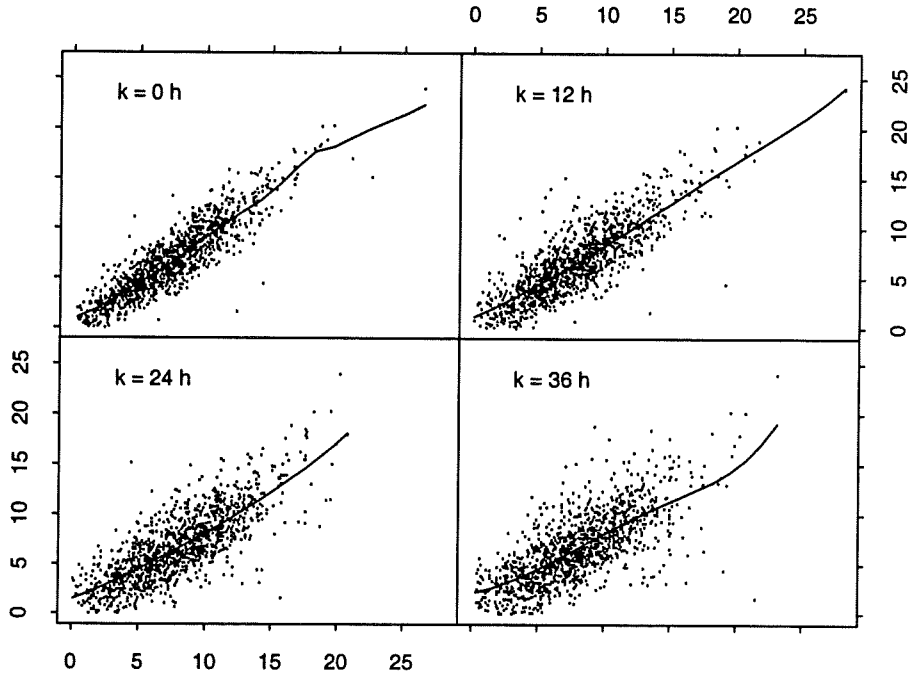

Figure 6.3: *(Rejsby) Observed wind speed [m/s] versus forecasted wind speed at level 31 [m/s] for a prediction horizon of 0 hours (top left), 12 hour (top right), 24 hour (bottom left) and 36 hour (bottom right). The line is the estimated relationship using local regression and 2. order polynomial approximation.*

The scatter in Figure 6.3 makes it difficult to evaluate visually, whether the relationship between observed and forecasted wind speed is sufficiently modelled by a linear regression

[2]This section exclusively analysis the relations between forecasted and observed wind speeds using wind speed 2 as the dependable variable.

model as (6.2), or whether a non-linear relationship as in

$$w_{t+k} = b_0(w^m_{t+k|t}) + e_{t+k} \tag{6.3}$$

is more appropriate. Here $b_0()$ is a non-linear function, which must be estimated. The function is estimated by local regression using a second order polynomial approximation and a fixed bandwidth as described in Section 5.2.1. The bandwidth has been optimized for the individual prediction horizons and wind farms using the procedure described in Section 5.4, but is in all cases in the range from 6 m/s to 12 m/s.

The estimated non-linear relationship between observed and forecasted wind speed is depicted in Figure 6.3 and Figure D.5 to D.8 for selected prediction horizons. When disregarding atypical behavior for extreme wind speeds, where the number of observations are very limited the estimates only display small deviations from linearity.

This impression/observation is confirmed by the model residuals. The R^2 for model (6.3) is found in Table 6.1 labelled "l30 m2" and "l31 m2". For Dræby the non-linearity is hardly detectable. Fjaldene, Hollandsbjerg and Sydthy show a consistent, but small improvement in the region of 0.01 for (6.3) when compared to the linear model (6.2). Finally, Rejsby shows a decrease in R^2 between 0.01 and 0.19. The large decreases (0.06 to 0.19) for the 12 hour, 30 hour and 36 hour prediction horizons are most likely due to some inconsistency between estimation and validation data set and the fact that R^2 is calculated on basis of the validation set. This could easily be wind direction related as Rejsby has a very marked wind direction dependency.

The local wind speed measurement will in most cases be influenced by local conditions such as obstacles in the vicinity of the anemometer, shading effects from surrounding wind turbines, etc. The result of these disturbances will be revealed as a wind direction dependency in the relationship between observed and forecasted wind speed.

One approach to allow for the influence of wind direction in the relation between observed and forecasted wind speed is to let the slope and intercept parameters in the linear model (6.2) vary as functions of the wind directions. The model thus becomes

$$w_{t+k} = b_0(\phi^m_{t+k|t}) + b_1(\phi^m_{t+k|t})w^m_{t+k|t} + e_{t+k} \tag{6.4}$$

where $b_0()$ and $b_1()$ are functions of (forecasted) wind direction to be estimated. The model (6.4) is estimated as a conditional parametric model as described in Section 5.2.1. By calculating the distances used in the estimation on a circle it is ensured, that the estimated functions $b_0()$ and $b_1()$ are continues between 0° and 360°. An optimal bandwidth has been identified by optimization for each model corresponding to a prediction horizon and a wind farm using the procedure described in Section 5.4. The identified bandwidths range from 50° to 300°, and it is observed, that for the individual wind farms the bandwidth is in general increasing, as the prediction horizon becomes larger.

The coefficients functions, $b_0()$ and $b_1()$, estimated for the prediction horizons 0, 12, 24 and 36 hours are plotted in Figure 6.4 for the Rejsby wind farm. The corresponding plots for Dræby, Fjaldene, Hollandsbjerg and Sydthy are found in Appendix D.2. The estimated coefficient functions display a similar pattern for all five wind farms: When wind speed from the analysis ($k = 0$) is used as input, the coefficient functions seems capable of describing the influence of local conditions in detail, but as the prediction horizon increases the level of

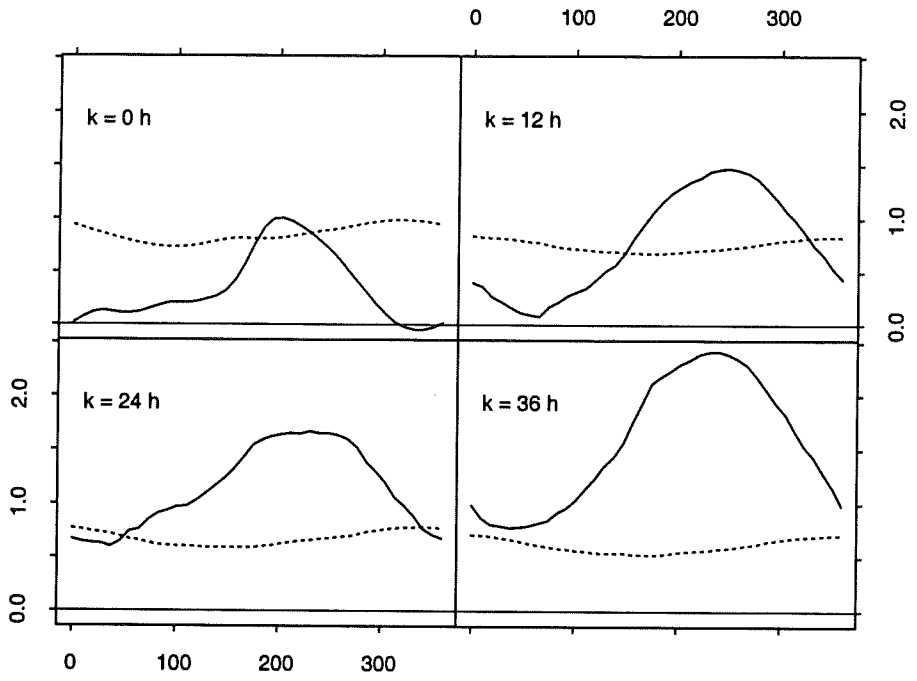

Figure 6.4: *(Rejsby) Estimated intercept, $b_0()$ (full line), and slope, $b_1()$ (dotted line), in (6.4) as a function of wind direction for a prediction horizon of 0 hours (top left), 12 hours (top right), 24 hours (bottom left) and 36 hours (bottom right). The coefficient functions indicate for all the depicted prediction horizons that for a given forecasted wind speed the expected value of the observed wind speed will increase as the wind direction shifts from east to west. This observation seams highly plausible as the Rejsby wind farm is located approximately 1.5km from the west coast of Jutland with a meteorology tower some 500m west of the wind farm.*

detail quickly diminishes until only a rudimentary pattern remains. A likely explanation for the observed behavior of the estimates is, that the increased uncertainty in the forecasts of wind speed and direction makes it impossible to distinguish the more abrupt changes in the wind field caused by the local conditions as the prediction horizon becomes larger. Details regarding the individual wind farms are referred to the captions of the figures.

The coefficient of determination for model (6.4) is found in Table 6.1 under label "l30 m3" and "l31 m3" for models using forecasts from level 30 and level 31, respectively. Comparing with the simple linear regression model (6.2) an increase in R^2 is found for all wind farms, when the forecasts from the analysis is used as input. The improvement ranges from 0.01 for Dræby and Fjaldene and up to 0.05 for Rejsby. As the prediction horizons increases the benefits from including the wind direction in the model become less noticeable, and for Dræby and Fjaldene the use of model (6.4) gives no clear advantage over the simple regression model. For Hollandsbjerg, Rejsby and Sydthy it remains advantageous to model the wind direction dependencies also for the higher prediction horizons, and especially Rejsby shows a very consistent improvement (≈ 0.03) for all prediction horizons.

Comparing the coefficient of determination for the models using forecasts from model layer 30 respectively model layer 31, it is seen that irrespective of the model the use of forecasts originating from level 31 will result in a 0 to 0.05 improvement of R^2 and especially Hollandsbjerg shows a very distinct improvement (0.03-0.05).

		Prediction horizon [*hours*]								
WF	Model	0	3	6	9	12	18	24	30	36
DR	l30 m1	0.76	0.69	0.68	0.65	0.65	0.62	0.57	0.51	0.45
DR	l30 m2	0.75	0.69	0.67	0.65	0.65	0.62	0.57	0.51	0.46
DR	l30 m3	0.77	0.70	0.69	0.65	0.65	0.62	0.56	0.50	0.44
DR	l31 m1	0.78	0.70	0.69	0.66	0.66	0.63	0.58	0.52	0.45
DR	l31 m2	0.78	0.70	0.69	0.65	0.66	0.63	0.58	0.52	0.47
DR	l31 m3	0.79	0.70	0.69	0.65	0.67	0.63	0.58	0.51	0.45
FJ	l30 m1	0.76	0.70	0.71	0.67	0.71	0.67	0.63	0.56	0.53
FJ	l30 m2	0.77	0.71	0.72	0.68	0.72	0.68	0.65	0.57	0.54
FJ	l30 m3	0.78	0.71	0.72	0.68	0.72	0.68	0.64	0.57	0.53
FJ	l31 m1	0.77	0.71	0.72	0.69	0.72	0.68	0.65	0.57	0.54
FJ	l31 m2	0.77	0.72	0.73	0.69	0.73	0.69	0.66	0.58	0.55
FJ	l31 m3	0.78	0.73	0.73	0.70	0.73	0.68	0.65	0.58	0.54
HO	l30 m1	0.72	0.65	0.64	0.64	0.60	0.59	0.55	0.49	0.43
HO	l30 m2	0.73	0.65	0.64	0.65	0.61	0.59	0.55	0.50	0.45
HO	l30 m3	0.74	0.68	0.65	0.66	0.61	0.60	0.56	0.48	0.42
HO	l31 m1	0.77	0.69	0.67	0.68	0.63	0.62	0.59	0.52	0.46
HO	l31 m2	0.78	0.69	0.68	0.69	0.64	0.62	0.59	0.52	0.48
HO	l31 m3	0.79	0.73	0.68	0.70	0.64	0.64	0.60	0.51	0.46
RB	l30 m1	0.80	0.75	0.73	0.73	0.70	0.66	0.64	0.60	0.55
RB	l30 m2	0.79	0.76	0.73	0.71	0.55	0.65	0.64	0.52	0.43
RB	l30 m3	0.85	0.79	0.77	0.77	0.74	0.70	0.67	0.63	0.58
RB	l31 m1	0.81	0.77	0.75	0.75	0.71	0.68	0.65	0.61	0.56
RB	l31 m2	0.81	0.77	0.74	0.73	0.52	0.66	0.65	0.55	0.47
RB	l31 m3	0.86	0.80	0.78	0.78	0.75	0.71	0.68	0.64	0.59
SY	l30 m1	0.80	0.75	0.72	0.71	0.71	0.69	0.64	0.55	0.47
SY	l30 m2	0.81	0.76	0.73	0.72	0.72	0.70	0.64	0.56	0.48
SY	l30 m3	0.82	0.77	0.74	0.74	0.73	0.70	0.65	0.56	0.48
SY	l31 m1	0.81	0.76	0.73	0.72	0.72	0.70	0.65	0.56	0.48
SY	l31 m2	0.82	0.76	0.74	0.73	0.73	0.70	0.66	0.57	0.49
SY	l31 m3	0.83	0.79	0.76	0.76	0.75	0.71	0.66	0.57	0.50

Table 6.1: *Coefficient of determination (R^2) for wind speed model (6.2), (6.3) and (6.4) (labelled "m1" to "m3") with forecasted wind speed from either model level 30 or model level 31 (labelled "l30" or "l31") as input and observed wind speed (w^2) as output. R^2 is in all cases estimated on basis of the validation data set as described in Section 5.4. The results are shown for selected prediction horizons between 0 hours (the analysis) and 36 hours. The estimated variance for the observed wind speed is listed below for the five wind farms: $s^2_{DR} = 4.79\,m^2/s^2$, $s^2_{FJ} = 5.35\,m^2/s^2$, $s^2_{HO} = 4.88\,m^2/s^2$, $s^2_{RB} = 13.0\,m^2/s^2$, $s^2_{SY} = 4.76\,m^2/s^2$.*

For reference the estimated variance of the model errors can be found in Table D.1 to D.5 in Appendix D.

6.1.2 Diurnal variations in observed and forecasted wind speed.

It is well known, that the thermal winds, which at many locations arise during sunny days, cause a mixing of the higher and lower layers in the atmosphere. Higher wind speeds are thus transfered from the upper to the lower part of the atmosphere during sunny days, which results in a diurnal variation of the wind speed for some locations.

In this section the diurnal variation in the observed wind speeds at the five wind farms is identified, and it is investigated, whether similar variations are present in the forecasted wind speeds from model layer 31 in the HIRLAM weather model.

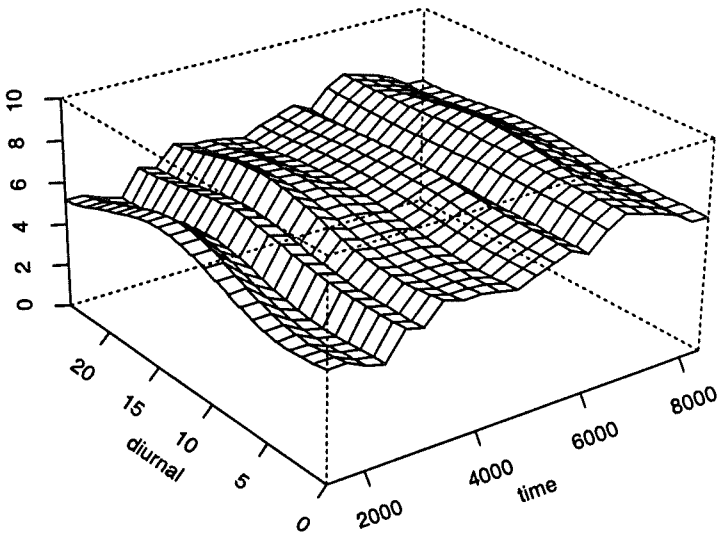

Figure 6.5: *(Rejsby) Annual variation in the estimated diurnal variation [m/s] versus time of day [hours] for the observed wind speed (w^2). Here the observation numbers 2000, 4000, 6000 and 8000 correspond to the dates 17.08.97, 08.11.97, 31.01.98 and 24.04.98 respectively. A forgetting factor corresponding to a memory time constant of 4 weeks is used in the estimation.*

Due to the very nature of this phenomenon the diurnal variations is more distinct during summer time than during winter time, and this annual variation has to be taken into consideration when estimating the diurnal variation. Figure 6.5 shows the estimated annual variation of the diurnal profile for the observed wind speed at the Rejsby wind farm using the model

$$w_t = b_0(h_t^{24}, t) + e_t \tag{6.5}$$

where h_t^{24} denote the time of day and $b_0(\ , t)$ is a time-varying coefficient function to be estimated. In the Figures D.13 to D.16 similar plots are shown for the wind farms at Dræby, Fjaldene, Hollandsbjerg and Sydthy. The model (6.5) is estimated as a local regression model using the recursive and adaptive method described in Section 5.2.2. By calculating the distances used in the estimation on a circle it is ensured, that the estimated functions

$b_0()$ is continues between 00:00 and 24:00. The estimation is carried out with a bandwidth of 12 hours and a forgetting factor corresponding to a memory time constant of 4 weeks.

For the wind farms at Dræby and Hollandsbjerg a diurnal variation in the observed wind speed is seen across the entire year, but, as expected, the variation is most distinct during summer time. The observed wind speed at Fjaldene hardly displays any diurnal variation at all, and the diurnal behavior of the wind speed at Rejsby and Sydthy falls in between these two extremes. The diurnal behavior of the wind speed is thus found to vary considerably between the five wind farms.

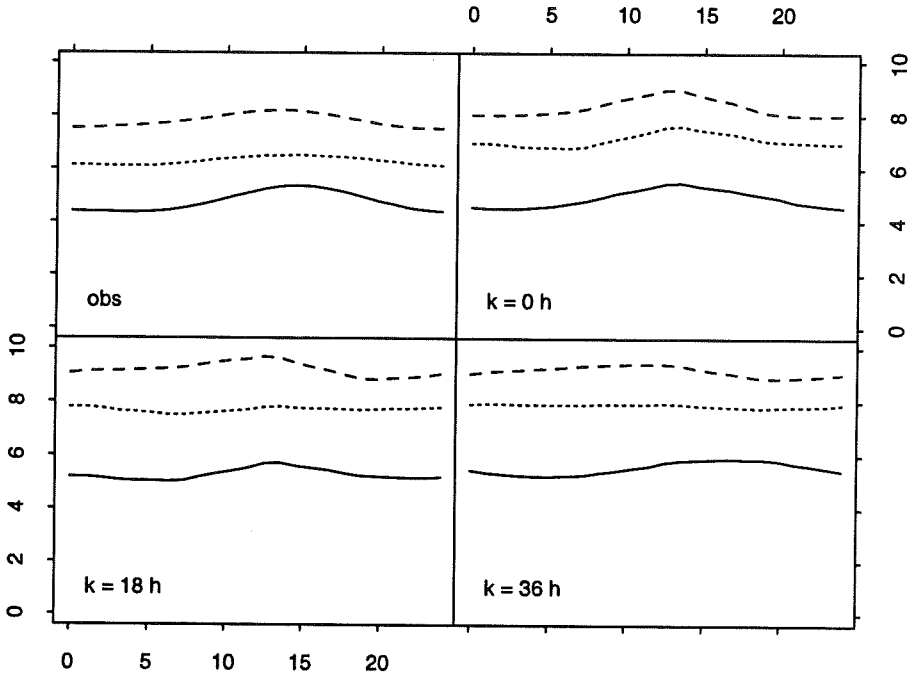

Figure 6.6: *(Rejsby) Estimated diurnal variation [m/s] versus time of day [hours] at 3th September 1997 (full line), 12th December 1997 (dotted line) and 22nd March 1998 (dashed line) for the observed wind speed (top left) as well as forecasted wind speed for a prediction horizon of 0 hours (top right), 18 hours (bottom left) and 36 hours (bottom right). A forgetting factor corresponding to a memory time constant of 4 weeks is used in the estimation.*

In order to evaluate whether the diurnal variation in the observed wind speed is sufficiently modelled by the HIRLAM weather model, the estimated diurnal variation for observed and forecasted wind speeds at Rejsby is plotted in the Figures 6.6 for three different time periods. The corresponding plots for Dræby, Fjaldene, Hollandsbjerg and Sydthy are found in Figure D.17 to D.20.

Considering the estimated diurnal profile for the forecasted wind speeds it appears from the figures, that the amplitude of the profile declines and simultaneously the shape of the profile becomes distorted as the prediction horizon increases. Comparing the profiles for observed and forecasted wind speeds it is furthermore seen, that a distinct variation in either the observed or forecasted wind speed does not necessarily recur in the other (see e.g. the figures for Dræby and Fjaldene).

It is thus concluded, that the diurnal variation in the wind speed can not with reason be assumed contained in the forecasts from the weather model, and consequently diurnal

profiles have to be included explicitly in the power prediction models formed in Section 6.5.

6.1.3 Conclusion and discussion

This section (6.1) considers the characteristics of the meteorological forecasts of wind speed generated by the HIRLAM model running at DMI as well as the relationship between observed wind speeds in five wind farms – Dræby, Fjaldene, Hollandsbjerg, Rejsby and Sydthy – and the corresponding forecasted wind speeds. The analysis is based on forecasts from level 30 (second lowest level $\sim$ 104m above ground level) and 31 (lowest level $\sim$ 32m above ground level) in the HIRLAM model, which are the two model layers closest to the surface.

It has been shown how fundamental characteristics such as mean value and variance of the forecasted wind speed change as a function of the forecast horizon. Especially the change in mean value is undesirable and should be countered by a statistical correction before further use of the meteorological forecasts of wind speed. This correction could e.g. be a simple scaling factor estimated individually for each forecast horizon.

The relationship between observed and forecasted wind speed has been modelled by a simple linear regression model, as a non-linear function of forecasted wind speed and as a regression model, where the slope and intercept coefficients are functions of the forecasted wind direction. When using coefficient of determination as a measure it is evident from Table 6.1 that the wind speed related non-linearities between between forecasted and observed wind speed is almost negligible as the improvements in R^2 when comparing to the simple linear regression model are at best marginal. For the shorter prediction horizons the influence of the wind direction is much more pronounced with improvements in R^2 ranging from 0.01 for the Dræby wind farm and up to 0.05 for the Rejsby wind farm. As the forecast horizon increases the influence of the forecasted wind direction decreases. This is probably due to the increased uncertainty in the forecasts of wind speed as well as wind direction which results in increased uncertainty in the inference of the wind direction dependency.

Discussion: As most of the wind direction dependency in the relationship between forecasted and observed wind speed is due to local phenomena in the vicinity of the anemometers such as shading effects from wind turbines or the meteorological tower (see Section 6.4.2) it seems questionable whether it is advantageous to build this information into a power prediction model using meteorological forecasts as input. It seems a better approach to filter the meteorological forecasts of wind speed through a simple linear model with model coefficient depending of the prediction horizon in order to ensure, that the mean value of the filtered forecasts of wind speed is independent of the prediction horizon. The wind direction dependency in the relationship between observed power production and forecasted wind speed should then be handled directly in the power prediction model.

It has been evaluated whether forecasts from the HIRLAM model layer 30 or model layer 31 are the most appropriate in this context. Using coefficient of determination for the estimated models as a measure it is apparent that models based on forecasts from model layer 31 gives the best description of the local wind speeds irrespective of which of the three different models that are used.

Finally the diurnal variation of observed as well as forecasted wind speeds have been investigated. As expected the diurnal variation of the observed wind speeds is found to follow a annual pattern with larger variations during summer time and only minor varia-

tions during winter time. The diurnal variation is found to vary greatly between the five wind farms ranging from a very distinct variation for the measured wind speed at Dræby and Hollandsbjerg to hardly any variation for the measured wind speed at Fjaldene. This pattern can not be recognized in the diurnal variation of the forecasted wind speeds and it is concluded, that the diurnal variation in the wind speed can not be assumed contained in the forecasts of wind speed from model layer 31 in the HIRLAM model.

6.2 Meteorological wind direction models

This section describes the initial investigation of the characteristics for the meteorological forecasts of wind direction provided by the meteorological weather model HIRLAM running at DMI. The data consists of the observed wind direction at the Dræby, Fjaldene, Hollandsbjerg, Rejsby and Sydthy wind farms as well as the HIRLAM forecasts from model level 30 and 31 for the five locations. The data set used in this investigation corresponds to the data set used in Section 6.1. That is the meteorological forecasts are the raw HIRLAM forecasts without any interpolation between forecast updates or within the hourly steps in the individual forecasts and the observations have been subsampled to form hourly values.

The purpose of the study described in this section is twofold:

- To evaluate whether the forecasts from HIRLAM model level 30 (second lowest layer $\sim$ 104 m above ground level) or level 31 (lowest layer $\sim$ 32 m above ground level) is the most appropriate for this application.

- To identify suitable models for the relation between observed wind speed and forecasted wind speed. One important consideration is here how the characteristics of the forecasted meteorological variables changes as a function of the prediction horizon.

As argued in the beginning of this chapter the subject of making (optimal) predictions of wind direction at a location will not be considered in this study. Consequently the analysis presented in this section is restricted to models describing the static relations between forecasted and observed wind direction. The models considered will be linear as well as non-linear, but as this section focuses on the static relationship between observed and forecasted wind speed only off-line estimation techniques will be used.

This section considers models for predicting the observed wind direction as a function of forecasted wind direction, that is models of the type

$$\phi_{t+k} = f_k(\phi^m_{t+k|t}) + e_{t+k}, \quad e_{t+k} \in N(0, \sigma_k^2), \tag{6.6}$$

where ϕ_{t+k} is the observed wind direction at time $t+k$, $\phi^m_{t+k|t}$ is the meteorological forecast of wind direction at time $t+k$ given at time t, and e_{t+k} is a noise term. Relations with diurnal or wind speed dependency has not been investigated. As indicated by the k subscript it is in (6.6) assumed that f_k is dependent of the prediction horizon.

The wind direction, as distinct from the remaining measurements, is measured on a discontinuous scale, which in this case give rise to difficulties in establishing a meaningful

definition of mean value and variance[3]. Thus the initial investigation of the characteristics for the meteorological forecasts of wind direction as a function of the prediction horizon is not based on the forecasts them self, but rather on the difference between the observed and forecasted wind directions

$$\widetilde{\phi^m}_{t+k|t} = ||\phi_{t+k} - \phi^m_{t+k|t}|| \tag{6.7}$$

where $\widetilde{\phi^m}_{t+k|t}$ is the model error at time $t+k$ for the forecast given at time t. Note that in (6.7) the difference between observed and forecasted values is measured as the circular distance. Bias ($\overline{\widetilde{\phi^m_k}}$) and variance ($s^2_{\widetilde{\phi^m_k}}$) for the HIRLAM model error can now be estimated as

$$\begin{aligned} \overline{\widetilde{\phi^m_k}} &= \frac{1}{N}\sum_{t=1}^{N} ||\phi_{t+k} - \phi^m_{t+k|t}|| \\ s^2_{\widetilde{\phi^m_k}} &= \frac{1}{N-1}\sum_{t=1}^{N} ||\phi_{t+k} - \overline{\widetilde{\phi^m_k}}||^2 \end{aligned} \tag{6.8}$$

where N is the number of observations in the data set.

Figure 6.7 depicts the estimated bias and error variance for the Rejsby wind farm. From the figure it is seen that after a initial decrease in bias corresponding to approximately 5° the estimated bias remains fairly constant across the prediction horizons whereas the estimated variance increases with the forecast horizon. A similar pattern is found for the other four wind farms. The corresponding plots for Dræby, Fjaldene, Hollandsbjerg and Sydthy are found in Appendix D.4.

If an average bias is estimated as an unweighted average of the bias estimates for the individual forecast horizons values ranging from -29° for Fjaldene up to 14° for Hollandsbjerg are found. The wind direction measurement equipment has been calibrated with an accuracy so that the expected bias for a measurement should be less that ±5°. The estimated bias of the error for the HIRLAM model thus exceeds the tolerance of the measurements for all five wind farms. The most likely explanation for the observed bias is that it can be attributed to local conditions such as the siting of the measurement equipment within the five wind farms as well as the siting of the wind farms theme self in combination with systematic errors in the forecasted wind directions for the HIRLAM model layers close to the ground.

6.2.1 Relations between observed and forecasted wind direction

Figure 6.8 shows scatter plots of observed wind speed versus forecasted wind speed at level 31 for prediction horizons of 0 hour (the analysis), 12 hours, 24 hours and 36 hours for the Rejsby wind farm. Similar plots for the Dræby, Fjaldene, Hollandsbjerg and Sydthy wind farms are found in Figure D.25 to D.28. When evaluating the scatter plots it should be noted

[3]The difficulties are easily illustrated by considering the following example: Suppose that we want to calculate the mean value of two observations, $\phi_1 = 2°$ corresponding to a northerly wind and $\phi_2 = 180°$ corresponding to a southerly wind. The arithmectical mean of the two observations is $\bar{\phi} = 91°$ corresponding to an easterly wind. If the northerly wind instead results in a reading $\phi_1 = 358°$ the mean now becomes $\bar{\phi} = 269°$ corresponding to a westerly wind!

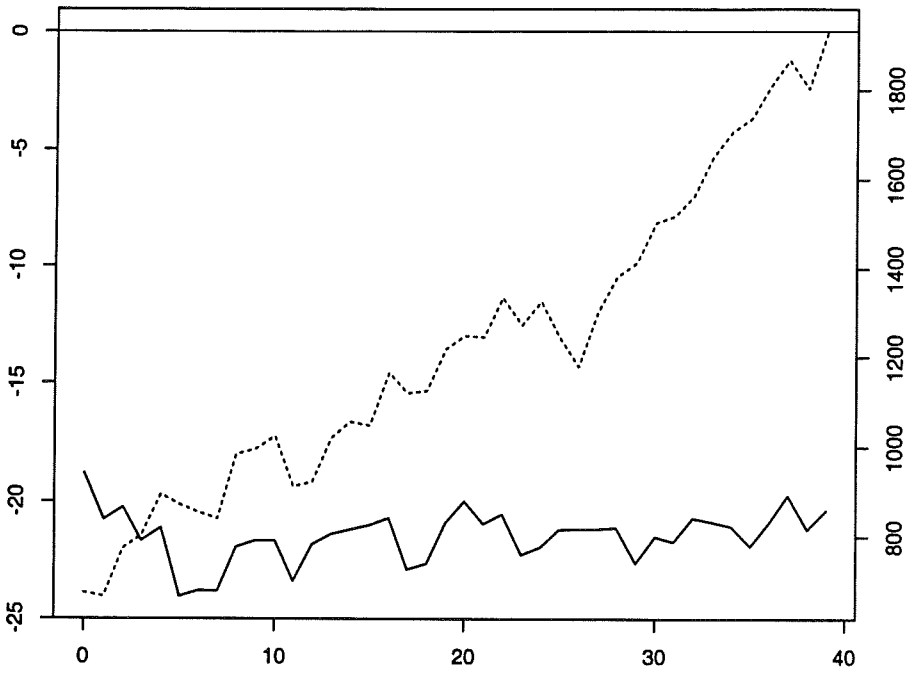

Figure 6.7: *(Rejsby) Estimated mean error (full line, left hand axis [°]) and error variance (dotted line, right hand axis [(°)^2]) versus prediction horizon (hours) for the forecasted wind direction at model level 31.*

that due to the discontinuity in the wind direction measure even an almost perfect forecasting model will show scatter in three regions: Along the diagonal (0°, 0°) to (360°, 360°) and in the region of (0°, 360°) and (360°, 0°). Even though the scatter is considerable, in particular for prediction horizons of 24 and 36 hours, the plots suggest that a bias correction might be sufficient. The model thus becomes

$$\phi_{t+k} = b_0 + \phi^m_{t+k|t} + e_{t+k} \tag{6.9}$$

where b_0 is the bias to be estimated. Model (6.9) is estimated using ordinary least squares as described in Section 5.1.1 minimizing the error term (6.7). The data set is separated into two independent sets as described in Section 5.4, where one set is used for estimation and the second set is used for model validation. The model as been estimated and evaluated using forecasts from both model layer 30 and 31. The estimated error variance for the validation data set is tabulated under label "l30 ml" and "l31 ml" for selected prediction horizons between 0 and 36 hours in Table 6.2 for the five wind farms.

The scatter in Figure 6.8 makes it difficult to evaluate whether the model bias for the HIRLAM model is independent of wind direction, or whether a wind direction dependent estimate of the bias as in

$$\phi_{t+k} = b_0(\phi^m_{t+k|t}) + e_{t+k} \tag{6.10}$$

is more appropriate. Here $b_0()$ is a non-linear function, which must be estimated. The function is estimated by local regression using a second order polynomial approximation and a fixed bandwidth as described in Section 5.2.1. The bandwidth has been optimized for the

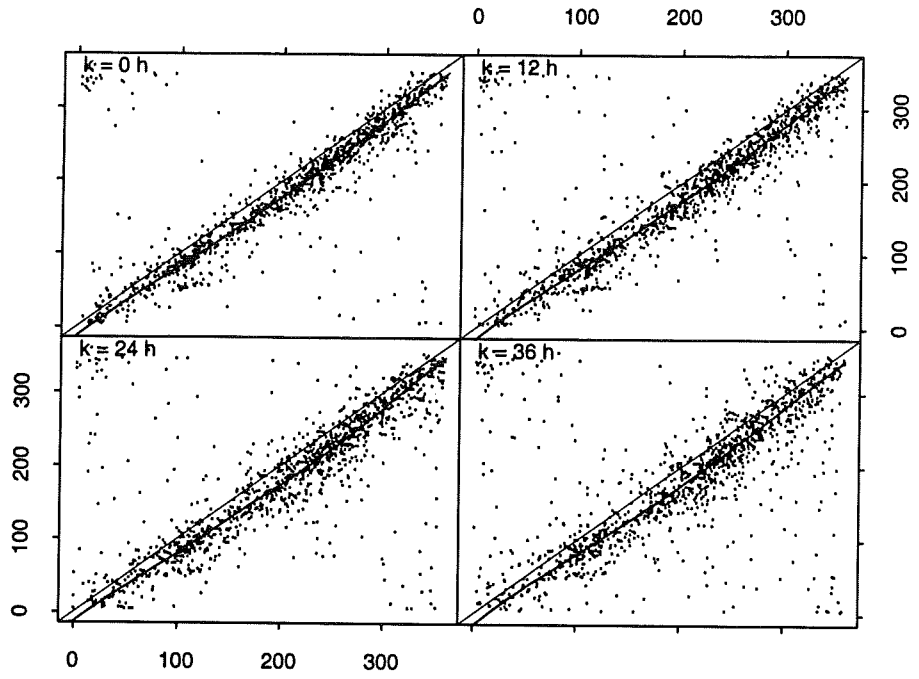

Figure 6.8: *(Rejsby) Observed wind direction* [°] *versus forecasted wind direction at level 31* [°] *for a forecast horizon of 0 hours (top left), 12 hour (top right), 24 hour (bottom left) and 36 hour. The line is the estimated relationship using local regression and 2. order polynomial approximation.*

individual prediction horizons and wind farms using the procedure described in Section 5.4, but is in all cases in the range from 81°to 148°. Restrictions have been introduced in the estimation of (6.10) in order to ensure that $\hat{b_0}(0°) = \hat{b_0}(360°) - 360°$.

The estimated non-linear relationship between observed and forecasted wind direction using model (6.10) is depicted for selected prediction horizons in Figure 6.8 for the Rejsby wind farm and in Figure D.25 to D.28 for the remaining four wind farms. The estimated error variance using wind direction forecasts from either model layer 30 or 31 as input is found in Table 6.2 labelled "l30 m2" and "l31 m2", respectively.

From the figures it is seen that the estimated non-linear relationship only displays small deviations from linearity. This impression/observation is confirmed by the model residuals. From Table 6.2 it is evident that within the individual wind farms the results obtained are very comparable regardless of how models and input layers are combined. The estimated model error variance differs markedly between the five wind farms especially for the shorter prediction horizons. The most likely explanation is that this is caused by the the differences in the siting of the measurement equipment within the five wind farms as well as the siting of the wind farms theme self.

Comparing the model error variance for the models using forecasts from model layer 30 respectively model layer 31, it seems rather random which model layer results in the smallest error variance irrespective of the model and wind farm considered.

		Prediction horizon [*hours*]								
WF	Model	0	3	6	9	12	18	24	30	36
DR	l30 m1	26.0^2	29.1^2	28.1^2	31.5^2	30.3^2	34.4^2	36.2^2	36.7^2	39.0^2
DR	l30 m2	26.0^2	28.9^2	28.1^2	31.0^2	29.3^2	33.3^2	34.9^2	36.1^2	37.9^2
DR	l31 m1	25.9^2	29.1^2	28.9^2	30.9^2	30.7^2	33.6^2	34.8^2	36.9^2	39.6^2
DR	l31 m2	26.0^2	29.0^2	29.0^2	30.3^2	29.6^2	32.4^2	33.5^2	35.8^2	38.5^2
FJ	l30 m1	26.1^2	31.1^2	26.7^2	30.8^2	30.6^2	32.9^2	36.6^2	38.1^2	40.7^2
FJ	l30 m2	25.8^2	30.9^2	26.3^2	30.3^2	30.2^2	32.9^2	36.3^2	37.8^2	40.1^2
FJ	l31 m1	25.7^2	31.6^2	28.8^2	30.2^2	30.0^2	31.9^2	36.5^2	37.9^2	40.4^2
FJ	l31 m2	25.3^2	30.8^2	28.3^2	29.8^2	29.6^2	31.9^2	36.1^2	37.4^2	39.6^2
HO	l30 m1	31.8^2	28.7^2	31.6^2	31.6^2	33.5^2	33.8^2	37.5^2	40.1^2	42.8^2
HO	l30 m2	32.2^2	28.5^2	31.6^2	31.2^2	33.6^2	33.8^2	37.3^2	40.0^2	41.6^2
HO	l31 m1	30.1^2	28.7^2	31.3^2	31.2^2	34.1^2	32.7^2	35.2^2	39.4^2	41.6^2
HO	l31 m2	30.3^2	28.3^2	31.3^2	31.0^2	33.9^2	32.6^2	34.8^2	39.2^2	40.6^2
RB	l30 m1	18.8^2	23.2^2	20.7^2	25.1^2	21.0^2	21.5^2	27.8^2	30.6^2	31.6^2
RB	l30 m2	18.5^2	23.0^2	20.6^2	25.3^2	21.0^2	22.1^2	27.9^2	30.8^2	31.6^2
RB	l31 m1	20.1^2	23.7^2	21.5^2	25.4^2	21.0^2	21.2^2	28.7^2	30.0^2	33.0^2
RB	l31 m2	20.0^2	23.5^2	21.3^2	25.4^2	21.1^2	21.9^2	29.0^2	30.2^2	33.3^2
SY	l30 m1	22.0^2	26.9^2	23.7^2	28.2^2	27.4^2	33.5^2	33.3^2	37.0^2	39.9^2
SY	l30 m2	22.1^2	26.8^2	23.5^2	28.3^2	27.2^2	33.5^2	33.5^2	37.5^2	40.2^2
SY	l31 m1	22.6^2	27.9^2	23.7^2	28.5^2	29.4^2	33.0^2	33.9^2	36.7^2	41.0^2
SY	l31 m2	22.6^2	27.5^2	23.5^2	28.5^2	29.3^2	33.0^2	34.2^2	37.3^2	41.1^2

Table 6.2: *Estimated model error variance for wind direction model (6.9) and (6.10) (labelled "m1" and "m2", respectively) with forecasted wind direction from either model level 30 or model level 31 (labelled "l30" or "l31") as input and observed wind direction as output. The model error variance is in all cases estimated on basis of the validation data set as described in Section 5.4. The results are shown for selected prediction horizons between 0 hours (the analysis) and 36 hours.*

6.2.2 Conclusion and discussion

This section (6.2) considers the characteristics of the meteorological forecasts of wind direction generated by the HIRLAM model running at DMI as well as the relationship between observed wind direction in five wind farms – Dræby, Fjaldene, Hollandsbjerg, Rejsby and Sydthy – and the corresponding forecasted wind direction. The analysis is based on forecasts from level 30 (second lowest level $\sim$ 104m above ground level) and 31 (lowest level $\sim$ 32m above ground level) in the HIRLAM model, which are the two model layers closest to the surface.

It has been shown how fundamental characteristics such as mean error and error variance of the forecasted wind direction change as a function of the forecast horizon. Especially the change in mean value is undesirable and should be countered by a statistical correction before further use of the meteorological forecasts of wind direction. This correction could e.g. be a simple bias factor estimated individually for each forecast horizon.

The relationship between observed and forecasted wind direction has been modelled by a simple linear regression model and as a non-linear function of forecasted wind direction.

When estimated error variance is used as a measure it is evident from Table 6.2 that the wind direction related non-linearities between forecasted and observed wind direction is almost negligible as the improvements in error variance when comparing to the simple linear regression model are at best marginal.

It has been evaluated whether forecasts from the HIRLAM model layer 30 or model layer 31 are the most appropriate in this context. Using the error variance for the estimated models as a measure no distinct differences between using forecasts from model layer 30 or 31 as input to the models were found.

6.3 Augmenting the meteorological data set

The model investigation in Section 6.1 and 6.2 is based on the raw HIRLAM forecasts. As described in Chapter 4 these forecasts cover a period from 0 to 48 hours ahead in hourly steps and is updated 4 times a day. No interpolation has been done between forecast updates or within the hourly steps in an individual forecast. This implies, that for each of the 49 horizons the forecasted wind speed or wind direction is only updated 4 times a day and consequently a prediction model as

$$y_{t+k} = f(x^m_{t+k|t}, ...) + e_{t+k}$$

has to be estimated on basis of 4 observations a day. Here y_{t+k} is an observed variable to be predicted (power) and $x^m_{t+k|t}$ is a meteorological forecast of a climatical variable (wind speed or direction).

In Section 6.1 and 6.2 the mean value and variance of the HIRLAM model error is found to vary fairly slowly with the prediction horizon for prediction horizons larger than 5 to 7 hours. It is thus an obvious idea to increase or *augment* the data set by applying the following interpolation scheme:

1. For each prediction horizon the meteorological forecasts of wind speed and direction are corrected for bias by applying model (6.2) and (6.9), respectively.

2. The models developed in Section 6.4 and 6.5 are based on 30 min (average) values. The corrected hourly forecasts are therefore interpolated to form half hourly values.

3. The (time) intervals between the updates of the meteorological forecasts are now filled by using the last available corrected and interpolated forecast and then shifting the (half hourly) values in the forecast one step backwards in each time step as illustrated in Table 6.3.

The augmented data set is generated on basis of the HIRLAM forecasts from model layer 31.

6.4 Power curve models

For a single wind turbine with no obstacles in its vicinity the power production is, disregarding the influence of ambient air temperature and humidity, only a function of the wind speed

Time	Prediction horizon				
	$k=0$	$k=1$	$k=2$	$k=3$	...
$t=t_0$	$w^m_{t_0\|t_0}$	$w^m_{t_0+1\|t_0}$	$w^m_{t_0+2\|t_0}$	$w^m_{t_0+3\|t_0}$	$\cdots$
$t=t_0+1$	$w^m_{t_0+1\|t_0}$	$w^m_{t_0+2\|t_0}$	$w^m_{t_0+3\|t_0}$	$w^m_{t_0+4\|t_0}$	$\cdots$
$t=t_0+2$	$w^m_{t_0+2\|t_0}$	$w^m_{t_0+3\|t_0}$	$w^m_{t_0+4\|t_0}$	$w^m_{t_0+5\|t_0}$	$\cdots$
$\vdots$	$\vdots$	$\vdots$	$\vdots$	$\vdots$	$\ddots$
$t=t_1$	$w^m_{t_1\|t_1}$	$w^m_{t_1+1\|t_1}$	$w^m_{t_1+2\|t_1}$	$w^m_{t_1+3\|t_1}$	$\cdots$
$\vdots$	$\vdots$	$\vdots$	$\vdots$	$\vdots$	$\ddots$

Table 6.3: *The meteorological forecasts are updated at time t_0 and t_1. The forecasts for a fixed prediction horizon, say $k=2$, in the time interval between the updates are generated by shifting the values in the forecast given at time t_0 one step backwards in each time step.*

"seen" by the turbine. In the static case[4] the relationship between power and wind speed is described by the turbine power curve specified by the manufacture of the wind turbine.

When the scope is changed from modelling the power output from a single free standing wind turbine to modelling the power production for an entire wind farm, it has to be taken into consideration, that the individual wind turbines now will create "wakes" disturbing the turbines standing behind. The influence of this effect on the power production depends on the layout of the wind farm as well as the wind direction. This section considers the relationship between power production in a wind farm and local values of wind speed and wind direction – in the following denoted the wind farm power curve. Often locally measured values of wind speed (and direction) will be affected by local conditions such as wind turbines in the nearby surroundings or the location of the measurement equipment on the meteorological tower. A wind farm power curve estimated on basis of measured values will thus reflect the combined influence of wind turbine characteristics, wind farm layout and placement of the anemometer.

The following topics concerning the identification and estimation of wind farm power curves are discussed in the subsequent sections:

- In Section 6.4.1 a method for creating an estimate of an undisturbed wind speed is suggested.
- The subject of identifying and estimating wind farm power curve models for a given wind speed is treated in Section 6.4.2. Models with as well as without wind direction dependencies are considered.
- The performance of the power curve models from Section 6.4.2 is evaluated in Section 6.4.3, when forecasted values of wind speed and direction are used to generate predictions of wind farm power output.

[4]If data is sampled (and averaged) at a rate, where the dynamics of the wind turbine is negligible, the power curve is also useful in the dynamic case. It should be noted though, that large fluctuations of the wind speed within a sample period will result in deviations from the power curve. This is caused by the non-linearities in the relationship between wind speed and power.

The data employed in this analysis is the half hourly data set described in Section 6.3, where the meteorological forecasts are interpolated between forecast updates as well as within the hourly steps in an individual update and the measurements are subsampled.

6.4.1 Area wind speed

Consider an imaginary wind speed measured in the undisturbed wind layers just above the wind farm. In the following this wind speed, w^a, will be denoted the area wind speed. Given a reliable model of the relationship between area wind speed and power production knowledge of the area wind speed will allow us to calculate the expected power output from the wind farm with high accuracy.

The transformation from area wind speed to measured wind speed at one of the two anemometers in a wind farm will, due to local phenomena such as shading effects from surrounding wind turbines and the meteorological tower, be dependent of wind direction. This dependency can be quite pronounced (See e.g. Fjaldene) and might together with the inevitably measuring noise severely compromise the identification and estimation of a reliable power curve model for the wind farm. In particular the measuring of wind speed is noise-prone.

This section describes, how an estimated area wind speed can be established using the analysis from the meteorological forecast model (HIRLAM) as well as measurements of the two wind speeds and the wind direction.

Assume that the HIRLAM analysis of the wind speed is an unbiased[5] estimate for the area wind speed (albeit a noisy one). Then an estimate of the area wind speed based on measurements can be established by formulating a model for the analysis wind speed as a function of measured wind speeds and wind direction.

Initial efforts made it clear, that the two measured wind speeds are too correlated to allow reliable estimation of models of the form

$$w^m_{t|t} = b_0(\phi_t) + b_1(\phi_t)w^1_t + b_2(\phi_t)w^2_t + e_t$$

where $w^m_{t|t}$ is the analysis[6], ϕ_t is the wind direction, w^1_t and w^2_t are wind speed 1 and 2, respectively, e_t is a noise term and finally $b_0()$, $b_1()$ and $b_2()$ are functions to be estimated. In the following a more successful two stage modelling approach will be described.

A simple relationship between analysis, one of the wind speed measurements and wind direction is given by

$$w^m_{t|t} = b^i_1(\phi_t)w^i_t + e_t \tag{6.11}$$

where w^i_t is either wind speed 1 or 2. The function $b^i_1()$ has been estimated using local regression with a second order polynomial approximation and fixed bandwidth. By calculating the distances used in the estimation on a circle it is ensured, that the estimated functions

[5]Unconditioned as well as conditioning on e.g. wind speed or wind direction.

[6]The 0 hour forecast, $w^m_{t|t}$, used in the estimation, will due to the augmenting of the meteorological forecasts consist of values derived from the forecasts for the first 6 hours in the individual updates. The analysis used in this section is thus a compound of the "proper" analysis and the 1 to 5 hour forecast of the meteorological weather model.

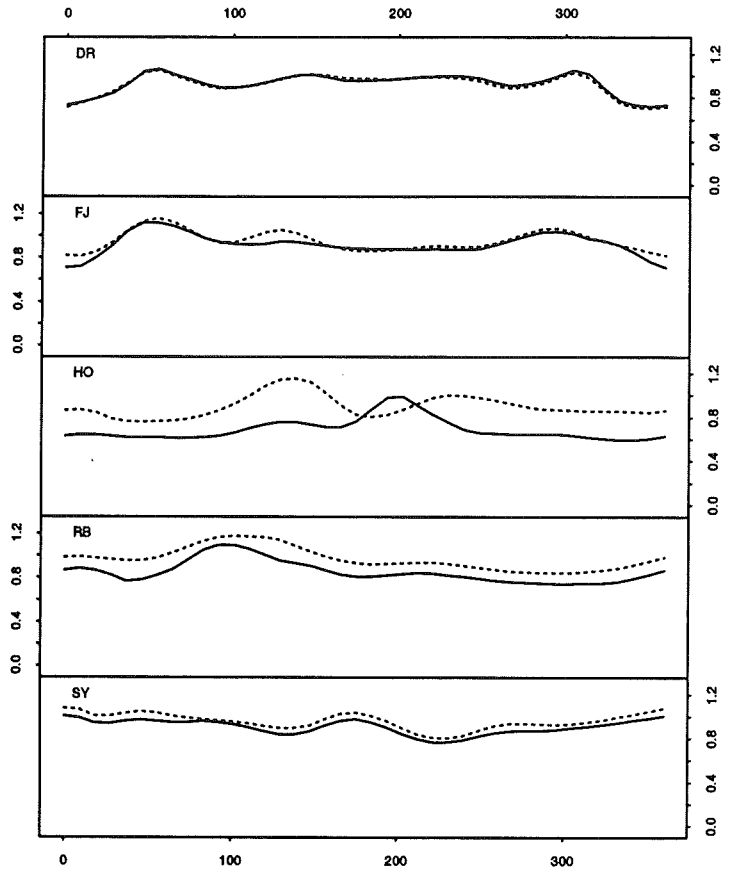

Figure 6.9: *(All wind farms) Estimated slope ($b_1()$) in model (6.11) as a function of wind direction when wind speed 1 (full line) or 2 (dotted line) are used as regressors. From top to bottom the estimates are from Dræby (DR), Fjaldene (FJ), Hollandsbjerg (HO), Rejsby (RB) and Sydthy (SY).*

$b_1^i()$ are continues between 0° and 360°. The bandwidth has been selected by optimization for each of the five wind farms using the procedure described in Section 5.4 and varies from 52° to 69°. The function estimates for the five wind farms are plotted in Figure 6.9.

Running (6.11) with either wind speed 1 or 2 as regressors will now produce two estimates for the area wind speed, where the influence of the wind direction (ideally) have been removed. The two estimates are combined into a single estimate using a simple regression model without intercept

$$w_{t|t}^m = \beta_1 \hat{b_1^1}(\phi_t) w_t^1 + \beta_2 \hat{b_1^2}(\phi_t) w_t^2 + e_t \tag{6.12}$$

or including intercept

$$w_{t|t}^m = \beta_0 + \beta_1 \hat{b_1^1}(\phi_t) w_t^1 + \beta_2 \hat{b_1^2}(\phi_t) w_t^2 + e_t \tag{6.13}$$

Here only the parameters β_0, β_1 and β_2 have to be estimated, as the functions $\hat{b_1^1}(\phi_t)$ and $\hat{b_1^2}(\phi_t)$ from (6.11) are estimated separately. The coefficient of determination for (6.11) with

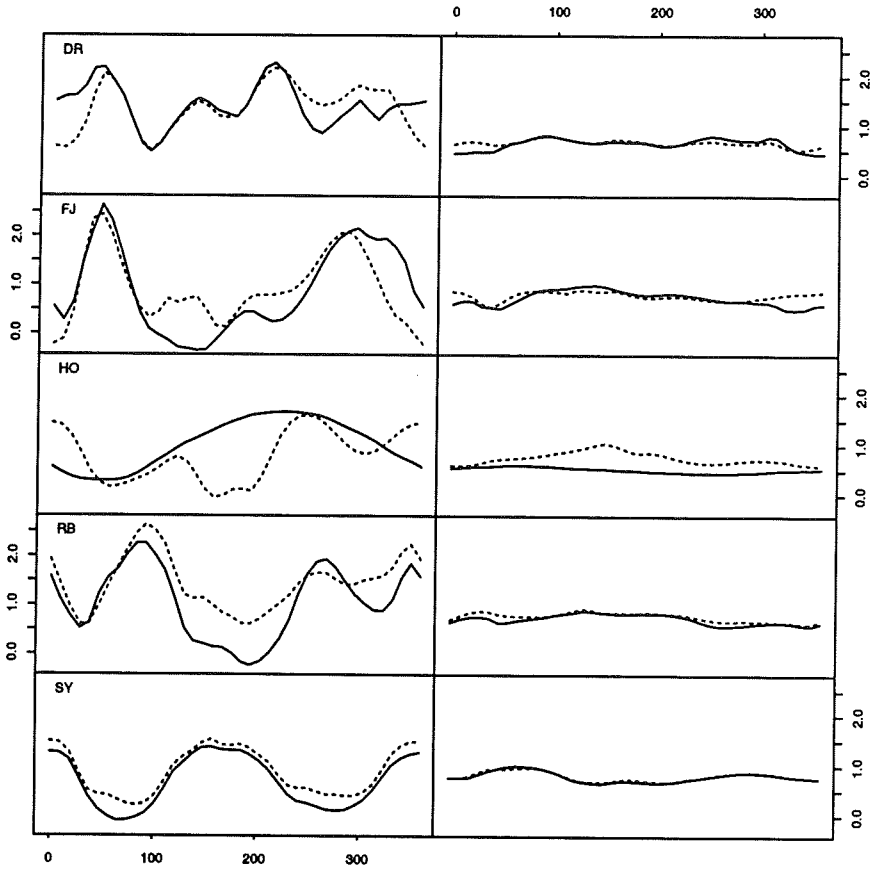

Figure 6.10: *(All wind farms) Estimated intercept ($b_0()$, left column) and slope ($b_1()$, right column) in model (6.14) as a function of wind direction when wind speed 1 (full line) or 2 (dotted line) are used as regressors. From top row to bottom row the estimates are from Dræby, Fjaldene, Hollandsbjerg, Rejsby and Sydthy.*

either wind speed 1 or 2 as input is listed in Table 6.4 labelled $m1_{w^1}$ or $m1_{w^2}$, respectively. Similarly the results for the combined models (6.12) and (6.13) are listed under $m1_c$ and $m1_c^I$, respectively. In all cases R^2 is estimated on basis of the validation data set as described in Section 5.4.

A natural extension of model (6.11) is to include a wind direction dependent intercept. The model thus becomes

$$w_{t|t}^m = b_0^i(\phi_t) + b_1^i(\phi_t) w_t^i + e_t \tag{6.14}$$

where $b_0^i(\phi_t)$ and $b_1^i(\phi_t)$ are coefficient functions to be estimated. (6.14) has been estimated using local regression with a second order polynomial approximation and fixed bandwidth, where the optimal bandwidth has been been found by optimization for each model using the procedure described in Section 5.4. With the exception of the wind speed 1 model for Hollandsbjerg, for which the optimization seems to have gone astray ($\alpha \approx 300°$), the bandwidths range from 52° to 85° for the individual models. The estimated coefficient functions for the five wind farms are plotted in Figure 6.10.

Again the two estimates for area wind speed established by using (6.14) with either wind speed 1 or 2 as regressors is combined by applying a simple regression model without intercept

$$w_{t|t}^{m} = \beta_1 \left[\hat{b}_0^1(\phi_t) + \hat{b}_1^1(\phi_t) w_t^1\right] + \beta_2 \left[\hat{b}_0^2(\phi_t) + \hat{b}_1^2(\phi_t) w_t^2\right] + e_t \tag{6.15}$$

or including intercept

$$w_{t|t}^{m} = \beta_0 + \beta_1 \left[\hat{b}_0^1(\phi_t) + \hat{b}_1^1(\phi_t) w_t^1\right] + \beta_2 \left[\hat{b}_0^2(\phi_t) + \hat{b}_1^2(\phi_t) w_t^2\right] + e_t \tag{6.16}$$

where β_0, β_1 and β_2 are the model parameters to be estimated. The coefficient of determination for (6.14) is tabulated in Table 6.4 labelled "$m2_{w^1}$" and "$m2_{w^2}$", when wind speed 1 or 2, respectively, is used as regressors. For the combined models (6.15) and (6.16) the estimated R^2 is listed under "$m2_c$" and "$m2_c^I$. In all cases R^2 is estimated on basis of the validation data set as described in Section 5.4.

	Wind farm				
Model	DR	FJ	HO	RB	SY
$m1_{w^1}$	0.69	0.65	0.69	0.74	0.76
$m1_{w^2}$	0.70	0.64	0.67	0.78	0.75
$m1_c$	0.68	0.64	0.69	0.78	0.76
$m1_c^I$	0.72	0.71	0.74	0.81	0.78
$m2_{w^1}$	0.71	0.70	0.69	0.77	0.78
$m2_{w^2}$	0.72	0.72	0.68	0.80	0.78
$m2_c$	0.72	0.72	0.71	0.80	0.78
$m2_c^I$	0.72	0.72	0.71	0.80	0.78

Table 6.4: *(All wind farms) Coefficient of determination (R^2) for the single wind speed model without intercept (6.11) or with intercept (6.14) using either wind speed 1 or 2 as regressors (labelled $m1_{w^i}$ and $m2_{w^i}$, where i is equal to either 1 or 2 for wind speed 1 or 2, respectively), for the combined models without intercept using estimated area wind speed from either (6.11) or (6.14) as regressors (labelled $m1_c$ and $m2_c$) and for the combined models with an intercept (labelled either $m1_c^I$ or $m2_c^I$). In all cases R^2 is estimated on basis of the validation data set as described in Section 5.4.*

When considering the single wind speed models (6.11) and (6.14) the table shows, that with the exception of Rejsby only small differences between using wind speed 1 or 2 as regressors are observed within the individual wind farms. It is also seen, that including an intercept term as in model "m2" results in a noticeable improvement comparing with model "m1" without intercept. Comparing the results for the two stage models makes it evident, that, if the single wind speed does not include an intercept term, it is beneficial to include an intercept in the combined model. Opposite it is also clear, that no significant improvement is achieved by including an intercept in the combined model if the single wind speed model already contains such a term. Comparing the results from the best of the two-stage models, "$m1_c^I$" and "$m2_c$", it is seen, that except for Hollandsbjerg only minor differences between the two models are observed. For Hollandsbjerg, though, the observed R^2 are clearly in favour of model "$m1_c^I$". Consequently the area wind speed used in Section 6.4.2 and 6.4.3

	Wind farm				
	DR	FJ	HO	RB	SY
$\hat{\beta}_0$	1.2546	1.0186	0.9150	1.2846	0.8361
$\hat{\beta}_1$	0.2280	0.7261	0.3918	0.0746	0.3314
$\hat{\beta}_2$	0.5180	0.0878	0.4297	0.7670	0.5155

Table 6.5: *(All wind farms) Estimated parameters in model (6.13).*

is estimated by applying "$m1_c^I$". The estimated model parameters in the combined model (6.13) are listed in Table 6.5 for the five wind farms.

The estimated variance of the model errors in model (6.11) to (6.16) is listed in Table E.1 for reference.

6.4.2 Identification and estimation of wind farm power curves

This section considers the relationship between power production in a wind farm and the related values of wind speed and direction in the area. The analysis is based on measured values of wind speed as well as the estimated area wind speed. Only measured values of wind direction is considered though. The relationship between power production and the analysis of wind speed and wind direction has also been estimated in the following. These estimates are primarily used in Section 6.4.3, which considers the prediction performance for the various models derived in this section. The analysis presented here is restricted to conditional parametric (non-linear) models describing the static relations between the dependent (power) and independent variables (wind speed and direction). The distribution of the wind speed measurements where only a (very) small fraction of the observations are in the upper range with full production in the wind farms implies that an increased uncertainty in the estimation relationship must be expected for the higher wind speeds. This section focuses on the static relationship between the dependent and the independent variables and thus only off-line estimation techniques will be used in this section.

A simple relationship between power production and wind speed without wind direction dependency is given by

$$p_t = b_0(w_t^i) + e_t \tag{6.17}$$

where p_t is the observed power production at time t, w_t^i is either wind speed 1 or 2, the area wind speed or the analysis wind speed at time t, $b_0()$ is a function (power curve) to be estimated and e_t is a noise term. (6.17) has been estimated using local regression with a second order polynomial approximation and fixed bandwidth, where the optimal bandwidth has been been found by optimization for each model using the procedure described in Section 5.4. Figure 6.11 shows the estimated power curves for the Rejsby wind farm when wind speed 1 and 2, the area wind wind speed and the analysis wind speed are used as input to (6.17). Similar plots for the remaining four wind farms are found in the Figures E.1, E.9, E.17 and E.28 in Appendix E.

When interpreting the estimated power curves it must be taken into consideration that the number of data points behind the estimate is very limited for the higher wind speeds. This

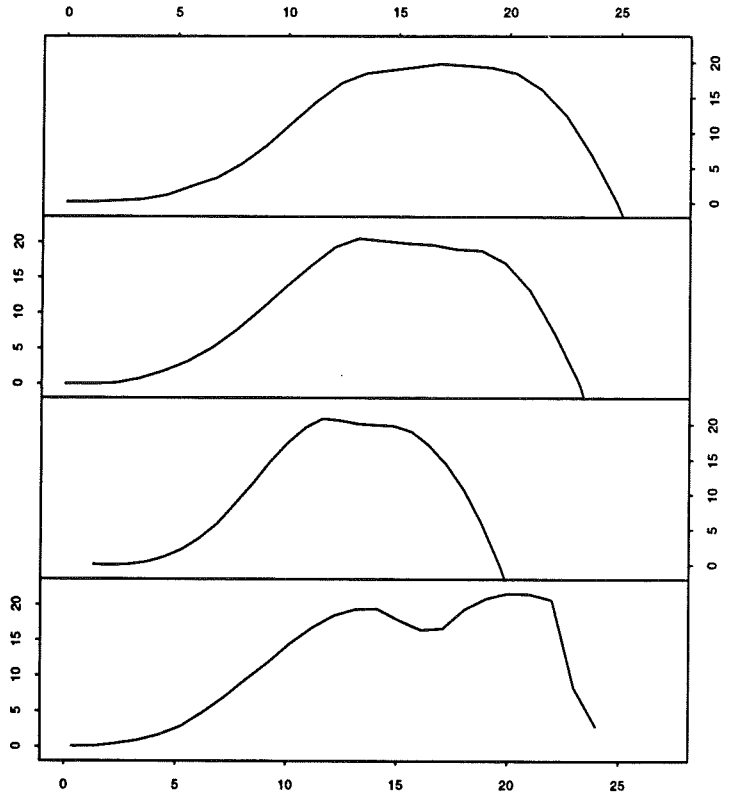

Figure 6.11: *(Rejsby) Estimated power curve as a function of from top to bottom wind speed 1 and 2, estimated area wind speed and the analysis.*

is in particular true for the power curve estimated for w^1 at Hollandsbjerg and for all wind speeds at Rejsby. In both cases the estimation has closer resemblance to an extrapolation for the top 5 m/s and should be regarded as such.

Comparing the power curves estimated on the basis of the two measured wind speeds with the stated power curves for the wind turbines installed in the five wind farms, see the Figures A.2, A.4, A.6, A.8 and A.10, it is seen that the maximum power production for the estimated power curve in most cases is reached at wind speeds well below maximum power production for the stated power curve. Comparing the hub heights for the wind turbines and the anemometers there seems to be a good agreement between the differences in the estimated and stated power curves and the differences in hub heigh for anemometers and wind turbines:

- *Dræby.* The estimated power curves for the two wind speed measurements reach maximum production just above 12 m/s whereas the wind turbines according to the stated power curve reach maximum production at 15 m/s. This suggests that wind turbines are subjected to higher wind speeds than the anemometers which seems reasonable as the wind turbines have a hub height of 31 m compared to 25 m for the anemometers. The estimated maximum production lies approximate 3% above rated maximum production[7] for the wind farm.

[7]The rated maximum production for a wind farm is simple calculated as the sum of the rated maximum

- *Fjaldene.* For the estimated power curves the maximum power production is obtained for measured wind speeds above 12 m/s compared to a maximum production for wind speeds above 15 m/s for the stated power curve. Again this corresponds well with the fact that the anemometers at 32 m above ground level (a.g.l.) are placed below the 42 m hub height of the wind turbines. The estimated maximum production is approximately 4% below the rated maximum power production for the wind farm.

- *Hollandsbjerg.* The top part of the estimated power curve is ill defined for wind speed 1 and it is thus difficult to judge exactly when maximum production is reached except that it happens somewhere above 15 m/s. For the power curve estimated on basis of wind speed 2 maximum power is achieved at 12 m/s. The wind turbines reach maximum production at 16 m/s according to the stated power curve so it seems that anemometer 1 at 26 m a.g.l. is subjected to similar or higher wind speeds and anemometer 2 at 13 m a.g.l. to lower wind speeds than seen by the wind turbines. As the wind turbines has a hub height of 26 m a.g.l. this seems reasonable. The estimated maximum production is approximately 9% below the rated maximum production for the wind farm.

- *Rejsby.* The estimated maximum power production is reached at an approximate wind speed at 14 m/s for both measured wind speeds – the top part of the estimated curve is not very well defined for wind speed 1 though. As the stated power curve for the wind turbines has maximum power at 15 m/s this indicates that the anemometers and the wind turbines are subjected to more or less the same wind speeds. This seems reasonable as the anemometers have a hub height of respectively 45 m and 46 m a.g.l. compared to a hub height of 46 m a.g.l. for the wind turbines. The estimated maximum power is close to 12% below the rated maximum production for the wind farm.

- *Sydthy.* For both wind speeds the estimated power curves reach maximum power at an approximate wind speed of 11 m/s whereas the stated power curve achieves its maximum power at 15 m/s. This corresponds well with the fact that the anemometers are located 20 m a.g.l. whereas the wind turbines have a hub height of 32 m a.g.l. The estimated maximum power is approximately 6% below the rated maximum production for the wind farm.

Comparing the power curves estimated on the basis of the area wind speed with the stated power curves it is seen that with the exception of Dræby there is a high degree of conformity between the shape of stated wind turbine power curve and estimated wind farm power curve. For all cases the maximum power production for the estimated power curve is reached at wind speeds below maximum power production for the stated power curve, though.

The power curves estimated on the basis of the analysis is less well defined than the power curves estimated on the basis of observed wind speeds[8]. Considering the added uncertainty

power production for the individual wind turbines in the wind farm – thus the influence of the layout of the wind farm is not taken into consideration.

[8]That is if the shape of the stated power curves for the wind turbines is expected to be reflected in the shape of power curve for the entire wind farm.

which arises when the power curve is estimated on basis of the analysis this is only to be expected.

The coefficient of determination for model (6.17) is listed in Table 6.6 labelled "$m1$" for the five wind farms with wind speed 1 ("w^1"), wind speed 2 ("w^2") as well as the area wind speed ("w^a") as input. In all cases R^2 is estimated on basis of the validation data set as described in Section 5.4.

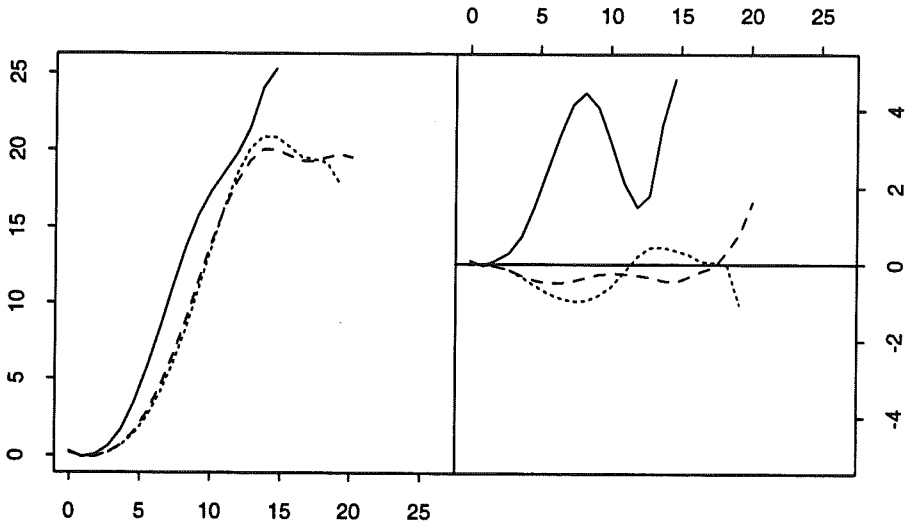

Figure 6.12: *(Rejsby) Power curve as a function of wind speed 2 and estimated locally around a wind direction of* 90° *(full line),* 200° *(dotted line) and* 300° *(dashed line). Each of the three curves is estimated using a fixed bandwidth of* 30° *for the wind direction and 5 m/s for the wind speed. Based on the plot the indicator function* $I(w_t^2)$ *used in (6.18) is set to 1 in the interval [2 m/s; 12 m/s] and 0 otherwise.*

In order to identify the characteristics of the wind direction dependencies power curves is estimated for specific wind directions. For each of the five wind farms three wind directions with a sufficient representation of high wind speeds in the vicinity is selected. Four power curves are then estimated: One "base" curve using the entire data set and the wind direction dependent curves with a fixed bandwidth of 30° around the selected wind directions. All the power curves are estimated using a fixed bandwidth of 5 m/s in the wind speed "dimension". The three wind direction dependent curves as well as the difference between base curve and the three wind direction dependent curves are plotted in Figure 6.12 for wind speed 2 at Rejsby. Similar plots for the remaining wind farms and the measured wind speeds, the area wind speed and the analysis are found from Figure E.2 and onwards in Appendix E.

When evaluating the wind direction dependencies using the aforementioned plots it must be taken into consideration that grouping the observations according to wind direction further diminishes the already small number of observations with a high wind speed for the individual groups. This may lead to poorly defined behavior in the high wind speed regime for the estimated curves – as confirmed by the plots where many examples of erratic behavior for the higher wind speeds are found.

Hence an upper limit on the wind speeds for which it is possible to estimate the wind speed dependency is introduced. Furthermore it is clear that below a certain wind speed

where power production ceases there will be no wind direction dependency in the power production. According to the plots this lower limit seems to be fairly independent of the wind direction.

Considering the wind direction dependency between these limits it is seen that for the great majority of the instances the observed pattern has a simple form which readily can be approximated by e.g. lower order polynomials. In order to model the influence of the wind direction model (6.17) is therefore extended with a polynomial term in wind speed where the coefficients are functions of wind direction. The model thus becomes

$$p_t = b_0(w_t^i) + I(w_t^i)\left[\sum_{j=0}^{N_p} b_1^j(\phi_t)(w_t^i)^j\right] + e_t \tag{6.18}$$

where ϕ_t is the observed wind direction, N_p is the order of the polynomial modelling of the wind direction dependency, $I()$ is an indicator function equal to 1 for wind speeds where the wind direction dependency should be modelled and zero otherwise, and finally $b_0()$ and $b_1^j()$ are functions of wind speed and wind direction, respectively, to be estimated. Model (6.18) belong to the model class named *additive models* in [Hastie and Tibshirani, 1990]. The overall model is estimated using the *back fitting* algorithm described in [Hastie and Tibshirani, 1990] wherein the individual terms have been estimated using local regression with a second order polynomial approximation and fixed bandwidth. By calculating the distances used in the estimation on a circle it is ensured, that the estimated functions $b_0()$ and $b_1()$ are continues between 0° and 360°. The optimal bandwidth has been been found by optimization for each model using the procedure described in Section 5.4. Figure 6.13 to 6.15 show the estimated power curves and wind direction dependencies for the Rejsby wind farm for N_p equal to 0, 1 and 2 when wind speed 1 and 2, the area wind speed and the analysis are used as input to (6.18). Similar plots for the remaining four wind farms are found in Figure E.6 to E.35 in Appendix E.

The coefficient of determination for model (6.18) is listed in Table 6.6 for the five wind farms labelled "$m2$", "$m3$" and "$m4$" for constant, first order and second order polynomial approximation of wind directions dependency, respectively. Results are listed when using wind speed 1 ("w^1"), wind speed 2 ("w^2") as well as the area wind speed ("w^a") as input. In all cases R^2 is estimated on basis of the validation data set as described in Section 5.4. Similarly Table E.2 in Appendix E lists the estimated model error variance.

The comments put forward regarding how the placement of the anemometers effects the estimated power curve given by (6.17) is also found to be valid for the estimates of the pure wind speed dependency, $b_0()$, in (6.18).

In general the estimated wind direction dependency displays a common pattern for a given wind speed and wind farm no matter whether a constant, first order or second order polynomial expansion is applied. In many cases the second order expansion shows a rather erratic behavior for the higher wind speeds indicating that the estimated wind direction dependency is unreliable for the higher wind speeds though. This notion is confirmed by Table E.2 where in most cases only minor decreases or direct increases in the estimated model error variance is seen when the order of the polynomial expansion of wind direction dependency is increased from first to second order. From Table E.2 it is seen that in all cases it is beneficial to extend the expansion of wind direction dependency from constant to first

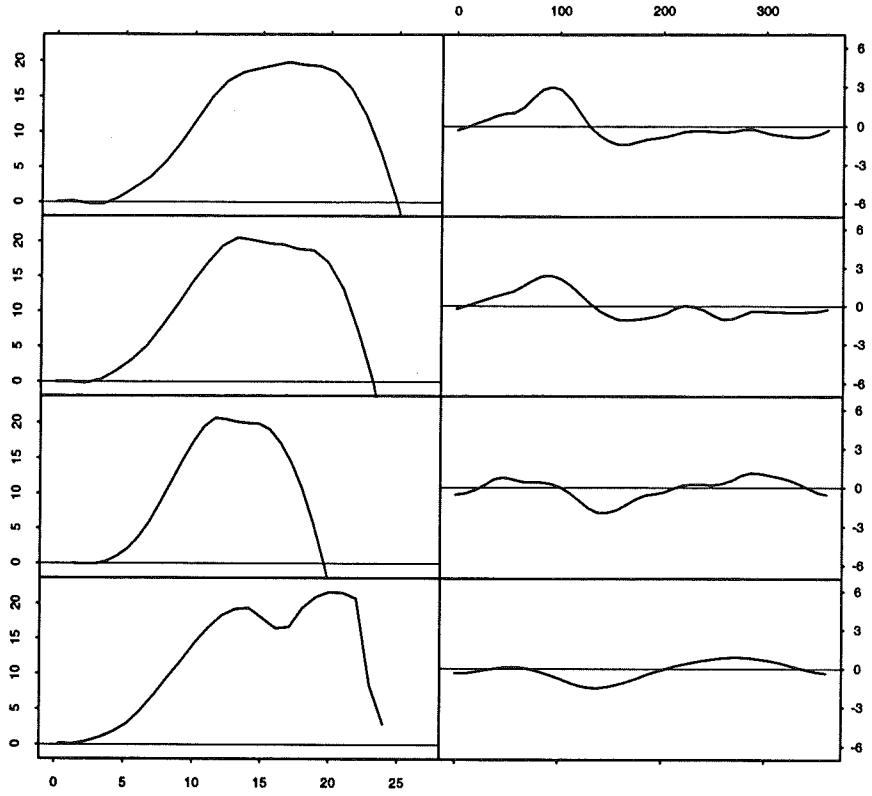

Figure 6.13: *(Rejsby) Estimated dependency on wind speed (left column) and wind direction (right column) in power curve model (6.18) with a constant approximation of the wind direction dependency. From top row to bottom row the estimates are calculated on the basis of wind speed 1 and 2, the area wind speed and the analysis.*

order. Thus it seems sensible to restrict model (6.18) to use first order expansion of wind direction dependency.

The estimated variance for the model errors is with the exception of Hollandsbjerg and to a lesser degree Rejsby comparable when the measured wind speeds are used as input to (6.17) and (6.18). For both Hollandsbjerg and Rejsby wind speed 1 shows markedly worse results compared to wind speed 2. The comparison of the results for "m1" and "m3" when measured wind speeds are used as input therefore take basis in the results obtained using wind speed 2. From Table E.2 it is seen that introducing wind direction dependency results in a reduction of model error variance ranging from 15% for Sydthy and up to 50% and 51% for respectively Dræby and Fjaldene. These findings correspond well to results obtained in a previously study, see [H. Madsen (Ed.), 1995], where wind farms at Mors and Ærø are investigated. When considering the estimated coefficient of determination in Table 6.6 values ranging from 0.97 for Dræby and Hollandsbjerg down to 0.91 for Sydthy are found for "m3".

The results obtained, when using the estimated area wind speed as input, do not give a clear picture of whether it is beneficial to use area wind speed in the estimation compared to measured wind speeds.

For the Dræby, Fjaldene, Rejsby and Sydthy wind farms it is seen that when the mea-

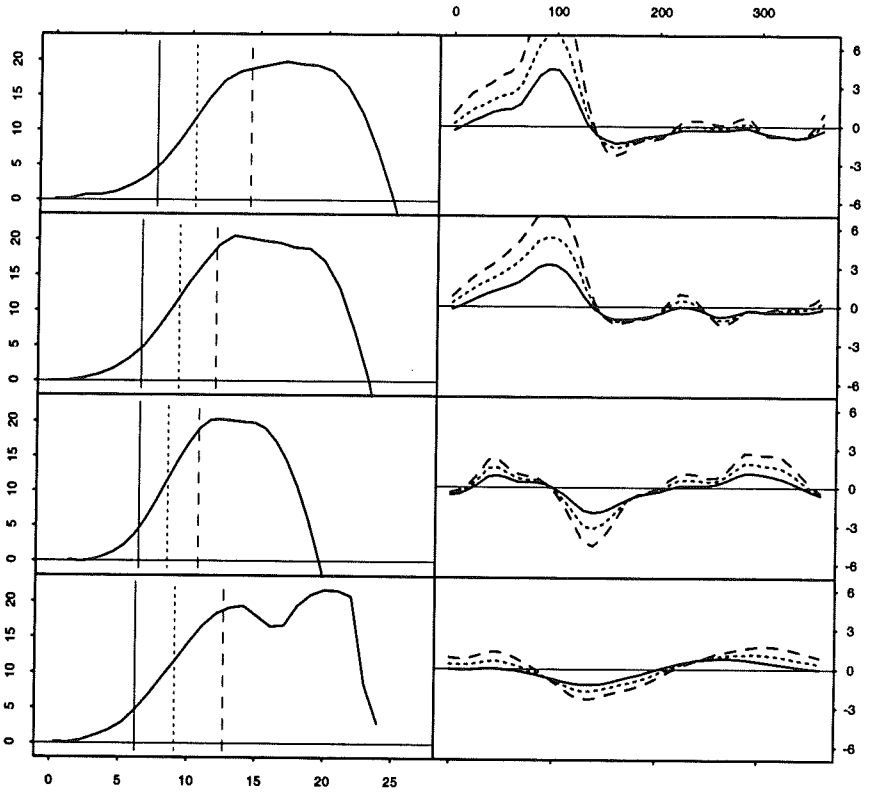

Figure 6.14: *(Rejsby) Estimated dependency on wind speed (left column) and wind direction (right column) in power curve model (6.18) with a first order polynomial approximation of the wind direction dependency. The three curves on the right hand plot gives the wind direction dependency at a wind speed corresponding to 20% (full line), 50% (dotted line) and 80% (dashed line) of rated power on the left hand curve. From top row to bottom row the estimates are calculated on the basis of wind speed 1 and 2, the area wind speed and the analysis.*

sured wind speeds are used as input to (6.18) the estimated wind direction dependency displays a similar pattern with only minor deviations between the two estimates. These four wind farms all have both their anemometers placed together in one meteorological tower at approximately the same height. This indicates that the differences in the wind speed measurements attributed to the location of the measurement equipment on the meteorological tower are either insignificant or difficult to model using (6.18) at least as long as the anemometers are placed at approximately the same height above ground level. Only for the Hollandsbjerg wind farm does the estimated wind direction dependency display a significant difference for the two measured wind speed, but this is attributed to the very distinct difference in the establishment of the two measurements. Here wind speed 1 is calculated as the average of two anemometers placed 26 m a.g.l. in two different meteorological towers situated in opposite ends of the wind farm whereas wind speed 2 is measured as normal by a single anemometer from a meteorological tower 13 m a.g.l. in the middle of the wind farm.

In general the wind direction dependency estimated using measured wind speeds as input does not give a clear indication of the situation or layout of the wind farm whereas local conditions influencing the anemometers them self are readily discerned. One reoccuring

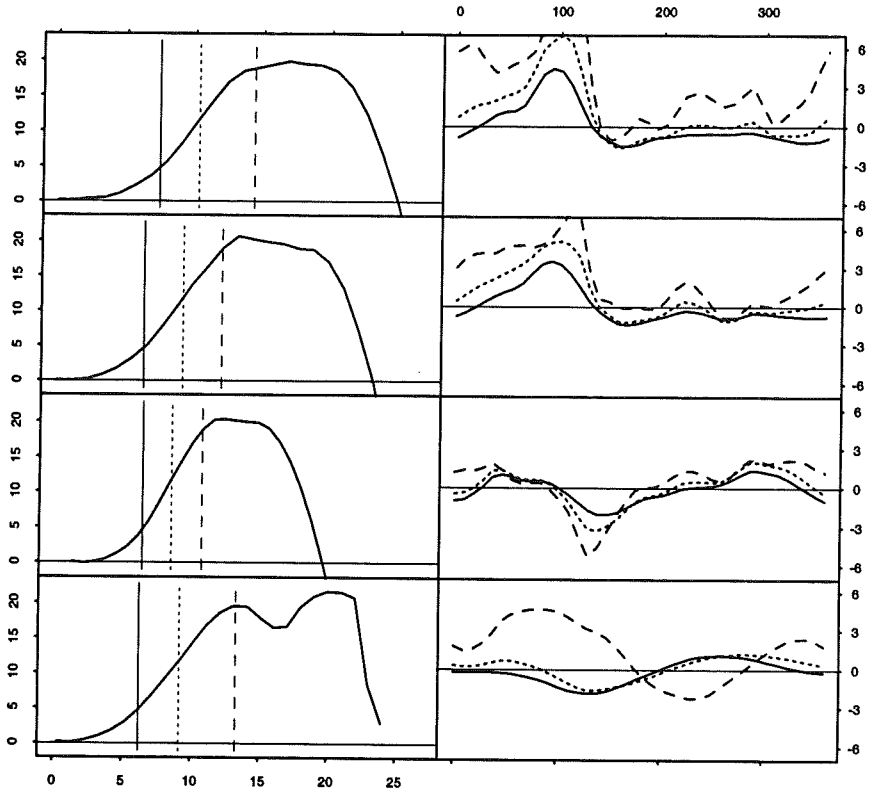

Figure 6.15: *(Rejsby) Estimated dependency on wind speed (left column) and wind direction (right column) in power curve model (6.18) with a second order polynomial approximation of the wind direction dependency. The three curves on the right hand plot gives the wind direction dependency at a wind speed corresponding to 20% (full line), 50% (dotted line) and 80% (dashed line) of rated power on the left hand curve. From top row to bottom row the estimates are calculated on the basis of wind speed 1 and 2, the area wind speed and the analysis.*

disturbance is the shading effect from wind turbines in the vicinity of the meteorological tower causing the anemometers to register an uncharacteristic low wind speed. The effect of this decrease in measured wind speed is that the wind direction dependency shows an *increase* in power production for the affected wind speeds. This phenomenon is clearly seen for Dræby at 220° and 315°, for Fjaldene at 50° and 300° and for Rejsby at 90°. The stated angels correspond to the wind directions for which the maximum effect of the shading is observed. For Sydthy a similar effect caused by shading from a small forest and Hurup town is observed for the northerly wind directions. The estimated wind direction dependency is, as demonstrated above, highly influenced by obstacles in the vicinity and thus no further attempts of analysing the estimated wind direction dependency will be made for the measured wind speeds.

The estimated wind direction dependency, when using area wind speed or the analysis wind speed as input to (6.18), seems in general to resemble what must be expected when the siting of the wind farms is considered and also the influence of the wind farm layout can in some cases be deducted from the estimated relationships. In the following some of the more specific results are outlined for each of the five wind farms:

	Wind farm				
Model	DR	FJ	HO	RB	SY
$m1\ w^1$	0.94	0.86	0.90	0.86	0.89
$m1\ w^2$	0.94	0.86	0.96	0.90	0.90
$m1\ w^a$	0.93	0.90	0.93	0.92	0.90
$m2\ w^1$	0.97	0.92	0.94	0.90	0.91
$m2\ w^2$	0.97	0.92	0.97	0.93	0.91
$m2\ w^a$	0.96	0.93	0.96	0.93	0.91
$m3\ w^1$	0.97	0.93	0.94	0.91	0.91
$m3\ w^2$	0.97	0.93	0.97	0.93	0.91
$m3\ w^a$	0.97	0.94	0.98	0.93	0.91
$m4\ w^1$	0.97	0.93	0.93	0.92	0.91
$m4\ w^2$	0.97	0.94	0.97	0.94	0.91
$m4\ w^a$	0.97	0.93	0.98	0.94	0.91

Table 6.6: *(All wind farms) Coefficient of determination (R^2) for the power curve model without wind direction dependency (6.17) or with wind direction dependency (6.18) using either wind speed 1 or 2, the area wind speed or the analysis as regressors. Label "m1" corresponds to (6.17) and "m2", "m3" and "m4" to (6.18) with constant, first order and second order polynomial expansion of the wind direction dependency, respectively. In all cases R^2 is estimated on basis of the validation data set as described in Section 5.4.The estimated variance for the observed power production is listed below for the five wind farms: $s^2_{DR} = 0.297[MW^2]$, $s^2_{FJ} = 4.31[MW^2]$, $s^2_{HO} = 0.664[MW^2]$, $s^2_{RB} = 43.9[MW^2]$, $s^2_{SY} = 3.71[MW^2]$.*

- *Dræby.* The dependency of wind speed and wind direction of the estimated power curve for Dræby is shown in Figure E.6 to E.8. For Dræby the influence of the wind farm layout is detected as two local minima at 130° and 290° corresponding to the north-west south-east axis along which the three rows of wind turbines are oriented. The more general pattern with a production above average for wind directions between 280° and 50° and below average for wind directions between 50° and 200° correspond to directions with on-shore respectively offshore winds for the Dræby wind farm sited on a northern shoreline of a small north-westward point.

- *Fjaldene.* The estimated wind direction dependency in the power curves for Fjaldene is shown in Figure E.14 to E.16. The estimated wind direction dependency using the area wind speed as input displays a pattern very similar to what is seen when the measured wind speeds are used as input. It is thus very likely that the influence of local conditions around the meteorological tower has not been eliminated from the area wind speed, which consequently is disregarded in the following. Considering the estimated wind direction dependency for the analysis two minima in the average power production is observed at 110° and 290°. This seems plausible as these angles corresponds to the north-west south-east orientation of the two rows of wind turbines at Fjaldene.

- *Hollandsbjerg.* The dependency of wind speed and wind direction in the estimated power curve for Hollandsbjerg is shown in Figure E.22 to E.24. Especially for the area wind speed the effects of the farm layout is here clearly seen in the wind direction dependency with (local) minima in the average power production at 120°, 300° and

360° corresponding to the orientation of the two rows of wind turbines which constitute the Hollandsbjerg wind farm. Layout or siting of the wind farms does not give any plausible explanation of the dip in average production found at 220° though.

- *Rejsby.* Figure 6.13 to 6.15 show plots of the estimated wind direction dependency in the power curves for Rejsby. From the plots is it seen that the power production is above average for wind directions between 200° and 330° and below average between 80° and 200°. As the Rejsby wind farm is situated some 1.5 km inland from the western coastline of Jutland this corresponds to a production above average for on-shore winds and a production below average for offshore winds.

- *Sydthy.* The estimated wind direction dependency in the power curves for Sydthy is shown in Figure E.33 to E.35. The figures show that the power production is above average for wind directions between 200° and 330° and below average for wind directions between 330° and 80°. When considering the siting of the Sydthy wind farm, which is placed along the western shoreline of a small peninsula, this seems reasonable as this correspond to directions with on-shore respectively offshore winds. It is difficult to see though what is accountable for the behavior between 80° and 200° where a small maximum is followed by another small minimum.

6.4.3 Predictions using the power curve

The wind farm power curve model developed in Section 6.4.2 is useful not only in describing the relationship between actual values of wind speed, wind direction and power production, but can also, given meteorological forecasts of wind speed and direction, be used to calculate forecasts of power production for the wind farm. The usefulness of such forecasts as input to dynamic forecasting models is investigated in Section 6.5.

The aim of the present section is to evaluate the performance for a selection of the wind farm power curve models developed in Section 6.4.2 when meteorological forecasts of wind speed and wind direction are used as input to the models in order to calculate power predictions for a wind farm.

The models selected are the power curve model (6.17) without wind direction dependency (model 1 or "m1") and the power curve model (6.18) with first order polynomial expansion of the wind direction dependency (model 3 or "m3"). The models have been estimated in Section 6.4.2 using either wind speed 2, the area wind speed or the analysis as input. The coefficient of determination for the power predictions are found in Table 6.7 for selected prediction horizons between 0 and 36 hours. The estimated prediction error variance for all models investigated in Section 6.4.2 are listed for reference in Table E.3 to E.7 in Appendix E.4.

The area wind speed has been constructed with the specific aim in mind, that models estimated using the area wind speed as input should be well suited for calculating power predictions by using meteorological forecasts as input to the models. From Table 6.7 it is seen that this is clearly not the case. The results obtained for the five wind farms with models estimated on basis of area wind speed are, with the exception of Fjaldene, noticeably inferior compared to the results obtained with models estimated on basis of the analysis.

		Prediction horizon $[\frac{1}{2}hours]$								
WF	Model	0	6	12	18	24	36	48	60	72
DR	$m1\ w^2$	0.71	0.68	0.66	0.65	0.63	0.59	0.54	0.48	0.41
DR	$m1\ w^a$	0.60	0.57	0.56	0.55	0.53	0.50	0.46	0.41	0.34
DR	$m1\ w^m$	0.71	0.67	0.66	0.64	0.62	0.59	0.54	0.47	0.40
DR	$m3\ w^2$	0.70	0.67	0.65	0.64	0.62	0.58	0.54	0.48	0.41
DR	$m3\ w^a$	0.60	0.57	0.57	0.55	0.54	0.51	0.46	0.40	0.33
DR	$m3\ w^m$	0.73	0.70	0.68	0.66	0.65	0.61	0.54	0.47	0.40
DR	$s_p^2[MW^2]$	0.363	0.362	0.361	0.361	0.362	0.363	0.363	0.364	0.365
FJ	$m1\ w^2$	0.77	0.75	0.74	0.74	0.73	0.68	0.63	0.55	0.50
FJ	$m1\ w^a$	0.77	0.75	0.74	0.74	0.72	0.68	0.62	0.54	0.49
FJ	$m1\ w^m$	0.78	0.76	0.75	0.75	0.74	0.70	0.64	0.56	0.51
FJ	$m3\ w^2$	0.74	0.71	0.70	0.70	0.69	0.64	0.58	0.50	0.45
FJ	$m3\ w^a$	0.71	0.68	0.67	0.67	0.65	0.61	0.55	0.46	0.42
FJ	$m3\ w^m$	0.79	0.76	0.75	0.75	0.74	0.69	0.63	0.56	0.51
FJ	$s_p^2[MW^2]$	4.92	4.91	4.90	4.90	4.91	4.93	4.93	4.95	4.96
HO	$m1\ w^2$	0.72	0.68	0.67	0.65	0.64	0.61	0.57	0.51	0.47
HO	$m1\ w^a$	0.67	0.64	0.63	0.62	0.60	0.56	0.52	0.47	0.42
HO	$m1\ w^m$	0.72	0.69	0.68	0.66	0.64	0.61	0.57	0.51	0.47
HO	$m3\ w^2$	0.69	0.66	0.65	0.63	0.62	0.59	0.56	0.51	0.46
HO	$m3\ w^a$	0.62	0.60	0.58	0.57	0.55	0.52	0.47	0.41	0.36
HO	$m3\ w^m$	0.74	0.72	0.71	0.69	0.67	0.63	0.59	0.53	0.48
HO	$s_p^2[MW^2]$	0.656	0.654	0.652	0.652	0.655	0.658	0.654	0.651	0.658
RB	$m1\ w^2$	0.77	0.75	0.73	0.71	0.69	0.65	0.60	0.54	0.48
RB	$m1\ w^a$	0.75	0.72	0.70	0.69	0.67	0.62	0.57	0.51	0.44
RB	$m1\ w^m$	0.77	0.75	0.73	0.71	0.70	0.65	0.61	0.55	0.48
RB	$m3\ w^2$	0.70	0.68	0.67	0.65	0.62	0.59	0.56	0.49	0.43
RB	$m3\ w^a$	0.76	0.73	0.72	0.70	0.69	0.63	0.58	0.51	0.44
RB	$m3\ w^m$	0.78	0.75	0.74	0.72	0.71	0.66	0.61	0.55	0.48
RB	$s_p^2[MW^2]$	41.30	41.3	41.2	41.2	41.2	41.3	41.3	41.6	41.8
SY	$m1\ w^2$	0.80	0.78	0.77	0.76	0.74	0.69	0.63	0.55	0.45
SY	$m1\ w^a$	0.78	0.75	0.74	0.73	0.72	0.65	0.59	0.50	0.39
SY	$m1\ w^m$	0.80	0.78	0.77	0.76	0.75	0.68	0.63	0.54	0.44
SY	$m3\ w^2$	0.78	0.76	0.75	0.74	0.73	0.67	0.60	0.52	0.43
SY	$m3\ w^a$	0.78	0.76	0.75	0.74	0.72	0.64	0.59	0.50	0.40
SY	$m3\ w^m$	0.81	0.79	0.78	0.77	0.75	0.69	0.63	0.55	0.46
SY	$s_p^2[MW^2]$	3.680	3.670	3.660	3.660	3.650	3.64	3.65	3.66	3.66

Table 6.7: *(All wind farms) Coefficient of determination (R^2) for model 1 without wind direction dependancy ("m1") and model 3 with first order polymomial approximation of the wind direction dependancy ("m3") from Section 6.4.2 when meteorological forecasts of wind speed and wind direction are used as input in order to calculate predictions of power production for the five wind farms. The models have been estimated using either wind speed 2, area wind speed or the analysis as input. In all cases R^2 is estimated on basis of the validation data set as described in Section 5.4. The estimated variance, s_p^2, for the observed power production in the five wind farms is also stated.*

Considering model 1 it is seen, that the prediction performance of models estimated on basis of wind speed 2 and the analysis is comparable. With the exception of Dræby it seems to be slightly advantageous to use models estimated on basis of the analysis though.

For models estimated with wind speed 2 as input it is also clear from the table, that the performance of the predictions is adversely affected when the wind direction dependency is included in the model. This is hardly surprising as the wind direction dependency estimated on basis of wind speed 2 to a large degree is dominated by local conditions affecting the anemometers rather than the actual power production in the wind farms. For further discussion of this topic refer to Section 6.4.2.

Considering models estimated using the analysis as input it is seen that, with the exception of Fjaldene, it is clearly beneficial to model the wind direction dependency and especially Dræby and Hollandsbjerg show a very distinct improvement in performance. There seems, however, to be a reduced improvement as the prediction horizon increases.

6.4.4 Conclusion and discussion

This section (6.4) considers the relationship between observed power production and observed as well as forecasted wind speed in five wind farms – Dræby, Fjaldene, Hollandsbjerg, Rejsby and Sydthy.

A derivative measure for the undisturbed wind field just above the area wind speed – the area wind speed – is suggested. The area wind speed is estimated on basis of a model describing the relationship between the HIRLAM analysis (or 0 hour forecast) of the wind speed in a wind farm and the local observations of the two wind speeds as well as the wind direction. The objective is to use the area wind speed to estimate a power curve for the wind farm which reflects the layout of the wind farm and the effects of the surroundings, but still is unaffected by local phenomena in the vicinity of the anemometers.

Power curves describing the relationship between observed power production and observed wind speeds, area wind speed as well as the HIRLAM analysis of the wind speed have been estimated using non-linear models. Models with as well as without wind direction dependency have been considered.

The power curves without wind direction dependancy and estimated using the observed wind speeds as input seems to give a good description of the physics in the wind farms. The differences between the estimated power curves for the wind farms and the power curve expected when considering the stated power curve given by the manufacture of the wind turbines in the wind farm can to a large extent be attributed to differences in hub height between wind turbines and anemometers. Furthermore there is also a good resemblence in curve shape and maximum power production between the estimated and expected power curves. Coefficient of determination (R^2) for the estimated power curve models range from 0.86 up to 0.96 depending on wind farm and the wind speed used as input.

When considering the wind direction dependant power curves the estimated wind direction dependency seeems to give a good indication of physical conditions in the wind farms. In general the wind direction dependency estimated using measured wind speeds as input does not give a clear indication of the situation or layout of the wind farm whereas local conditions influencing the anemometers them self such as shading effects from nearby wind turbines are readily discerned. The wind direction dependency estimated using area wind

speed or the analysis wind speed as input by contrast seems to resemble what must be expected when the siting of the wind farms is considered and also the influence of the wind farm layout can in some cases be deducted. When comparing with the power curves estimated without wind direction dependencies improvements in R^2 ranging from 0.01 to 0.07 depending on wind farm and wind speed used as input are observed.

The results obtained, when using the estimated area wind speed as input, do not give a clear picture of whether it is beneficial to use area wind speed in the estimation compared to measured wind speeds. As expected, though, the use of the area wind speed as input seems to reduce the wind direction dependancy in the power curves for most of the wind farms.

The performance of the power curve models have been evaluated when using meteorological forecasts of wind speed and direction as input in order to calculate predictions of the power production for the wind farms. The power curves models investigated are the power curve model without wind direction dependency as well as the most promissing of the wind direction dependant models estimated using either wind speed 2, the area wind speed or the analysis as input. The results have been evaluated using R^2 as a measure.

When comparing the R^2 obtained for the models estimated using the area wind speed as input with the R^2 for the models estimated on basis of the analysis it is readily seen that the analysis models show a markedly better performance in all cases except Fjaldene where only a minor improvement is seen.

In the context of prediction it seems generally to be advantageous to use models estimated on basis of the analysis and this is especially true for the models with wind direction dependency. Furthermore it is found that, with the exception of Fjaldene, it is clearly beneficial to model the wind direction dependency and especially Dræby and Hollandsbjerg show a very distinct improvement in performance. There seems, however, to be a reduced improvement as the prediction horizon increases. For the two prediction horizons 0 hours and 36 hours the R^2 values range from between 0.73 and 0.81 for Dræby and Sydthy, respectively, and down to between 0.40 and 0.51 for Dræby and Fjaldene, respectively.

6.5 Power prediction models

This section presents results concerning the issue of modelling and predicting the power production in a wind farm. The considered models take local measurements of power, wind speed and wind direction as well as forecasted values of wind speed and wind direction as input. The study is based on the half hourly data set described in Section 6.3, where the meteorological forecasts are interpolated between forecast updates as well as within the hourly steps in an individual update and the measurements are subsampled.

The models are all linear in the parameters and the parameter estimation is conducted using the adaptive on-line method (RLS estimation) described in Section 5.1.2. The prediction horizon range from half an hour to 39 hours in half hourly steps, thus the prediction horizon for the models investigated range from 1-step to 78-step.

Three different approaches for formulating multi step prediction models can be conceived:

1. The model is formulated and estimated as a 1-step prediction model. The k-step ($k \geq 2$) predictions are then obtained by using the 1-step prediction model recursively.

2. The model is formulated as a 1-step prediction model. The k-step prediction model is then formulated explicitly as a function of the parameters in the 1-step prediction model.

3. The model is formulated directly as a k-step prediction model.

The advantage of the first two methods is that most of the standard time series analysis tools are best suited for 1-step prediction models. The disadvantage of method 1) is that the recursive use of an insufficient model will, as the prediction horizon is increased, lead to a too high increase in the discrepancy between the predicted and the observed values. For the second approach the disadvantage is that the k-step prediction model is formulated as a non-linear (and for higher k rather complex) function of the parameters belonging to the 1-step prediction model. This means that the approach is unsuitable for RLS estimation and often even for LS estimation.

The third approach suffers from none of the previously mentioned drawbacks. First of all it is possible to formulate linear models and secondly different prediction horizons can be covered by different models which match the model structure needed for the prediction horizon. Combined with adaptive estimation of the model parameters this enables the modelling system to cope with slowly time varying dynamics. The disadvantage of the third method is, as previously mentioned, that many of the time series analysis tools are best suited for 1-step prediction models. The model development thus becomes more like a "trial and error" approach.

For the reasons mentioned above all prediction models in the following have been formulated directly as k-step prediction models.

The considered models all belong to the class of autoregressive models with exogenous input, where the input is transformed values of locally measured and forecasted wind speeds[9].

[9]The transformation of wind speed is necessary, as the relationship between power production and wind speed is non-linear.

In Figure 6.16 scatter plots of observed power versus forecasted wind speed for selected forecast horizons are shown for the Rejsby wind farm. The line is the estimated relationship using local regression with second order polynomial approximation as described in Section 5.2.1. The bandwidth used in the estimation is found by optimization for the individual forecast horizons using the procedure described in Section 5.4. The corresponding plots for the wind farms at Dræby, Fjaldene, Hollandsbjerg and Sydthy are found in Figure F.1 to F.4 in Appendix F. From the figures it is seen, that the estimated relationship between observed power and forecasted wind speed depends on the forecast horizon. For Fjaldene, Rejsby and Sydthy the estimated curves still resemble the power curves previously estimated in Section 6.4.2, but with growing distortion as the forecast horizon increases. For Dræby and Hollandsbjerg the non-linearity in the relationship between observed power and forecasted wind speed seems more appropriately approximated by a second order expansion of wind speed than by a power curve. The models investigated in the following employ either a second order expansion or the power curves estimated in Section 6.4.2 in the transformation of wind speed. An alternative approach is to estimate a power curve for the individual forecast horizons. This has not been considered further, as the computational requirements are assessed to be too high to render the implementation of such an approach practical.

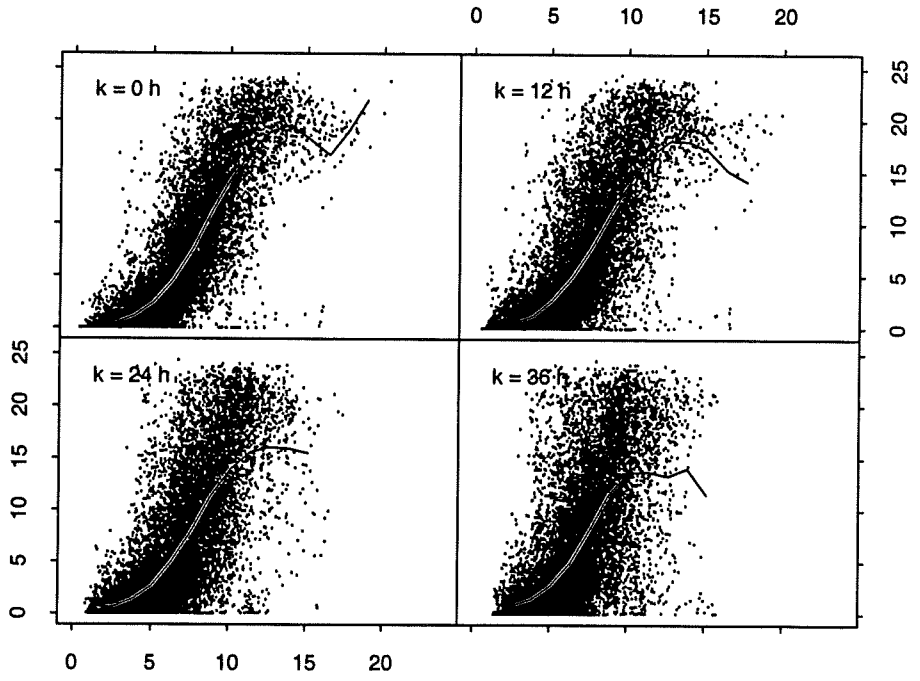

Figure 6.16: *(Rejsby) Observed power production [MW] versus forecasted wind speed [m/s] for a forecast horizon of 0 hours (top left), 12 hours (top right), 24 hours (bottom left) and 36 hours (bottom right). The line is the estimated relationship using local regression and 2. order polynomial approximation with a bandwidth of 3.4, 5.1, 4.6 and 4.1 [m/s] for the 0, 12, 24 and 36 hours forecasts, respectively.*

Models fitted to the original power series as well as models fitted to the square root transformed power series are considered. The square root transformation of power is motivated by the skew density of the power distribution (see e.g. [H. Madsen (Ed.), 1995] or

[Joensen, 1997]), but, as the model is fitted to the transformed power series, the prediction performance in the original power series must be expected to be (slightly) compromised.

When a model fitted to the square root transformed power series is used to predict in the original power series, a systematic bias is introduced in the predictions, and in [Joensen, 1997] it is suggested to eliminate this bias. The calculation of the correction necessary is in general complicated, but in [Tong, 1990] the following second order Taylor approximation of the correction term is proposed

$$\begin{aligned} y &= f(x) \\ g &= f^{-1} \\ E[x_{t+k}|t] &= E[g(y_{t+k})|t] \\ &\doteq g(\hat{y}_{t+k}) + E[(y_{t+k} - \hat{y}_{t+k})g'(\hat{y}_{t+k})|t] + \frac{1}{2}E[(y_{t+k} - \hat{y}_{t+k})^2 g''(\hat{y}_{t+k})|t] \\ &= g(\hat{y}_{t+k}) + \frac{1}{2}g''(\hat{y}_{t+k})V[\hat{e}^y_{t+k}|t] \end{aligned} \tag{6.19}$$

where x and y is the original and transformed process, respectively, f is the transformation function, $\hat{y}_{t+k}$ is the k-step prediction of y given at time t and finally $\hat{e}^y_{t+k}$ is the k-step prediction error. If the prediction errors can be assumed identically distributed and thus have a time-invariant variance, (6.19) reduces to

$$E[x_{t+k}|t] \doteq g(\hat{y}_{t+k}) + \frac{1}{2}g''(\hat{y}_{t+k})V[\hat{e}^y_k] \tag{6.20}$$

where the term $V[\hat{e}^y_k]$ now is (approximately) time-invariant.

Using (6.20) the following bias correction for power predictions based on models fitted to the square root transformed power series ($f = \sqrt{}$) is obtained

$$\hat{p}_{t+k} = \begin{cases} (\widehat{\sqrt{p_{t+k}}})^2 + s^2_{\sqrt{p}} & \text{if } \widehat{\sqrt{p_{t+k}}} >= 0 \\ s^2_{\sqrt{p}} - (\widehat{\sqrt{p_{t+k}}})^2 & \text{if } -s^2_{\sqrt{p}} < \widehat{\sqrt{p_{t+k}}} < 0 \\ 0 & \text{if } \widehat{\sqrt{p_{t+k}}} \leq -s^2_{\sqrt{p}} \end{cases}$$

where $\hat{p}_{t+k}$ is untransformed k-step power prediction, $\widehat{\sqrt{p_{t+k}}}$ is the k-step prediction in the square root transformed power series, and $s^2_{\sqrt{p}}$ is the estimated prediction error variance in the square root transformed power series.

The results for two models suggested in previous studies are listed for reference. The models, which are denoted $WPPT1$ and $WPPT2$ in the following, were found to be the most suitable in [H. Madsen (Ed.), 1995] and [Nielsen and Madsen, 1996], respectively. The $WPPT1$ model given as

$$\begin{aligned} \sqrt{p_{t+k}} &= a_1\sqrt{p_t} + b^o_1\sqrt{w_t} + b^o_2 w_t + \\ &\quad c^c_1 \cos\frac{2\pi h^{24}_{t+k}}{24} + c^s_1 \sin\frac{2\pi h^{24}_{t+k}}{24} + m + e_{t+k} \end{aligned} \tag{6.21}$$

is based entirely on local measurements in the wind farm, whereas the $WPPT2$ model given

as

$$\sqrt{p_{t+k}} = a_1\sqrt{p_t} + b_2^o w_t + b_1^m\sqrt{w_{t+k|t}^m} + b_2^m w_{t+k|t}^m + c_1^c \cos\frac{2\pi h_{t+k}^{24}}{24} + c_1^s \sin\frac{2\pi h_{t+k}^{24}}{24} + m + e_{t+k} \quad (6.22)$$

also utilizes forecasts of wind speed from the national weather service. Here p_t is the observed power at time t, w_t is the observed wind speed at time t, $w_{t+k|t}^m$ is the forecasted wind speed at $t+k$ given at time t, h_{t+k}^{24} is time of day at time $t+k$, e_{t+k} is a noise term, and a_1, b_2^o, b_1^m, b_2^m, c_1^c, c_1^s and m are the time-varying model parameters to be estimated. In the previous model studies it has not been possible to determine optimal forgetting factors for model (6.21) and (6.22). Instead a forgetting factor of $\lambda = 0.999$ has been used in the estimation for all prediction horizons.

Also the results for the naive or persistent predictor

$$p_{t+k} = p_t + e_{t+k} \quad (6.23)$$

are stated for reference. The naive predictor is discussed more comprehensively in Section 5.3.2.

The model selection procedure as well as the various full models[10], within which the model selection takes place, are described in Section 6.5.1, and the results obtained by the selected models are found in Section 6.5.2.

6.5.1 Model selection

Two widely used methods in the development of statistical models are forward and backward selection. In the forward selection procedure the model terms are added one at a time starting with the most significant term, until no further terms are significant, whereas the backward selection procedure starts with the full model and then removes the least significant terms, until all terms remaining in the model are significant. It is well known, however, that a model selection procedure based on either forward or backward selection often will fail to identify the optimal model (See e.g. [Miller, 1990]). The optimal model is in this case the model, which minimizes the least squares error using either a validation data set or forward validation and thus only contains significant terms. Therefore the model selection procedure applied in this study is based upon exhaustive search among all possible combinations of the model terms in the full model. As an exhaustive search in the set of models corresponding to a single prediction horizon is very time consuming, computational wise, the model selection is only conducted for a subset of the prediction horizons consisting of the 1, 3, 6, 9, 12, 18, 24, 30 and 36 hours prediction horizons. For each prediction horizon k in the subset the following model selection procedure is used:

- First the full model containing all possible terms, which should be investigated, is established.

[10]The full model here denotes the model containing all terms, which aspire to be included in the final model.

- The model selection must be expected to be influenced by the forgetting factor (λ) used in the RLS estimation. It is therefore important, that a sensible λ is chosen prior to the model selection. This is necessary, as even for a rather limited number of terms in the full model, say 10 to 15 terms, the number of possible combinations is to large to allow an optimization of the forgetting factor for the individual models. For this aim a model containing a representative set of the terms in the full model is selected, and an "optimal" λ is established for this model. This is accomplished by optimizing λ for each of the five wind farms and then calculate the "optimal" λ as the average of these five optimal λ's.

- Employing the previously optimized forgetting factor the model set consisting of all possible permutations of the terms in the full model are estimated and evaluated. Using mean square error as a performance measure the five most promising models for each of the five wind farms are selected and the results are summarized in a table for each k.

- From the table the final model is constructed. A term is included in the model, if it appears in more than half (13 or more) of the models listed in the table.

- Once again the optimal λ is determined using the same procedure as applied previously, but this time for the final model.

In the following three different (full) models are subjected to the model selection scheme described above. The predictions for all three models are restricted, so that they always are positive and less than or equal to the rated maximum power for the wind farm in question.

The full model 1 is an extension of the $WPPT2$ model (6.22), where the autoregressive part of the model is increased, the transformation of observed wind speed to power is by the full second order polynomial expansion of wind speed and finally the modelling of the diurnal profile is extended to a third order Fourier transformation. The full model thus becomes

$$\begin{aligned}\sqrt{p_{t+k}} &= a_1\sqrt{p_t} + a_2\sqrt{p_{t-1}} + \\ &\quad b_1^o\sqrt{w_t} + b_2^o w_t + b_1^m\sqrt{w_{t+k|t}^m} + b_2^m w_{t+k|t}^m + \\ &\quad \sum_{i=1}^{3}[c_i^c \cos\frac{2i\pi h_{t+k}^{24}}{24} + c_i^s \sin\frac{2i\pi h_{t+k}^{24}}{24}] + m + e_{t+k}\end{aligned} \tag{6.24}$$

where a_i, b_i^o, b_i^m, $i \in [1,2]$, c_j^c, c_j^s, $j \in [1,2,3]$ and m are the time-varying model parameters to be estimated.

For the investigated subset of prediction horizons the best five sub-models of (6.24) for each of the five wind farms are listed in the Tables F.2 to F.10 and using the tables the final model 1 listed in Table 6.8 is selected. The coefficient of determination for the final model is found in Table 6.11 labelled "m1".

k	λ	Model
2	0.9978	$1+\sqrt{p_t}+\sqrt{p_{t-1}}+\sqrt{w^m_{t+2\|t}}+w^m_{t+2\|t}+\cos^{24}_{t+2}+\sin^{24}_{t+2}$
6	0.9984	$1+\sqrt{p_t}+\sqrt{p_{t-1}}+\sqrt{w^m_{t+6\|t}}+w^m_{t+6\|t}+\cos^{24}_{t+6}+\sin^{24}_{t+6}$
12	0.9987	$1+\sqrt{p_t}+\sqrt{w^m_{t+12\|t}}+w^m_{t+12\|t}+\cos^{24}_{t+12}+\sin^{24}_{t+12}$
18	0.9988	$1+\sqrt{p_t}+w_t+\sqrt{w^m_{t+18\|t}}+w^m_{t+18\|t}+\cos^{24}_{t+18}+\sin^{24}_{t+18}+\cos^{12}_{t+18}+\sin^{12}_{t+18}$
24	0.9991	$1+\sqrt{p_t}+\sqrt{w_t}+\sqrt{w^m_{t+24\|t}}+w^m_{t+24\|t}+\cos^{24}_{t+24}+\sin^{24}_{t+24}$
36	0.9993	$1+\sqrt{p_t}+\sqrt{w^m_{t+36\|t}}+w^m_{t+36\|t}+\cos^{24}_{t+36}+\sin^{24}_{t+36}+\cos^{12}_{t+36}+\sin^{12}_{t+36}$
48	0.9994	$1+\sqrt{p_t}+\sqrt{w^m_{t+48\|t}}+w^m_{t+48\|t}+\cos^{24}_{t+48}+\sin^{24}_{t+48}+\cos^{12}_{t+48}+\sin^{12}_{t+48}$
60	0.9995	$1+\sqrt{p_t}+\sqrt{w^m_{t+60\|t}}+w^m_{t+60\|t}+\cos^{24}_{t+60}+\sin^{24}_{t+60}+\cos^{12}_{t+60}+\sin^{12}_{t+60}$
72	0.9994	$1+\sqrt{p_t}+\sqrt{w^m_{t+72\|t}}+w^m_{t+72\|t}+\cos^{24}_{t+72}+\sin^{24}_{t+72}$

Table 6.8: *(Model 1) The optimal models with corresponding optimal forgetting factors, λ, identified from the full model given by (6.24) and listed for a subset of the prediction horizons, k (in half hours). For clarity the model parameters are omitted.*

The full model 2 contains the same model terms as (6.24), but without the square root transformation of power and wind speed terms. The full model may be formulated as

$$\begin{aligned} p_{t+k} &= a_1 p_t + a_2 p_{t-1} + \\ &\quad b^o_1 w_t + b^o_2 (w_t)^2 + b^m_1 w^m_{t+k|t} + b^m_2 (w^m_{t+k|t})^2 + \\ &\quad \sum_{i=1}^{3} [c^c_i \cos \frac{2i\pi h^{24}_{t+k}}{24} + c^s_i \sin \frac{2i\pi h^{24}_{t+k}}{24}] + m + e_{t+k} \end{aligned} \tag{6.25}$$

where a_i, b^o_i, b^m_i, $i \in [1,2]$, c^c_j, c^s_j, $j \in [1,2,3]$ and m are the time-varying model parameters to be estimated.

Using the Tables F.12 to F.20, where the best five sub-models of (6.25) are listed, the final model 2 in Table 6.9 is chosen. The coefficient of determination for the final model is found in Table 6.11 labelled "m2".

The full model 3 employs the power curves estimated in Section 6.4.2 in the transformation of observed and forecasted wind speed to power and contains also an additional term

k	λ	Model
2	0.9981	$1 + p_t + p_{t-1} + w^m_{t+2\|t} + (w^m_{t+2\|t})^2 + \cos^{24}_{t+2} + \sin^{24}_{t+2}$
6	0.9984	$1 + p_t + p_{t-1} + w^m_{t+6\|t} + (w^m_{t+6\|t})^2 + \cos^{24}_{t+6} + \sin^{24}_{t+6}$
12	0.9988	$1 + p_t + w^m_{t+12\|t} + (w^m_{t+12\|t})^2 + \cos^{24}_{t+12} + \sin^{24}_{t+12} + \cos^{12}_{t+12} + \sin^{12}_{t+12}$
18	0.9990	$1 + p_t + w_t + w^m_{t+18\|t} + (w^m_{t+18\|t})^2 + \cos^{24}_{t+18} + \sin^{24}_{t+18} + \cos^{12}_{t+18} + \sin^{12}_{t+18}$
24	0.9989	$1 + w_t + w^m_{t+24\|t} + (w^m_{t+24\|t})^2 + \cos^{24}_{t+24} + \sin^{24}_{t+24} + \cos^{12}_{t+24} + \sin^{12}_{t+24}$
36	0.9991	$1 + w^m_{t+36\|t} + (w^m_{t+36\|t})^2 + \cos^{24}_{t+36} + \sin^{24}_{t+36} + \cos^{12}_{t+36} + \sin^{12}_{t+36}$
48	0.9994	$1 + w^m_{t+48\|t} + (w^m_{t+48\|t})^2 + \cos^{24}_{t+48} + \sin^{24}_{t+48} + \cos^{12}_{t+48} + \sin^{12}_{t+48}$
60	0.9995	$1 + w^m_{t+60\|t} + (w^m_{t+60\|t})^2 + \cos^{24}_{t+60} + \sin^{24}_{t+60} + \cos^{12}_{t+60} + \sin^{12}_{t+60}$
72	0.9994	$1 + w^m_{t+72\|t} + (w^m_{t+72\|t})^2 + \cos^{24}_{t+72} + \sin^{24}_{t+72} + \cos^{12}_{t+72} + \sin^{12}_{t+72}$

Table 6.9: *(Model 2) The optimal models with corresponding optimal forgetting factors, λ, identified from the full model given by (6.25) and listed for a subset of the prediction horizons, k (in half hours). For clarity the model parameters are omitted.*

in the diurnal profile. The full model is given as

$$\begin{aligned} p_{t+k} &= a_1 p_t + a_2 p_{t-1} + \\ &\quad b^o_1 P^o_{pc}(w_t, \theta_t) + b^m_1 P^m_{pc}(w_{t+k|t}, \theta^m_{t+k|t}) + b^{24}_1 P_{di}(h^{24}_{t+k}) + \\ &\quad \sum_{i=1}^{3} [c^c_i \cos \frac{2i\pi h^{24}_{t+k}}{24} + c^s_i \sin \frac{2i\pi h^{24}_{t+k}}{24}] + m + e_{t+k} \end{aligned} \tag{6.26}$$

where a_1, b_2, b^o_1, b^m_1, c^c_i, c^s_i, $i \in [1,2,3]$ and m are the time-varying model parameters to be estimated. Furthermore P^o_{pc} and P^m_{pc} are the estimated power curve functions used in the transformation of observed and forecasted wind speed, respectively, and finally P_{di} is the diurnal variation in power production estimated using the model

$$\begin{aligned} p_{t+72} &= b_0(h^{24}_{t+72}, t) + e_t \\ P_{di}(h^{24}_{t+k}) &= \hat{b_0}(h^{24}_{t+k}, t) \end{aligned} \tag{6.27}$$

where b_0 is a time-varying coefficient function to be estimated. (6.27) is estimated by local regression using a second order polynomial approximation and a fixed bandwidth of 6 hours as described in Section 5.2.2. The forgetting factor used corresponds to a memory time constant of 3 weeks. By calculating the distances used in the estimation on a circle it is ensured, that the estimated functions $b_0()$ is continues between 00:00 and 24:00. Before (6.27) is used as input to (6.26), the diurnal mean of the estimate has to be removed in order not to disturb the estimation of the level parameter m.

k	λ	Model
2	0.9970	$p_t + p_{t-1} + p^m_{t+2\|t} + \cos^{24}_{t+2} + \sin^{24}_{t+2}$
6	0.9987	$1 + p_t + p^m_{t+6\|t} + \cos^{24}_{t+6} + \sin^{24}_{t+6} + \cos^{12}_{t+6} + \sin^{12}_{t+6}$
12	0.9990	$1 + p_t + p^m_{t+12\|t} + \cos^{24}_{t+12} + \sin^{24}_{t+12} + \cos^{12}_{t+12} + \sin^{12}_{t+12} + \cos^{8}_{t+12} + \sin^{8}_{t+12}$
18	0.9990	$p_t + p^m_{t+18\|t} + \cos^{24}_{t+18} + \sin^{24}_{t+18} + \cos^{12}_{t+18} + \sin^{12}_{t+18}$
24	0.9991	$p_t + p^m_{t+24\|t} + \cos^{24}_{t+24} + \sin^{24}_{t+24} + \cos^{12}_{t+24} + \sin^{12}_{t+24}$
36	0.9988	$p^m_{t+36\|t} + p^{24}_{t+36} + \cos^{24}_{t+36} + \sin^{24}_{t+36} + \cos^{12}_{t+36} + \sin^{12}_{t+36}$
48	0.9989	$1 + p^m_{t+48\|t} + p^{24}_{t+48} + \cos^{24}_{t+48} + \sin^{24}_{t+48} + \cos^{12}_{t+48} + \sin^{12}_{t+48}$
60	0.9986	$1 + p^m_{t+60\|t} + p^{24}_{t+60} + \cos^{24}_{t+60} + \sin^{24}_{t+60} + \cos^{12}_{t+60} + \sin^{12}_{t+60} + \cos^{8}_{t+60} + \sin^{8}_{t+60}$
72	0.9982	$1 + p^m_{t+72\|t} + p^{24}_{t+72} + \cos^{24}_{t+72} + \sin^{24}_{t+72} + \cos^{12}_{t+72} + \sin^{12}_{t+72} + \cos^{8}_{t+72} + \sin^{8}_{t+72}$

Table 6.10: *(Model 3) The optimal models with corresponding optimal forgetting factors, λ, identified from the full model given by (6.26) and listed for a subset of the prediction horizons, k (in half hours). Here $p^m_{t+k|t}$ is the forecasted wind speed at time $t+k$ given at time t transformed to power by one of the estimated power curves from Section 6.4.2 and p^{24}_{t+k} is the estimated diurnal variation using (6.27). For clarity the model parameters are omitted.*

In the model selection the transformation of observed as well as forecasted wind speed is handled by a power curve estimated with observed wind speed as input and without wind direction dependency (Model "$m1\ w^2$" in Section 6.4.3). The best five sub-models of (6.26) for each of the five wind farms are listed in the Tables F.22 to F.30 and using the tables the final model 3 listed in Table 6.10 is selected. The coefficient of determination for model 3 without wind direction dependency in the power curves is found in Table 6.11 labelled "$m3a$". The benefits of using power curves with wind direction dependency in model 3 are also investigated, and the results are listed in Table 6.11 labelled "$m3b$". Here the transformation of observed and forecasted wind speed to power is obtained by two different power curves estimated using observed wind speed and the analysis, respectively. For both power curves the wind direction dependency is modelled by a first order polynomial expansion in wind speed (Model "$m3\ w^2$" and "$m3\ w^m$" in Section 6.4.3).

When considering the final models 1 to 3 the following features are observed:

- The transformed meteorological wind speeds are needed in the models for all prediction horizons.
- For the shorter prediction horizons the models rely on observed values of power, and to a less extent, wind speed, but as the prediction horizon increases the emphasis shifts to terms related to diurnal variation. For model 2 and 3 no observations enter the models corresponding to prediction horizons larger than or equal to 18 hours!

- The tables in Appendix F show, that the differences in performance between the best five models within a given wind farm and prediction horizon are (very) small. Consequently, if the model selection procedure is based on finding the model which maximizes the coefficient of determination for a given data set, some non-significant model terms are likely to be present in the selected model. The effect of this is to some extent countered by the model selection procedure applied in this section where a model term only enters the final model if it is found to be significant for a majority of the five investigated wind farms.

6.5.2 Model results

The prediction performance obtained for the three models identified in the previous section are compared in Table 6.11, where the coefficient of determination (R^2) for the models given in Table 6.8 to 6.10 are listed together with the coefficient of determination for the reference models: The naive predictor (6.23), $WPPT1$ (6.21) and $WPPT2$ (6.22). For reference the corresponding estimates of prediction error variance are found in Table F.31. In order to facilitate the comparison of the achievements of the various models with the performance of the naive predictor, the prediction error variance for the models is tabulated in Table F.31 as a fraction of the prediction error variance for the naive predictor.

The benefits of introducing meteorological forecasts into the models are most clearly illustrated by comparing the performance of the $WPPT1$ and $WPPT2$ models. These two models are very similar with respect to model terms as well as forgetting factors, and the main difference is, that $WPPT2$ contains additional terms incorporating forecasted wind speeds as model input. Using Table 6.11 it is seen, that already for a prediction horizon of 3 hours a very noticeable increase in R^2 is found for the $WPPT2$ model. As the prediction horizons increases the difference between the two models escalates in favour of the $WPPT2$ model, and for a prediction horizon of 36 hours the improvement range from 0.30 for the Dræby wind farm (DR) up to 0.44 for the Rejsby wind farm (RB).

The following considers the achievements of the three models identified in Section 6.5 when comparing with the $WPPT2$ model identified in [Nielsen and Madsen, 1996].

Model 1 (labelled "$m1$" in Table 6.11) can be considered as a straight forward optimization of the previously developed model $WPPT2$ with respect to models terms and forgetting factor. When comparing with the $WPPT2$ model a small improvement in R^2 ranging from 0 to 0.01 is seen for Dræby, Fjaldene (FJ), Hollandsbjerg (HO) and Rejsby, whereas no improvement in R^2 is found for Sydthy (SY).

Model 2 (labelled "$m2$") is fitted to the original power series whereas model 1, $WPPT1$ and $WPPT2$ are fitted to the square root transformed power series with the resulting deterioration of the performance. For model 2 an increase in R^2 ranging from 0 to 0.03 is seen for Dræby, Fjaldene, Hollandsbjerg and Rejsby when comparing with the $WPPT2$ model, and the improvement seems to escalate with increasing prediction horizon. For Sydthy model 2 shows a decrease in R^2 ranging from 0 to 0.01 compared to the $WPPT2$ model.

Model 3 employs a more accurate transformation between forecasted wind speed and power than any of the previous models $WPPT2$, model 1 or model 2. Considering model 3 without wind direction dependency in the transformation between wind speed and power (labelled "$m3a$") an increase in R^2 ranging from 0 to 0.06 is found when comparing with

		Prediction horizon $[\frac{1}{2}hours]$								
WF	Model	2	6	12	18	24	36	48	60	72
DR	*NAIVE*	0.88	0.64	0.30	0.02	-0.20	-0.46	-0.54	-0.69	-0.78
DR	*WPPT*1	0.88	0.69	0.46	0.31	0.21	0.12	0.09	0.07	0.08
DR	*WPPT*2	0.89	0.77	0.71	0.68	0.66	0.61	0.54	0.45	0.38
DR	*m*1	0.89	0.78	0.71	0.69	0.66	0.61	0.54	0.45	0.38
DR	*m*2	0.90	0.78	0.72	0.69	0.67	0.62	0.55	0.46	0.40
DR	$m3_a$	0.90	0.78	0.72	0.69	0.67	0.63	0.55	0.48	0.43
DR	$m3_b$	0.90	0.79	0.74	0.71	0.69	0.65	0.57	0.49	0.43
FJ	*NAIVE*	0.89	0.67	0.37	0.14	-0.05	-0.33	-0.45	-0.57	-0.63
FJ	*WPPT*1	0.89	0.70	0.48	0.33	0.24	0.13	0.10	0.07	0.07
FJ	*WPPT*2	0.90	0.80	0.76	0.75	0.72	0.66	0.59	0.53	0.49
FJ	*m*1	0.90	0.80	0.76	0.75	0.73	0.67	0.59	0.54	0.50
FJ	*m*2	0.90	0.80	0.76	0.75	0.73	0.67	0.61	0.55	0.50
FJ	$m3_a$	0.90	0.81	0.77	0.76	0.74	0.68	0.61	0.55	0.51
FJ	$m3_b$	0.90	0.81	0.77	0.77	0.75	0.69	0.61	0.55	0.51
HO	*NAIVE*	0.87	0.62	0.27	-0.03	-0.26	-0.50	-0.62	-0.81	-0.86
HO	*WPPT*1	0.87	0.67	0.45	0.31	0.22	0.15	0.11	0.08	0.07
HO	*WPPT*2	0.89	0.78	0.73	0.70	0.67	0.61	0.56	0.51	0.46
HO	*m*1	0.89	0.78	0.73	0.70	0.67	0.62	0.57	0.52	0.47
HO	*m*2	0.89	0.79	0.74	0.71	0.69	0.63	0.59	0.54	0.49
HO	$m3_a$	0.89	0.79	0.74	0.72	0.69	0.64	0.60	0.54	0.50
HO	$m3_b$	0.89	0.80	0.76	0.74	0.72	0.66	0.61	0.55	0.50
RB	*NAIVE*	0.86	0.65	0.35	0.12	-0.05	-0.28	-0.41	-0.50	-0.56
RB	*WPPT*1	0.87	0.68	0.46	0.32	0.23	0.12	0.05	0.02	0.00
RB	*WPPT*2	0.88	0.78	0.72	0.69	0.66	0.60	0.55	0.48	0.44
RB	*m*1	0.88	0.78	0.72	0.69	0.66	0.61	0.56	0.49	0.45
RB	*m*2	0.88	0.78	0.73	0.69	0.66	0.61	0.56	0.50	0.46
RB	$m3_a$	0.88	0.79	0.74	0.71	0.68	0.64	0.59	0.53	0.49
RB	$m3_b$	0.88	0.79	0.74	0.72	0.69	0.64	0.60	0.54	0.49
SY	*NAIVE*	0.92	0.75	0.48	0.26	0.09	-0.18	-0.30	-0.39	-0.45
SY	*WPPT*1	0.92	0.76	0.54	0.39	0.29	0.18	0.14	0.10	0.07
SY	*WPPT*2	0.93	0.83	0.77	0.74	0.72	0.66	0.59	0.52	0.46
SY	*m*1	0.93	0.83	0.76	0.74	0.72	0.66	0.59	0.52	0.46
SY	*m*2	0.93	0.83	0.76	0.74	0.71	0.65	0.58	0.52	0.46
SY	$m3_a$	0.93	0.84	0.77	0.75	0.73	0.68	0.62	0.56	0.52
SY	$m3_b$	0.93	0.85	0.79	0.77	0.76	0.70	0.64	0.58	0.54

Table 6.11: *(All wind farms) Coefficient of determination (R^2)for model 1 ("m1"), model 2 ("m2") and model 3 ("$m3_a$" or "$m3_b$") stated in Table 6.8, 6.9 and 6.10, respectively. In model 3 the power curve models identified in Section 6.4.2 are used to transform wind speed to power production. Here model 3_a uses power curves without wind direction dependency whereas model 3_b employs power curves with first order polynomial approximation of the wind direction dependency. The results for the naive predictor, WPPT1 and WPPT2 given by (6.23), (6.21) and (6.22), respectively, are listed for reference.*

the $WPPT2$ model and again the increase in model performance is largest for the longer prediction horizons. If wind direction dependent power curves are employed in model 3 (labelled "$m3b$") improvements in R^2 ranging from 0 to 0.08 are found. With the exception of Sydthy, which shows a consistent improvement for all but the lowest prediction horizons, the benefits of including wind direction seems to be largest for prediction horizons between 6 and 24 hours.

When considering the simple models without power curve transformation of wind speed it is clear, that a distinct improvement of the prediction performance can be achieved by utilizing model 2 fitted to the original power series in favour of any of the models fitted to the square root transformed power series. This improvement can be achieved without any additional computational requirements. It is also clear, however, that replacing the second order polynomial transformation of wind speed to power in model 2 by a power curve transformation improves the performance for all wind farms and this considerably in the case of Dræby, Rejsby and Sydthy. The applicability of on-line estimation of power curves without wind direction dependency using the methods outlined in Section 5.2.2 is demonstrated in [Nielsen et al., 1999a], whereas further studies are necessary before on-line estimation of wind direction dependent power curves using a recursive back fitting algorithm can be considered feasible.

6.5.3 Conclusion and discussion

This section (6.5) considers the issue of modelling and predicting the power production in five wind farms – Dræby, Fjaldene, Hollandsbjerg, Rejsby and Sydthy – using on-line observations of power production, wind speed and wind direction as well as meteorological forecasts of wind speed and wind direction.

The models investigated belong to the class of linear autoregressive models with exogenous input and are formulated directly as k-step prediction models. The input is transformed values of observed wind speed as well as forecasted wind speed, where the transformation is either by a second order polynomial expansion or by the power curves estimated in Section 6.4.2. The model parameters are estimated adaptively in order to accommodate slow changes in the system using the Recusive Least Squares algorithm with exponential forgetting. The prediction horizon range from half an hour to 39 hours in half hourly steps, thus the prediction horizon for the models investigated range from 1-step to 78-step.

The model selection procedure applied in this study is based upon exhaustive search among all possible combinations of the model terms in a full model containing all terms which are candidate to be included in the final model. An exhaustive search consumes a large amount of computational resources and thus the model selection is only conducted for a subset of the prediction horizons consisting of the 1, 3, 6, 9, 12, 18, 24, 30 and 36 hours prediction horizons.

Three different (full) models have been investigated. The full model 1 is an extension a model identified in a previous study [Nielsen and Madsen, 1996] (the $WPPT2$ model) where the autoregressive part of the model is increased, the transformation of observed wind speed to power is by the full second order polynomial expansion of wind speed and finally the modelling of the diurnal profile is extended to a third order Fourier transformation. The model is fitted to the square root transformed power series. The full model 2 contains the

same terms as model 1, but without the square root transformation of the power series. The full model 3 replaces the second order polynomial expansion with the power curves estimated in Section 6.4.2 in the transformation of observed and forecasted wind speed to power and also contains an additional term in the diurnal profile. Model 3 has been estimated employing power curves with as well as without wind direction dependencies.

Some important characteristics are noted for the three (final) models resulting from applying the selection procedure on the three full models. First of all the transformed meteorological wind speeds are needed in the models for all prediction horizons. Secondly for the shorter prediction horizons the models rely on observed values of power, and to a less extent, wind speed, but as the prediction horizon increases the emphasis shifts to terms related to diurnal variation. For model 2 and 3 no observations enter the models corresponding to prediction horizons larger than or equal to 18 hours!

Model 1 can be considered as a straight forward optimization of the previously developed model $WPPT2$ with respect to models terms and forgetting factor. When comparing with the $WPPT2$ model a small improvement in R^2 ranging from 0 to 0.01 is seen for Dræby, Fjaldene (FJ), Hollandsbjerg (HO) and Rejsby, whereas no improvement in R^2 is found for Sydthy (SY).

For model 2 an increase in R^2 ranging from 0 to 0.03 is seen for Dræby, Fjaldene, Hollandsbjerg and Rejsby when comparing with the $WPPT2$ model, and the improvement seems to escalate with increasing prediction horizon. For Sydthy model 2 shows a decrease in R^2 ranging from 0 to 0.01 compared to the $WPPT2$ model.

Model 3 employs a more accurate transformation between forecasted wind speed and power than any of the previous models $WPPT2$, model 1 or model 2. Considering model 3 without wind direction dependency in the transformation between wind speed and power an increase in R^2 ranging from 0 to 0.06 is found when comparing with the $WPPT2$ model and again the increase in model performance is largest for the longer prediction horizons. If wind direction dependent power curves are employed in model 3 improvements in R^2 ranging from 0 to 0.08 are found. With the exception of Sydthy, which shows a consistent improvement for all but the lowest prediction horizons, the benefits of including wind direction seems to be largest for prediction horizons between 6 and 24 hours.

For the two prediction horizons 1 hours and 36 hours the R^2 values for model 3 estimated without wind direction dependency range from between 0.88 and 0.93 for Rejsby and Sydthy, respectively, and down to between 0.43 and 0.52 for Dræby and Sydthy, respectively.

Chapter 7

Upscaling

The WPPT model is based on on-line measurements from 14 wind farms at different locations, a total of 117 MW.

The total installed wind power capacity in the Jutland-Funen supply area amounts to 989 MW (specification as of October 1, 1998).

The problem of predicting the total wind power production in the supply area, when knowing the behaviour of the 14 wind farms, is referred to as the upscaling problem.

7.1 Regional upscaling

The starting point is that measurement of wind speed and wind power production from 14 different locations (hereafter referred to as reference wind farms) takes place every five minutes. These measurements have been recorded for more than two years.

For the rest of the wind turbines in the supply area (hereafter referred to as free wind turbines), only monthly or quarterly readings of power production are available. This means that no detailed information about the pattern of production exists for the major part of the wind capacity. This implies that the true value of total wind power output minute by minute is absent.

However, it is evident from all available information that wind speed differs according to location, and there are considerable differences in the utilisation time for different wind turbines. This statement points to a method where upscaling is carried out region by region. Yet, without detailed information about the total wind power output, the approach to this issue should be a pragmatic rather than a highly advanced.

7.1.1 Definition of regional areas

The division of the supply area into regional areas has been accomplished according to the following criteria:

- Grouping of free wind turbines depending on utilisation time.
- Linking of reference wind farms and groups of free wind turbines according to proximity.
- Preferably two (or more) reference wind farms in each regional area.

The result of the analysis is presented in Figure 7.1 and in Table 7.1.

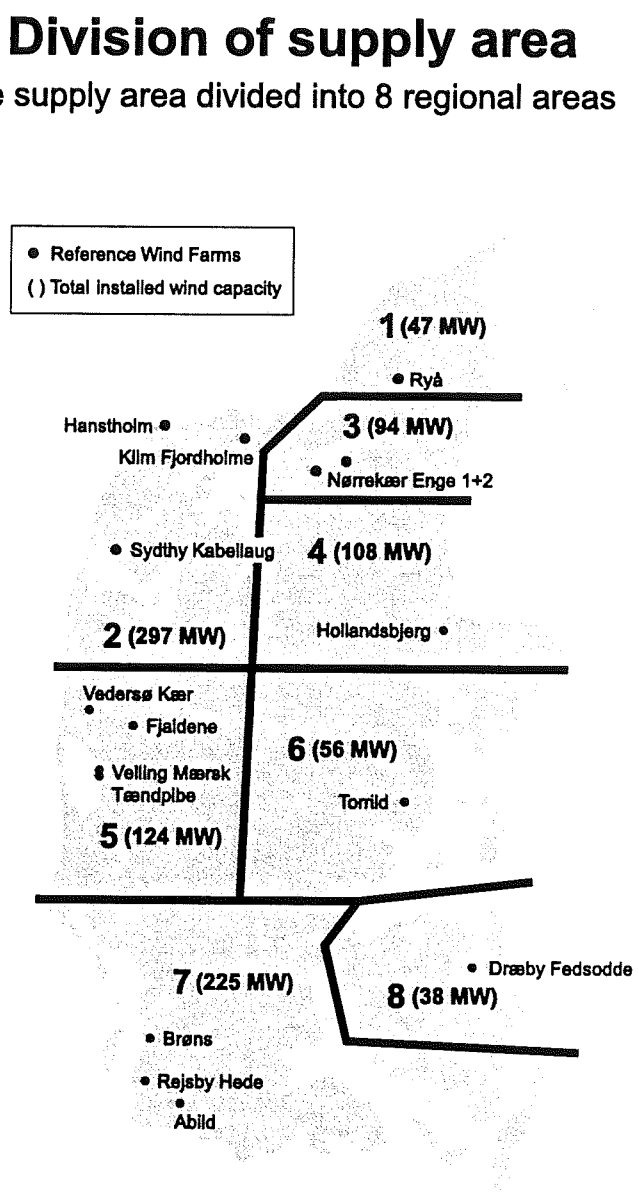

Figure 7.1: *Division of supply area into regional areas (MW-specifications as of October 1, 1998)*

In Table 7.1 below the division is presented along with information about the wind capacity and utilisation time for 1997 within each regional area.

The standard deviation of the utilisation time within each area is in the order of 100-200 hours. This fact signifies that an upscaling, no matter how advanced it is carried out, cannot guarantee that the wind power production in a local area (or the power production from an individual wind turbine) will be precise.

A natural consequence of no specific knowledge on the production behaviour of free wind turbines must be that if the utilisation time for reference wind turbines (TU^{ref}) and free wind turbines (TU^{free}) within a certain area is identical, there will be no need at all for

Area	WC^{ref} [MW]	TU^{ref}	WC^{free} [MW]	TU^{ref}
1	2.58	1.591	44.3	1.958
2	30.05	2.295	266.9	2.334
3	17.28	1.445	76.9	1.756
4	4.50	1.191	103.5	1.894
5	27.31	1.966	96.9	1.948
6	2.70	1.577	52.8	1.814
7	29.70	2.128	194.9	2.044
8	2.64	1.393	35.7	1.745

Table 7.1: *Installed wind capacity for the reference wind farms (WC^{ref}) and the free wind turbines (WC^{free}) within each area. Also the recorded utilization time for 1997 is listed for the reference wind farms (TU^{ref}) and the free wind turbines within each area (TU^{free}).*

upscaling (except from the simple upscaling WC^{free}/WC^{ref}, where WC^{free} and WC^{ref} is the installed wind capasity for the free wind turbines and the reference wind farms within a given area, respectively).

What can be seen from Table 7.1, however, is that the utilisation time for groups of free wind turbines and reference wind farms differs. To compensate for this behaviour a correction based on the recorded utilization times is introduced in the upscaling. The final upscaling function is given as

$$p_{tot}(t) = \sum_{i=1}^{8} \frac{WC_i^{ref}TU_i^{ref} + WC_i^{free}TU_i^{free}}{WC_i^{ref}TU_i^{ref}} p_i(t) \tag{7.1}$$

where $p_{tot}(t)$ is the total power production in the supply area and $p_i(t)$ is the sum of the power production within the reference wind farms in area i.

7.2 Substituting wind farms

The WPPT model is based on on-line measurements from 14 reference wind farms. For each of the locations a prediction of the wind power production is calculated. The production figures of the reference farms in the same area are added up and the total sum is used when upscaling. During on-line operation it must be expected that the individual wind farms experience "drop outs" or lacking recordings. The upscaling is then based on the remaining reference farms. In this situation there is a need for substituting wind farms. Table 7.2 below specifies the first and second substituting wind farms for each of the 14 reference wind farms. The principle is that the reference wind farms within the same regional area act as substitutes for each other. In situations where this solution is not possible, the principle of geographical proximity applies.

7.3 Conclusion

In the project a rather simple solution to the upscaling problem has been defined.

Reference wind farm	Tb 1997	1. substitute	2. substitute
Ryå	1.591	Nørrekær Enge 1+2	Hollandsbjerg
Hanstholm	2.725	Sydthy Kabellaug	Klim Fjordholme
Klim Fjordholme	2.080	Sydthy Kabellaug	Hanstholm
Sydthy Kabellaug	2.870	Hanstholm	Klim Fjordholme
Nørrekær Enge 1+2	1.445	Ryå	Hollandsbjerg
Hollandsbjerg	1.191	Nørrekær Enge 1+2	Torrild
VedersøKær	1.846	Fjaldene	V. Mærsk/Tændpibe
Fjaldene	1.950	VedersøKær	V. Mærks/Tændpibe
V. Mærsk/Tændpibe	2.034	Fjaldene	VedersøKær
Torrild	1.577	Hollandsbjerg	Dræby Fedsodde
Brøns	1.738	Abild	Rejsby Hede
Rejsby Hede	2.234	Brøns	Abild
Abild	1.630	Brøns	Rejsby Hede
Dræby Fedsodde	1.393	Hollandsbjerg	Torrild

Table 7.2: *Reference wind farms and substituting wind farms.*

The main reason for choosing a pragmatic approach was the lack of detailed information about the total wind power output.

In the near future, however, it is foreseen that detailed measurements of production from almost all wind turbines in the service area will be available due to changing market conditions. Data consisting production values with a 15 minute sampling period will be collected off-line and made available for Eltra with a delay of a few days.

With such data on hand it will be possible to refine and improve the upscaling procedure.

Chapter 8

Utility experiences

This chapter is a summary of Elsam experience using the Wind Power Prediction Tool (WPPT).

Different versions of WPPT have been used in the control centres of Elsam and Eltra since October 1997. Basically the prediction model has remained the same in all versions, but with currently corrections of minor and larger errors as well as changes resulting from of user suggested improvements. The latest version, WPPT 2.1, was put into operation in September 1998.

The general experience described in this paper may be from the whole period, but the actual examples and figures originate from the latest version.

8.1 Description of framework

This section describes the framework or the connections in which the WPPT is used.

During the course of this project the electricity sector in the western part of Denmark has been divided into Eltra as the transmission company with the system responsibility and Elsam as the commercial production company. Furthermore, the number of installed wind turbines in the area has increased considerably. Thus, the necessity of a tool for on-line prediction of the power production from the wind turbines is obvious.

In the past period of experience (1998) Elsam has been responsible for the economic load dispatch of the production from the primary power stations, when the priority production has received its share. Elsam has also been in charge of the balance responsibility for the whole Eltra/Elsam area. The distribution of the responsibilities between Elsam and Eltra might change in the future, though.

Elsam's production apparatus consists of 6 primary power stations with 12 units of between 250 and 650 MW, in total approximately 4,250 MW. All units but one gas-fired 400 MW unit are coal-fired. All units are CHP units (Combined Heat and Power) with the possibility of a considerable production of district heating. Furthermore, there are a large number of local CHP units of between 1 and 100 MW, in total approximately 1,400 MW, and finally the wind turbines of approximately 1,000 MW. These units (except for 125 MW of utility owned wind turbines) are treated as priority production, which means that they have the prior claim to sell the electricity produced. The local power units are only governed

by the consumption of district heating and by a three-step tariff defining a diurnal variation in the price payed for the electricity produced.

The high-voltage network in the western part of Denmark is connected via AC cables to Germany and DC cables to Norway and Sweden. Through these cables electricity is exchanged under different agreements with business partners abroad.

8.2 Planning with wind-based electricity production

An important input to the production planning is a good prediction of the electricity consumption, which has to be covered. In the Elsam/Eltra area the total consumption is calculated as production minus export, which all can be measured on-line. Thus not measured production covering part of the consumption will distort the picture of the actual consumption. Therefore the large penetration of wind based electricity production in the Eltra/Elsam area has necessitated that this production is measured on-line (partly supplemented by scaling) and enters into the production planning as a production plan.

Long-term plans (weeks/months ahead) are made as a mean value of the expected annual production, possibly adjusted by a statistically decided seasonal and daily variation.

In Elsam's daily planning WPPT is used to produce the short-term plans of the wind-based electricity production.

The planning of the production at the large primary power stations is made by means of a system for economic load dispatch. The prediction of the wind-based electricity production of WPPT is an input of this optimalization. At first WPPT predictions are checked by an experienced operator who may adjust the predictions on the basis of his knowledge of the weather from other sources or due to obvious errors in the predictions.

8.2.1 Wind predictions

Generally WPPT makes very good predictions but the operator may change them manually. This has typically been the case when:

- The weather is unstable, e.g. due to heavy depressions in a limited geographic area. This will give brief but large fluctuations of the predicted production and it is a well-known fact that it is very difficult to date and estimate such fluctuations correct. Therefore, the operator often chooses to "smooth" the prediction to avoid that the uncertain part of the wind predictions will disturb the load dispatch.

- There are obvious errors in the prediction. This may be due to erroneous measurements or failing wind speed forecasts from the DMI.

- The WPPT is at initial load start after errors or software updating. Normally a backup of the model database is made every midnight. If it is intact an initial load start can be carried out within a few hours. If it is not intact or cannot be used due to changes of the models, the models are to be "trained" by throughput of the data from at least 7 days (the measurements from the wind farms and the wind speed forecasts from the DMI from the last 7 days).

- The WPPT is defective. This has only been the case very few times.

8.2.2 The Operator's possibilities to act

For the time being the first phase of the daily planning of the next day's production from midnight to midnight is to be finished at 8:30 am on the day before. Ideally we should therefore have 40-hour predictions from WPPT, and thus the possible 39 hours are rather on the small side.

The WPPT calculates a new prediction every half-hour on the basis of the latest wind speed forecast from the DMI and updated measurements from the wind farms. Thus, for a given point of operation the uncertainty of the predictions decreases the closer to the point of operation one get. This enables the operator to adjust the production plan currently within the restrictions set by the production apparatus, the agreements with external partners (foreign business agreements) and the possibilities on the commodity exchange for electrical power. These restrictions give different possibilities of regulating the production and change of agreements on exchange of electricity as regards quantity and time of delivery dependent on how close to the point of operation one are.

The operator's possibilities to act are illustrated below:

- *Internal possibilities.* With Elsam's own production apparatus the operator has the following possibilities of regulating an imbalance between production and consumption/sale:

  - *Running reserve.* Normally Elsam plans to have a running reserve at the large power stations of approximately 5% of the maximum load - i.e. 150 to 200 MW. Thus, at least 150 to 200 MW can immediately be regulated up and down regardless of the production plan. Furthermore, additional reserve capacity is sold (reserved) to Eltra (the independent system operator). This is to cover the uncertainties in the prediction of load as well as in the predictions of production at the local co-generation units and the wind turbines. Also the uncertainty in the need for district heating from the primary power stations is taken into consideration. Regulation within the running reserve can be done without large additional expenditures.
  - *Regulation of district heating.* All primary units are CHP units, which produce district heating and electricity at the same time. These units can change the relation between the electricity and district heating production within certain limits. Furthermore, the district heating production can to some extent be varied independent of the district heating consumption, because the CHP units are attached to hot water accumulator-tanks with a storage capacity corresponding to several hours of consumption. As long as heat is stored in the accumulator it is possible to increase the electricity production from the unit by stopping the district heating production and instead cover the district heating consumption with heat from the accumulator. This can be started without any notable costs. On the contrary the unit can be put to a complete stop in the case, where there is no need for the electricity production and the accumulator can cover the district

heating consumption. However, this implies starting costs when the unit is to be re-started, and therefore this method is not used very often.

  - *Oil support operation.* All coal-fired units can change the fuel to oil during operation and thus decrease the electricity production with some MW. However, this is done at the expense of the considerable higher price on oil.

- *External possibilities.* The external possibilities, which the operator can use in order to adjust the production to consumption/sale, are to change the sales and purchase agreements with foreign (and gradually also domestic) partners. At present there are the following types of sales and purchase possibilities:

  - *Guaranteed power agreement.* A so-called guaranteed power agreement with Norway (Statkraft) makes it possible to import between 0 and 600 MW. The import plan can be changed without any costs up until 5 hours before the time of exchange.
  - *Power exchange trade.* Elsam trades on the Nordic power exchange for electricity - called NordPool. The purchase and sales offers are reported to the power exchange before 11.30 AM for the following day. The final purchases/sales cannot be changed later, however, bilateral contracts on counter purchase could be agreed. Balance power is purchased and sold on an hourly basis to compensate for imbalance on the market. The price for balance power varies a great deal depending on the supply and demand.
  - *Long-term contract.* The number of long-term contracts on purchase and sale can vary. These contracts can be deviated with high costs as a consequence.
  - *Other trade.* Furthermore, trading with electricity is done with several domestic and foreign partners - quantity and timetable being variable. The spot trade can be agreed every day before 9 am for the next day. The terms for deviations from these agreements differ from each other, but can be expensive. Spot trade in the present 24 hours can also happen with an hour's notice, if transfer capacity is available on the foreign connections (is agreed with Eltra).

8.3 The importance of the predictions for the operation planning

Considering the number of wind turbines in the Elsam/Eltra system today it is necessary to have some kind of prediction for their electricity production. The consequence of having 1000 MW of installed wind power in the system should be evaluated in the context of an annual minimum and a maximum load in the Elsam/Eltra area of approximately 1200 MW and 3700 MW, respectively. The largest gradient found in the wind-based electricity production is approximately 300 MW/h sustained over a period of 2-3 hours. This can be compared with the load change of approximately 650 MW/h over a period of 2 hours, which very predictable with respect to size as well as time occurs every morning.

The performance goal for WPPT is to be capable of predicting the wind-based electricity production with an accuracy of 50 MW up to 36 hours in advance. This is not possible yet,

but the predictions are much better than the ones an experienced operator can give on the basis of weather forecasts from known public available sources (radio, TV, Internet, etc). The predictions are the basis for the economic load dispatch and trade in electricity from day to day and hour to hour.

The natural consequence of large uncertainty is that the system has to operate with a large running reserve. A increase to 300-400 MW in the running reserve will for Elsam mean running of an extra unit, which otherwise was not necessary. This means DKK 30-40,000.- per 24 hours in extra costs. This could be avoided in periods of stabile wind conditions or periods with not wind at all, but if it is necessary for e.g. 100 days a year it means an extra cost of DKK 3-4 million a year.

The prediction horizon of 39 hours is normally too short a period/time-scale on which to base a stop/start of the units, but the saving is approximately DKK 100-150,000.- for every avoided stop/start of a unit.

8.4 Examples from the daily planning

To illustrate the quality of the predictions as well as emphasize the importance of the predictions for the daily operation three examples from the daily planning, which was negatively or positively influenced by the predictions for the wind-based electricity production, have been analysed in the following.

8.4.1 Example 1 (17 October, 1998)

On 17 October 1998 the wind power production was characterized by large fluctuations (See Figure 8.1). The deviation between the actual production and the prediction given at 10.30 am the day before was too large to be covered by the running reserve in the period from 5 pm to 7:30 pm and the missing power would have had to be purchased from NordPool at a total price of approximately DKK 16,000. The prediction given at 4.30 pm the day before was so much better, that the deviation could be countered by the normal means of regulation without any additional costs compared to a perfect forecast.

8.4.2 Example 2 (24 October, 1998)

On 24 October the wind power production stayed around 100 MW during the first part of the day. From noon the wind power began to increase and at midnight maximum production was reached (See Figure 8.2). The prediction from WPPT given at 10.30 am the day before had indicated a less changeable course of the wind production. At 8 pm the deviation was approximately 250 MW which was covered by the running reserve and by changing the heat to power ratio on some of the CHP units. Consequently the deviation was handled without considerable costs. The situation was worsened by the fact that the operator had written up the WPPT prediction by 100 MW at the time.

At midnight the production was approximately 250 MW higher than predicted, which could by handled the normal means of regulation without any additional costs compared to a perfect forecast.

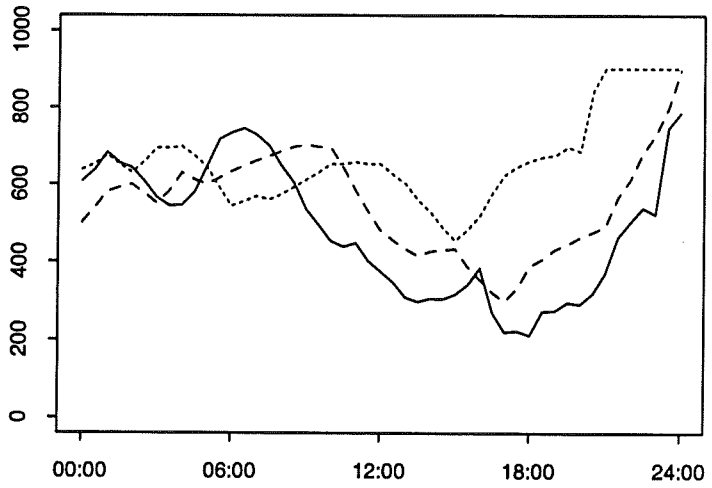

Figure 8.1: *Measured (up-scaled) wind-based electricity production 17 October, 1998 (full line) compared with the WPPT prediction from 10:30 am (dotted line) and 4:30 pm (dashed line) the day before.*

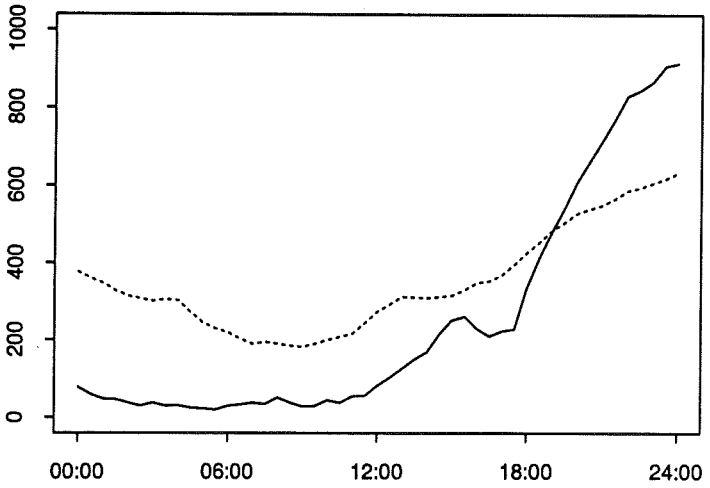

Figure 8.2: *Measured (up-scaled) wind-based electricity production October 24, 1998 (full line) compared with WPPT-forecast from 10:30 am the day before (dotted line).*

8.4.3 Example 3 (9 November, 1998)

On 9 November the wind power production was marked by a large peak around noon (See Figure 8.3). This course of the wind power production was accurately predicted the day before and consequently the full economical value could be gained.

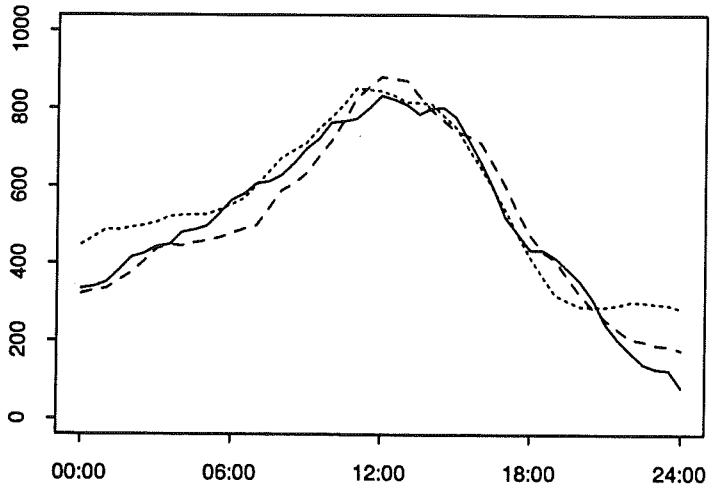

Figure 8.3: *Measured (up-scaled) wind-based electricity production 9 November, 1998 (full line) compared with WPPT-forecast from 9:30 am (dotted line) and 9:30 pm (dashed line) the day before.*

8.5 Using WPPT

8.5.1 Operation

The graphical interface in WPPT has been developed in close co-operation with the users and the latest version of WPPT has a very nice operational interface. The necessary menus and plots are implemented and are used logically and with reasonable response times.

8.5.2 Operational reliability

WPPT software

After a few corrections in the first versions WPPT is very reliable. Only a very few unintentional stops of the system have occurred in the previous year.

Collection of measurement values

The measurement equipment in the wind farms has shown a number of errors. Especially the anemometers have had errors due to mechanical problems. These errors are not always automatically discovered by WPPT, why a better detection of such errors is needed. It should also be possible to manually "disconnect" bad measurements.

Meteorological forecasts

The transmission of the forecasts from the DMI has been interrupted a few times. Mostly it has been due to errors in the public Internet, but interruptions have also been caused by errors or maintenance work on the internal mail-server at Elsam.

8.5.3 Suggestions for improvements

It has been pointed out that the following improvements of the latest version of WPPT could be desirable:

- Manual choice of the most optimal wind speed measurements.
- Plot of manually chosen historic prediction of a certain hour.
- Better error detection for measurements for wind and power.

8.6 The wind turbines' influence on the network losses

At the end of 1998 there are installed approximately 1000 MW wind power in the Eltra area. These wind turbines have all been connected to the distribution network (60 kV and lower voltage levels), and the majority of the wind turbines are connected to the 10 kV network. This section illustrates the wind turbines' influence on the network losses in the power system. The matter is complex, why only general assessments are taken into consideration.

On the basis of experience it can be assumed that the average network losses in a power system with mainly large power stations connected to the transmission network (150 kV and 400 kV networks) in the Eltra area are divided as indicated below in Table 8.1.

Network	Average network losses
0.4 kV network	$> 4\%$
10 kV network	$\approx 2\%$
60 kV network	$< 2\%$
150 and 400 kV networks	$< 2\%$

Table 8.1: *Average network losses distributed between voltage levels in the network.*

Table 8.1 shows that the majority of the total network losses are to be found in the low voltage levels. Bearing this in mind, the wind turbines' influence on network losses in the various voltage levels is explained in the following.

8.6.1 0.4 kV network

The wind turbines do not influence on the network losses in the 0.4 kV network, as the connection point normally is in the 10 kV network or in the higher voltage level networks.

8.6.2 10 kV network

The wind turbines increase the network losses in the 10 kV network, partly because the majority of the wind turbines that are connected to the 10 kV network are connected to a "collecting network" [1], and partly because the wind turbines are concentrated in relatively limited regional areas, where the installed capacity is considerably higher than the consumption in the area.

8.6.3 60 kV network

Apart from the wind turbines a large number of local CHP units (total capacity approximately 1400 MW by the end of 1998) are also connected to the distribution network. These combined heat and power units obviously affect the losses in the network too, which makes it difficult to distinguish between the consequences of wind turbines and the consequences of CHP units on the 60 kV level and higher voltage levels.

The general tendency is that in areas with many wind turbines and CHP units, the 60 kV network losses are increased, in areas with few wind turbines and CHP units, the 60 kV network losses are reduced. It has earlier been investigated how the network losses in a 60 kV point in the network (a.c. sub-station, a transmission line etc.) change according to the capacity of the installed local CHP production in terms of a percentage share of the maximum load in the point, see Table 8.2.

Inst. capacity	Wind power	Local CHP	Wind power + CHP (1:1)
0%	0%	0%	0%
50%	35%	45%	45%
100%	40%	40%	65%
150%	20%	-25%	50%
200%	-30%	-150%	10%

Table 8.2: *Reduction in network losses (expressed in percentages) as a function of the installed capacity in terms of percentages of the maximum yearly load in the point investigated.*

Table 8.2 shows that in areas (points in the 60 kV network), where the installed capacity does not exceed the maximum load, the reduction in the network losses is relatively high. But in the points, where it exceeds the capacity, the reduction decreases to disappear entirely at capacities higher than approximately. 1.5-2.0 times the maximum load.

It is estimated that the average network losses in total are reduced in the 60 kV network compared to a situation with exclusively large power stations. However, marginal reasoning in a 60 kV area will often show that new wind turbines increase the network losses.

[1] A network, which solely collects the production from wind turbines. The construction of "collecting networks" (or other network upgradings due to wind turbines are financed by a equalisation arrangement in order to divide the cost equally on all consumers in the Eltra area. In 1995 the costs amounted to DKK 11 million, in 1996 to DKK 62 million and in 1997 to DKK 65 million.

8.6.4 150 kV and 400 kV networks

It is assumed that the wind turbines in total reduce the network losses in the 150 kV and the 400 kV networks. However, the assessment is somewhat complex in this situation too, as surplus production, which has to be exported, does occur in the Eltra area at different times of the year.

The compelled export increases the transit in the transmission lines and the interconnections to other systems, which increase the network losses in the 150 kV and 400 kV networks. But as it to a high degree is the heat-bound production and thereby the local CHP units and power stations that cause the surplus, the additional losses cannot be ascribed to the wind turbines alone.

8.6.5 Summary

The first wind turbines reduced the network losses in the 10 kV, 60 kV, 150 kV and the 400 kV networks, but today the wind turbines represent a relatively large part of the total production capacity, and as it in addition is concentrated in regional areas with a low consumption, there are no network savings attached to the wind turbines any longer. New wind turbines in these areas increase the network losses.

The net result of the wind turbines' influence on the network losses is probably close to zero. The additional losses in the 10 kV network are at a conservative estimate assumed to be in the same order as the savings on the network losses in the overall network.

Chapter 9

Implementation

WPPT is implemented as two fairly independent parts – a numerical part and a presentation part – in the following denoted WPPT-N and WPPT-P, respectively. Data exchange between the two subsystems is implemented via a set of files. A file based interface between WPPT-N and WPPT-P has been chosen for portability reasons as it is foreseen that WPPT will have to run on wide range of platforms. Currently WPPT have been successfully tested on HP Unix systems, Digital VMS systems as well as PC systems running Linux.

WPPT-N is meant to be running continuously whereas any number of WPPT-P processes can be running at a given time, i.e. WPPT is not restricted to be used by only one user at a time. In the following two sections WPPT-N and WPPT-P is presented in more detail.

9.1 The Numerical Part of WPPT (WPPT-N)

WPPT-N is implemented in ANSI C and is designed to be straight forward to port to a new platform for which an ANSI C compliant compiler is available.

WPPT-N can by and large be considered to consist of five major modules: data input (measurements and meteorological forecasts), data validation, model estimation and prediction, up-scaling module and finally performance logging and data output for WPPT-P. The measurements are given as 5 minute average values and the data validation is carried out on the 5 minute values before these are subsampled to form the 30 minute values used by the models. The meteorological forecasts are given as hourly values which are interpolated to form 30 minute values before being used in the models. A brief description of the functionality within each module is given in the following:

- *Data input.* The data interface for exchanging measurements and meteorological forecasts between the local SCADA system and WPPT-N is established via a set of plain ASCII files. An ASCII file interface has been selected for two reasons:

  1. The interface is simple to establish on a wide range of systems.
  2. The input files provide a historic database for the measurements. This is very helpful for fine tuning of the models as well as further model development.

  The input files are checked for consistency both with respect to timing as well as the number of values.

- *Data validation.* Experience has shown that despite large efforts on-line measurements are prone to failures (errors). It is therefore essential to have some sort automatic error classification of the measurements not only for protecting the models against the influence of erroneous measurements, but also in order to ease the surveillance tasks for the operators (see Section 9.2).

  - Range check. The measurements are checked versus predetermined minimum and maximum values.
  - Stationarity check. The measurements are checked for stationarity, i.e. are hung on a constant value. Measurements of wind speed and power are allowed to become stationary around 0 for longer periods of time but otherwise stationary measurements are discarded as erroneous.
  - Confidence check. Here the output models describing the relationship between related measurements, e.g. wind speed and power production, are compared with the actual measurements. If a measurement falls outside some predefined confidence bands provided by the model, it is classified as erroneous. This test is only implemented in a provisional version in the current release of WPPT.

  Only the measurements are subject to the data validation methods described above, and the validation of the meteorological forecasts is left with the quality control of the national weather service.

- *Model estimation and prediction.* Each wind farm has a set of models covering the prediction horizon (30 minutes up to 39 hours) in steps of 30 minutes. Each model is a k-step prediction model for which estimation of model parameters and prediction of wind power is implemented as described in Section 5.1.2. The model implemented is the WPPT version 2 model – see Section 6.5. Every 30 minutes a new 39 hour prediction is calculated for the power production of each wind farm. During periods, where model input is marked as erroneous, the model estimation is inhibited in order to protect the model from the influence of bad data and the predictions for the actual park are marked as being unavailable.

- *Up-scaling.* Both power production measurements and predictionss for the selected wind farms are up-scaled and summarized so as to calculate an estimate for the power production in the entire Jutland-Funen supply area. For each wind farm a number of substitution wind farms have been defined and in case the values for a wind farm becomes marked as unavailable the wind farm in question is replaced by one of its predefined substitutes in the up-scaling.

- *Performance logging.* Every 30 minute the updated 39 hour predictions for the reference wind farms as well as the total prediction for the entire supply area are logged and saved in individual files.

- *Data output for WPPT-P.* Finally the interface files between WPPT-N and WPPT-P are updated (5 minute values as well as 30 minute values).

It should be stressed, that the models applied in WPPT-N are self calibrating, they so to speak learn from the observed data as time goes by, thereby rendering re-calibration superfluous. On the other hand this means, that they have to run for some time, typically 7 - 14 days, before the predictions can be considered to be reliable. To overcome this drawback in applying self calibrating models some additional features have been incorporated into WPPT-N:

- Accelerated learning allows WPPT-N to be started back in time and then use historical input files to calibrate the models before moving into real time operation.
- A backup of the current model state is generated every day at midnight. The backup ensures that the system will be able to restart quickly in case of power interrupts, system reboot or similar.

9.2 The Presentation Part of WPPT(WPPT-P)

WPPT-P is implemented in ANSI C++ and is based on the X11 and Motif graphical libraries. It has been tested under VMS, HP Unix and Linux and is expected to run on any platform for which X11, Motif and an ANSI C++ compliant compiler is available.

In the configuration used by Elsam/Eltra WPPT-N is a rather large system taking 70 measurements and 14 meteorological forecasts as input. Thus WPPT-P has to serve several purposes:

1. Display the 39 hour prediction of the total wind production in the Jutland-Funen supply area.
2. Provide an overview over the climatical conditions and the power production throughout the supply area.
3. Provide an overview of the current status for the measurement equipment installed in the wind farms.
4. Display detailed information for each wind farm for diagnostic purposes, e.g. if a prediction seems to be unrealistic the detailed plot for the wind farms can be used to determine the reason for the bad prediction.
5. Act as interface to the upscaling algorithm described in Chapter 7.

The need for providing both an overview as well as detailed information is reflected in the design of WPPT-P. The main window together with a number of plots directly accessible from the menu bar on the main window provides the operators with an overview of the system state whereas the system engineer has access to more detailed information through a set of sub-windows dedicated to the individual wind farms.

The following sections provide an overview of the functionality build into WPPT-P.

9.2.1 The Main Window

The main window consists of four elements - menu bar (top), map area (left), value field (right) and information field (bottom) - as shown in Figure 9.1.

- *The menu bar* provides access to some system functionality as well as the overview plots described in Section 9.2.2.
- *The map area* contains a map of the Jutland/Funen area where the location of each reference wind farm is marked by a wind farm symbol. The symbol consists of a reference code for the wind farm (W*) (top), a number giving the farms current production as a percentage of the rated power (left) and a wind rose indicating the current wind direction and wind speed (right). In case a measurement error has been detected in the wind farm the symbol turns red to alert the operator to the error. Furthermore clicking on a symbol with the mouse opens the corresponding wind farm window (See Section 9.2.3).
- *The value field* provides some key figures regarding the current system state. The fields 1 and 2 from the top show the calculation time for the current power prediction and the initiation time for the calculation of the last meteorological forecast recieved, respectively. Field 3 shows the total rated wind power in the Jutland/Funen area as registered by WPPT-N. The fields 4 and 5 give the current estimate of the total power production as a 5 minute and 30 minute average, respectively, and finally the fields 6 to 15 present the current power prediction for selected prediction horizons.
- *The information field* provides the system engineer with a bulletin board to relay relevant information to the users of WPPT.

9.2.2 Plots available from the Main Window

A number of plots regarding the observations and the predictions of the total power production are available from the menu bar in the main window.

- *Plot of observations.* In order to provide a mean for comparing the measurements from the 14 wind farms relative power production, wind speed, wind direction and ambient air temperature for the 7 northern and 7 southern wind farms can be plotted together (See Figure 9.2 for an example).
- *Plot of power predictions.* The predicteded power production in the Eltra/Elsam supply area for the next 39 hours is presented together with the observed power production for the last 6 hours in a plot (Figure 9.3). The plot also presents some emperic uncertainity bands for the prediction. By default the 5% and the 95% quantiles are displayed but other quantiles are available if more appropriate. In order to provide an overview of the prediction performance for the total power production the observed power production is plotted together with historical predictions for selected prediction horizons (Figure 9.4).

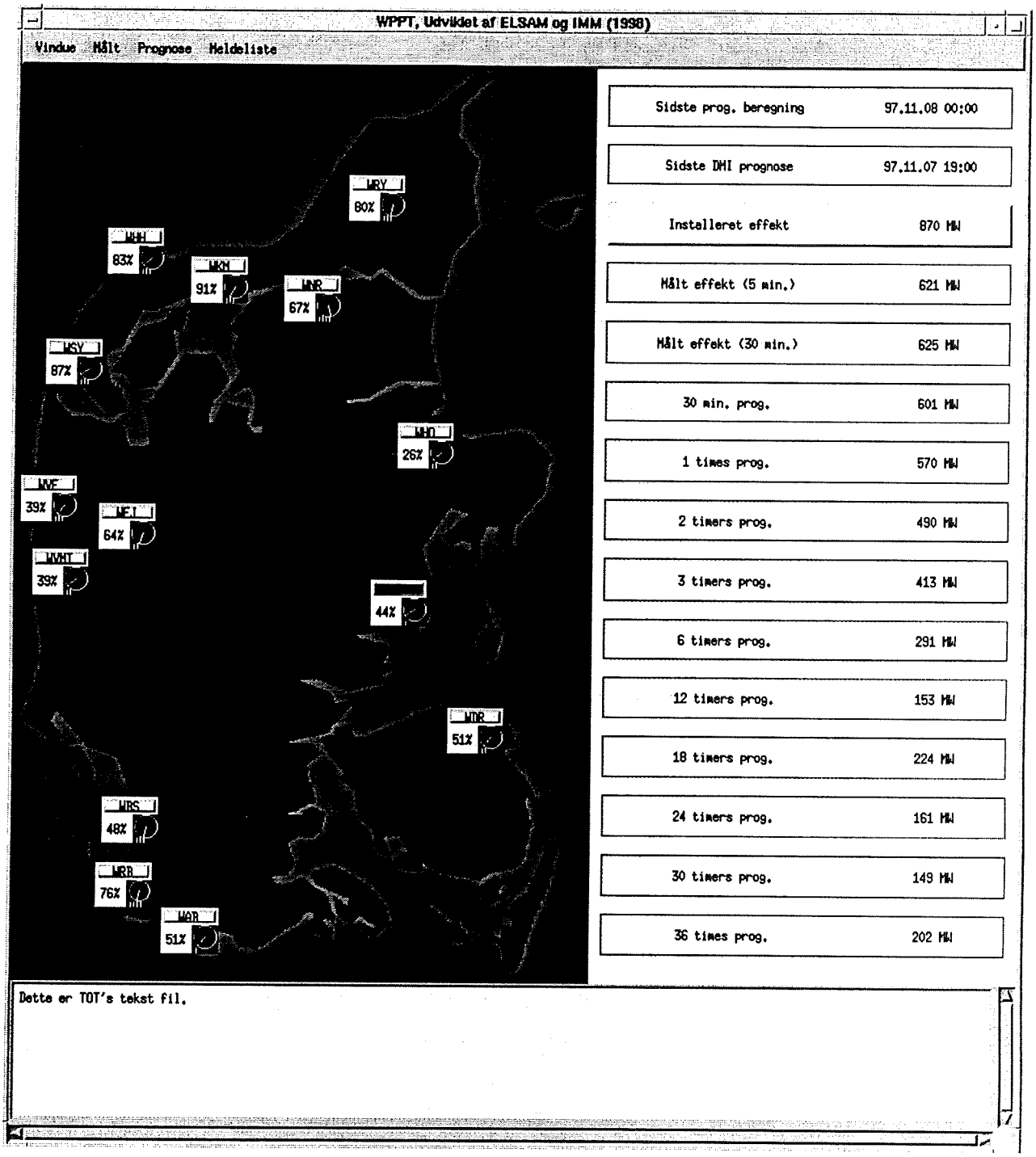

Figure 9.1: *Main window in WPPT-P. The menu bar (top) provides access to some system functionality as well as the overview plots. The map area (left) contains a map of the Jutland/Funen area where the location of each reference wind farm is marked by a wind farm symbol. Dedicated windows for the individual wind farm windows can be accessed by selecting the corresponding wind farm symbol with the mouse. The value (right) field provides some key figures regarding the system state for instance current and predicted power production in the supply area. The information field (buttom) provides the system engineer with a bulletin board to relay relevant information to the users of WPPT.*

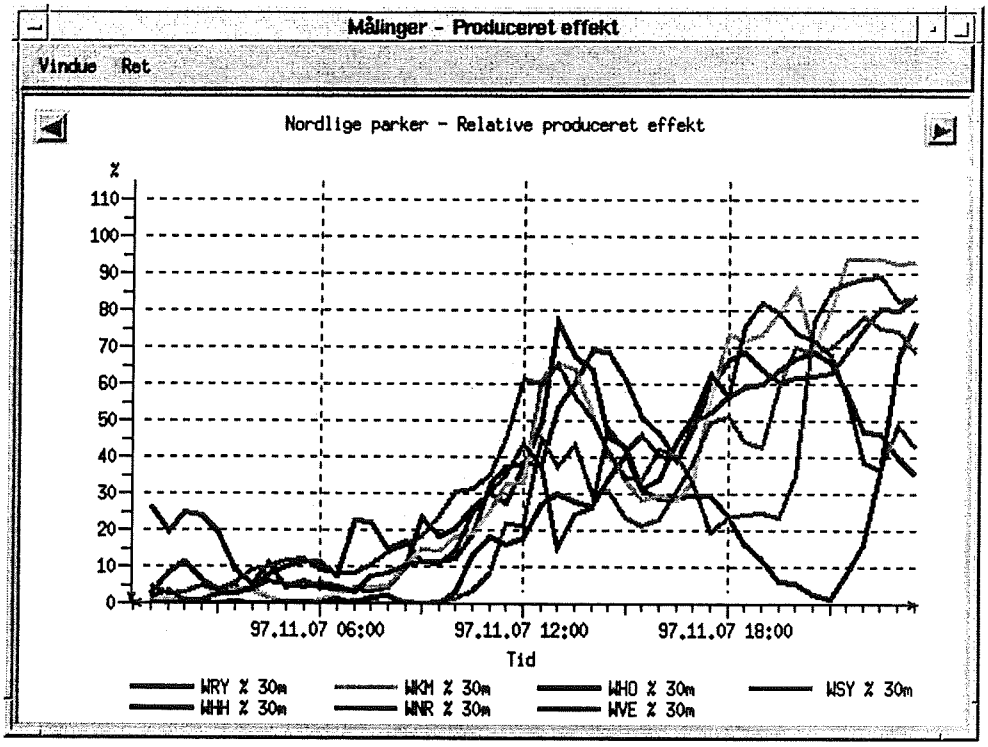

Figure 9.2: *The relative power production for the Northern wind farms. The plot covers the last 24 hours.*

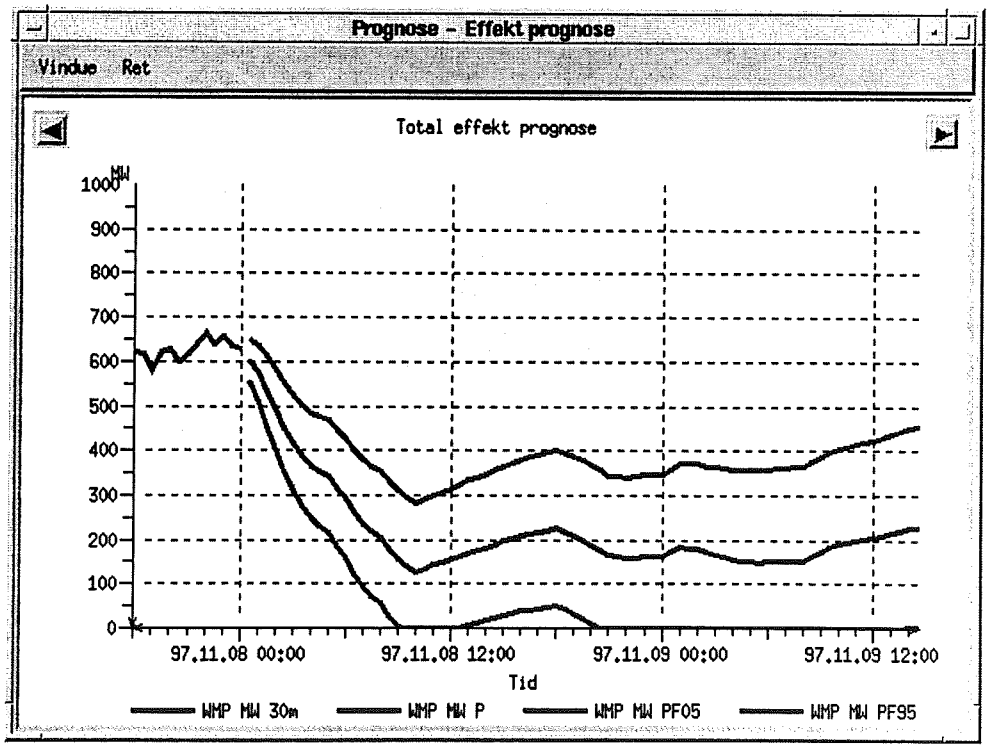

Figure 9.3: *Plot of the predicteded total power production for the next 39 hours together with the most recent observed values. The plot also include estimated uncertainity bands for the prediction.*

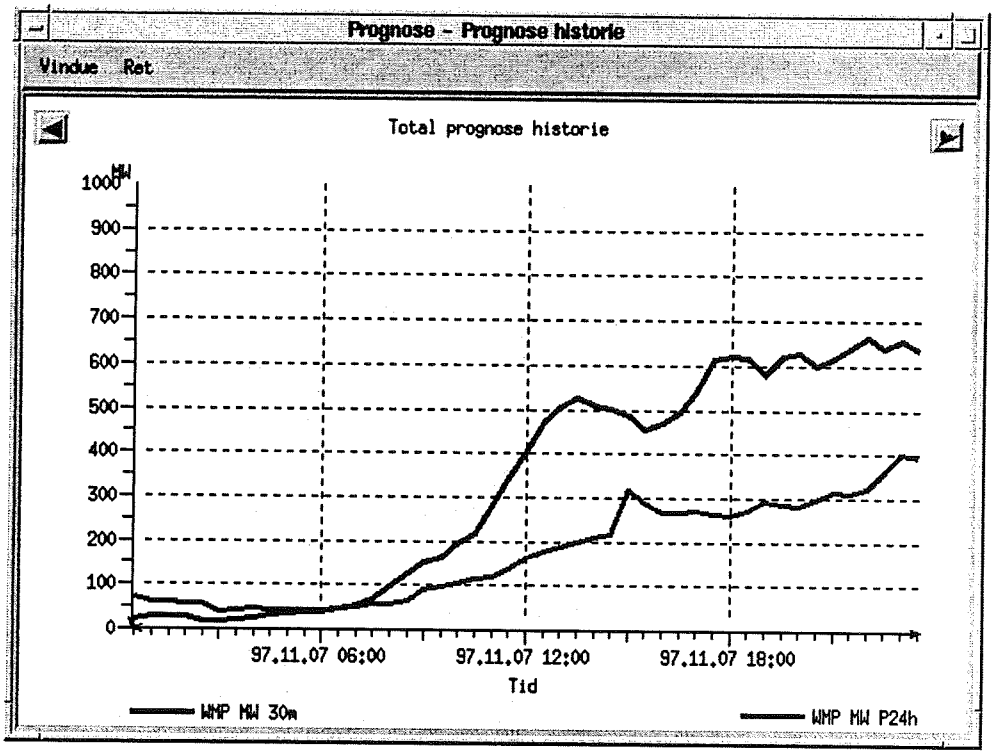

Figure 9.4: *Plot of the observed power production together with the historical 24 hour predictions. Also the 6 hour, 18 hour, 24 hour and 36 hour predictions can be selected for comparison.*

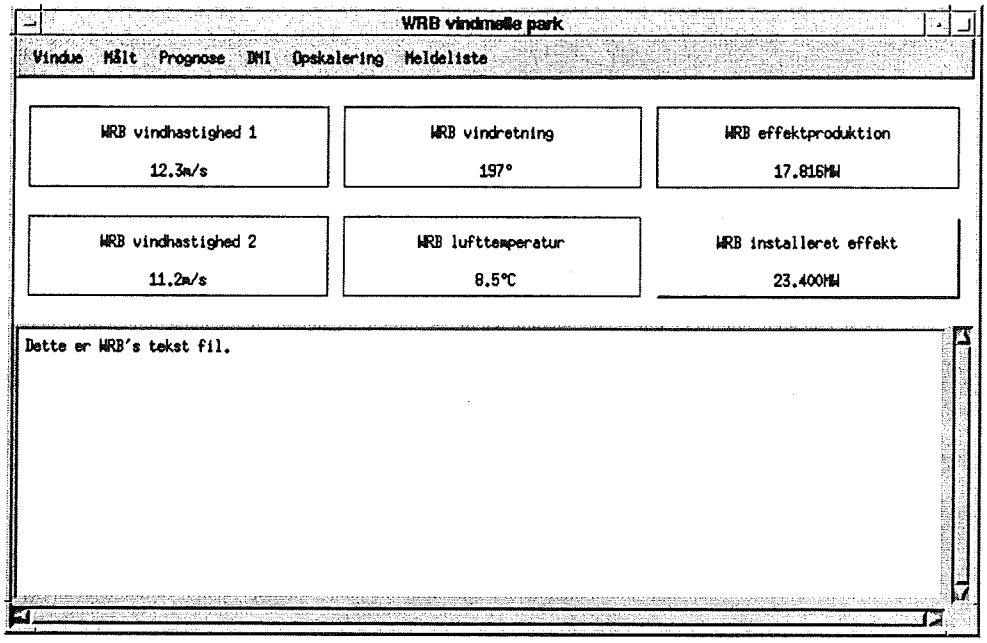

Figure 9.5: *The wind farm window in WPPT-P.*

9.2.3 The Wind Farm Window

The wind farm windows consists of three parts: a menu bar (top), a measurement value field (middle) and an information field (bottom).

- *The menu bar* gives access to some system functionality as well as a large number of plots for the wind farms (See Section 9.2.4).
- *The measurement value field* displays the most resent 5 minute values for the wind farm measurements (two wind speeds, wind direction, air temperature and power production). In case a measurement has been classified as faulty the measurement in question is marked by a red background colour. The last field shows the rated power for the wind farm as registered by WPPT-N.
- *The information field* provides the system engineer with a bulletin board where information concerning the wind farm can be relayed to the operators.

9.2.4 Plots Available from the Wind Farm Window

The wind farm window gives the user access to a number of plots which falls into 3 separate categories:

- *Plots of observations.* Plots of the 30 minute average values versus time are accessible directly via the menu bar for all of the five measurements (See Figure 9.6 for an example) but WPPT-P also enables the user to compose new plots where the various measurements can be plotted against each other.

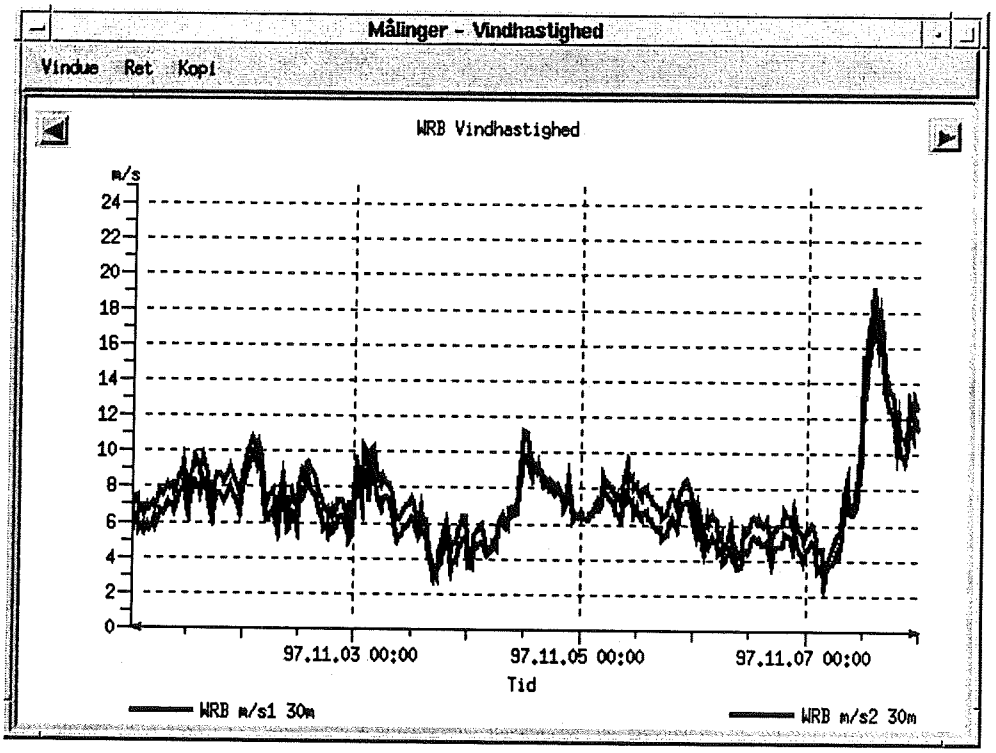

Figure 9.6: *Plot of the two wind speed measurements. By default the plot covers the most recent 7 days.*

- *Plots derived from the power production predictions.* Here the user has the possibility of plotting the predicted power production for the wind farm (Figure 9.7), the historical predictions for the wind farm as well as the uncertainty quantiles for the current prediction.

- *Plots derived from the meteorological forecasts.* Gives access to a plot of the most recent meteorological forecast of wind speed (Figure 9.8) as well as a plot of the historical performance for the meteorological forecasts.

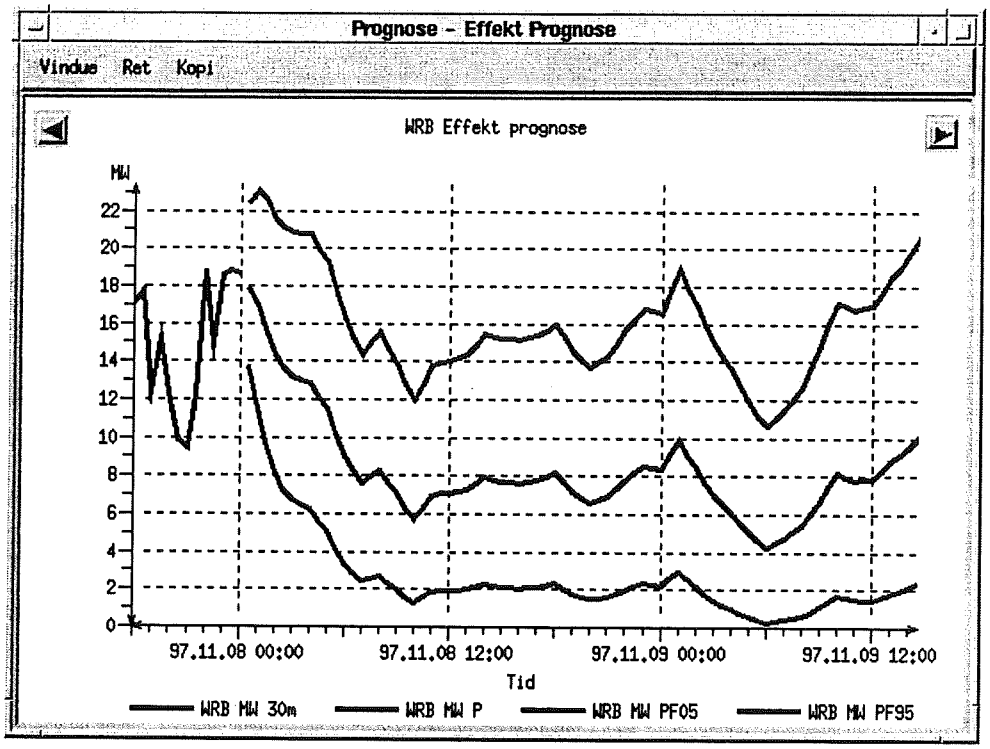

Figure 9.7: *Plot of the predicted power production for the next 39 hours including the estimated uncertainty bands for the prediction together with the most recent observed values.*

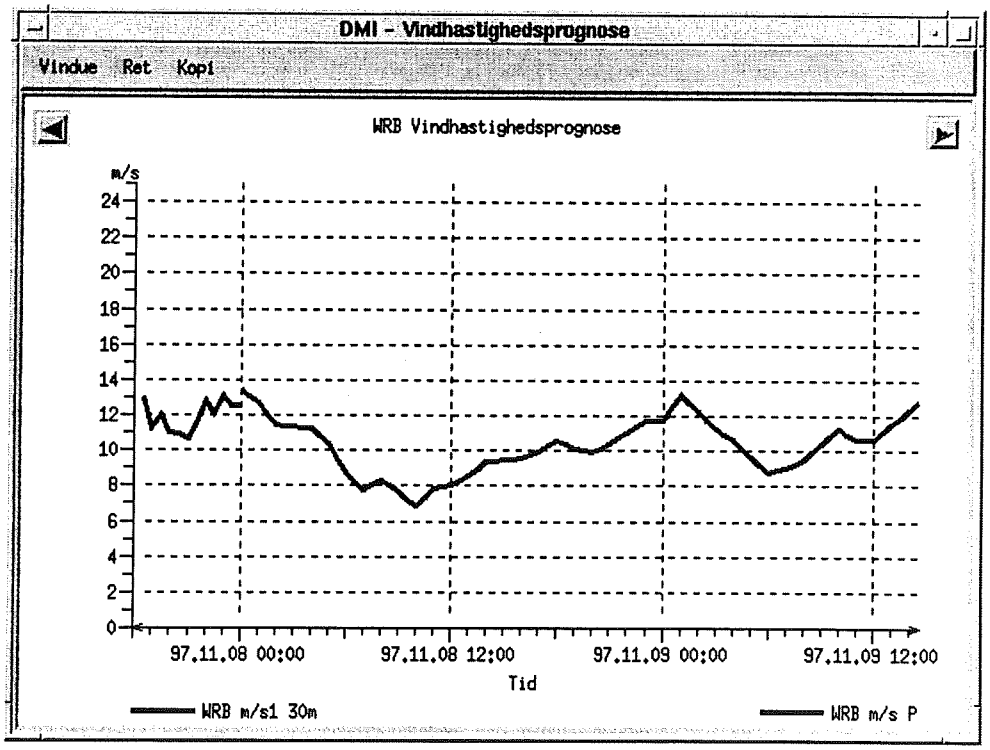

Figure 9.8: *Plot of the meteorological forecasted wind speed for the next 39 hours together with the most recent observed values.*

9.2.5 The upscaling dialogue

The upscaling dialog provides access to the constants used in the upscaling function described in Chapter 7. In case of longer lasting errors in a wind farm the dialogue allows the system engineer to disable the wind farm in question and thus remove it from the upscaling.

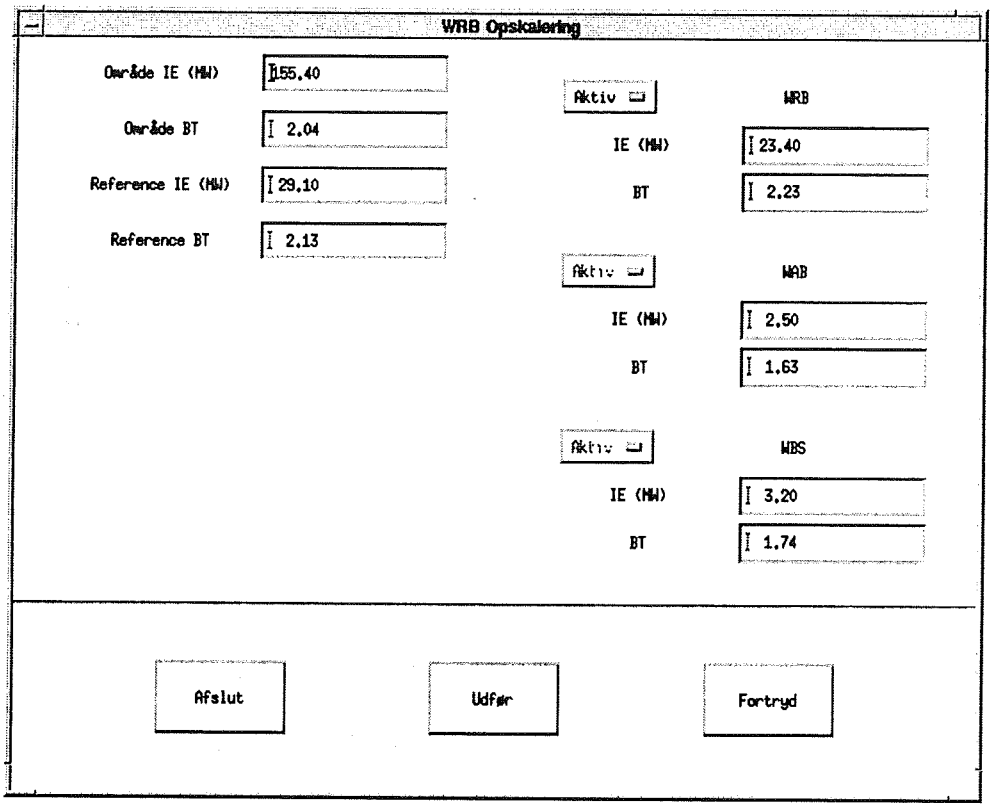

Figure 9.9: *The upscaling dialogue window in WPPT-P. The fields in the righthand column displays the rated power and utilization time for the reference wind farms in a sub-area. The toggle switch associated with each wind farm allows the system engineer to disable indivdual wind farms from the upscaling. The fields in the lefthand column display the constants used in the upscaling of the power production in the sub-area. These are rated power and utilization time for the free wind turbines in the sub-area as well as rated power and utilization time for the reference wind farms in the sub-area.*

9.2.6 Options Available from a Plot Window

All plots can be printed if a postscript printer is available at the site. Furthermore each plot can be tailored by the user through a dialogue box. The dialogue box allows the user to change the time period considered, the scaling of the axis and, for some plots, the plot variables.

The following contains a brief description of the various options:

- *Time period.* Allows the user to select start and end date for the data plotted. Option modes:
  - **Fast**. The start/end date of the plot is fixed to a given date set via the scrollbar or the entry fields.

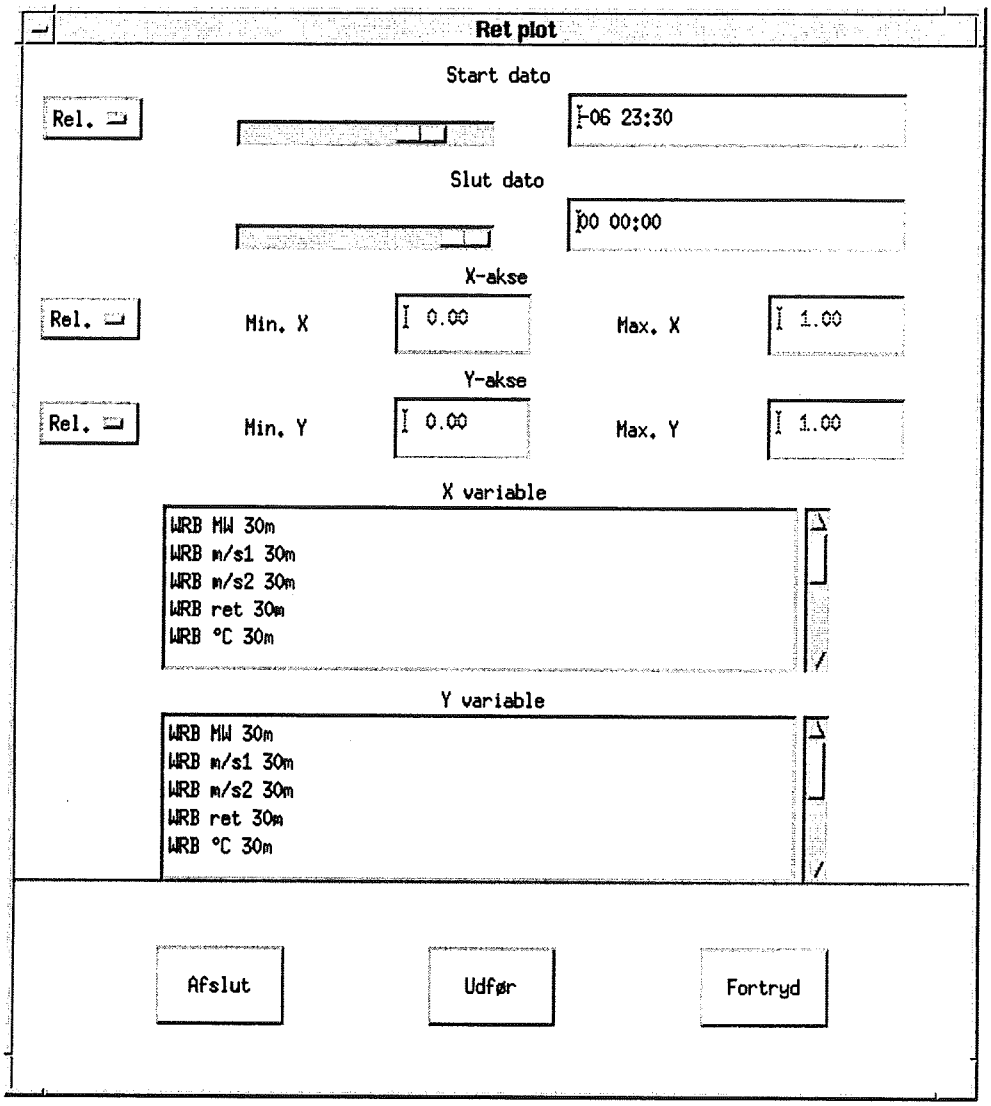

Figure 9.10: *The plot window dialogue box. Through this dialogue the user can change the time period considered, the scaling of the axis and, for some plots, the plot variables.*

  - **Rel.** The start/end of the plot is set as an offset relative to the current time.

- *Axis scaling.* Allows the user to select the scaling of the x- and y-axis. Option modes:
  - **Fast.** The axis scaling is a fixed value set through the min/max entry fields.
  - **Rel.** The scaling is automatically selected according to the extreme values in the data set.

- *Plot variables.* Allows the user to select the variables to plot and the plot type (x-y plot or time series plot).